Effects of power ultrasound on the pore solution, hydration and mechanical properties of Portland cement pastes and mortars

By

Ahmad Ehsani

BSc, MSc

October 2020

Effects of power ultrasound on the pore solution, hydration and mechanical properties of Portland cement pastes and mortars

By

Ahmad Ehsani

A thesis submitted in partial fulfilment of the University's requirements for the Degree of Doctor of Philosophy

October 2020

“From many of the usual category distinctions through which we make sense of our lives – liquid/solid, smooth/rough, natural/artificial, ancient/modern, base/spirit – concrete manages to escape, slipping back and forth between categories. […] concrete has a tendency to ‘double’, to be two opposite things at once”

Professor **Adrian Forty**
Concrete and Culture: A Material History

.

Library Declaration and Deposit Agreement

Content removed on data protection grounds

Certificate of Ethical Approval

Applicant:

Ahmad Ehsani

Project Title:

Ultrasonic treatment of waste pozzolans to improve cementitious property of binders

This is to certify that the above-named applicant has completed the Coventry University Ethical Approval process and their project has been confirmed and approved as Low Risk

Date of approval:

11 February 2020

Project Reference Number:

P103095

Acknowledgements

This interdisciplinary thesis dissertation relies on interactions and time spent with many people. I would like to express my sincere gratitude to each of them.

My first thanks go to Prof. Eshmaiel Ganjian who gave me the opportunity to delve into researching this topic and diligently helped me to do this work. I would like to thank him for his involvement towards this project and in keeping me motivated. His excellent guidance, support, and knowledge are greatly appreciated and of great value.

I would also like to thank Prof. Timothy J. Mason who provided me with an opportunity to study the fundamentals of power ultrasound and sonochemistry as well as their widespread interdisciplinary research opportunities. In addition to providing guidance and feedback, his personal bespoke ultrasonic equipment made any of this research a possibility.

My thanks and appreciation also go out to Prof. Mark Tyrer whose diligent support was of critical importance to this work. I was very lucky to benefit from his extensive knowledge and expertise in the area of cement chemistry throughout this work and I hugely learnt from his feedback along with constructive and encouraging discussions.

Special thanks to Dr Olivier Hass who substantially helped me to develop the automated dilatometry test setup for the measurement of chemical shrinkage of cement pastes.

Another important gratitude goes to all the friendly technicians at the laboratory of the School of Energy, Construction and Environment who helped me to set up the experimentations. I am further indebted to Dr Mark Bateman who provided his excellent guidance and feedback on the development of a reliable method for the ICP-OES analysis. In addition, I am grateful to Ms Raluca Barza, Mr Daniel Dugdale and Dr Richard Collins, the staff at the Analytical Laboratory in the Faculty of Health and Life Science for their assistance with the ICP-OES measurements and particle size analysis. I am also thankful to Dr John Graves for the fruitful discussions and his assistance with coating samples for microscopy.

I also wish to acknowledge the support of the Henry Royce Institute through the Royce PhD Equipment Access Scheme enabling access to STA and XRD facilities at Royce@Imperial; EPSRC Grant Number EP/R00661X/1. Very special thanks to Mr Richard Sweeny at the Royal School of Mines, Imperial College London for his assistance with the XRD and TGA analyses.

And last but not least, my biggest thanks to my wife, Elaheh, for all the unconditional support you have shown me through this intense work and looking after our young playful son, Ryan. You have been amazing!

Abstract

The present study investigates in detail the effects of the direct application of power ultrasound (PUS) at several frequencies and power densities to Portland cement (PC) pastes and mortars. The ultrasound frequencies of 26, 67 and 132 kHz that respectively correspond to power densities of 0.011, 0.007 and 0.003 W/cm^3 were deployed to treatments of fresh cement pastes and mortars. These various ultrasound intensities were generated using a large bespoke, multi-frequency ultrasonic bath. A fixed ultrasonic bath operating at 40 kHz with a power density of 0.014 W/cm^3 was also used to study the effects of PUS on the particle size distribution (PSD) of PC.

In the first part of the study, changes in the PSD parameters of PC based on wet dispersion in both isopropanol (IPA) and deionised water (DI water) were determined using laser diffraction method. Next, ultrasound at various frequencies was directly applied to the fresh PC pastes at water-to-cement (w/c) ratios of 0.50 and 0.80. The chemical composition of the pore solution extracted from the fresh and hardened cement pastes were examined using the inductively coupled plasma optical emission spectrometry (ICP-OES) technique after applying ultrasound for various periods. The work presents a robust ICP-OES method developed to quantify both Ca, K, Na and S as the high-concentration analytes, and Al, Fe, Mg and Si as the low-concentration analytes in the PC paste pore solution. Additionally, hydrate assemblages were identified by X-ray diffraction (XRD). A semi-quantification of important components was performed using data obtained by thermogravimetric analyses (TGA/DTG). The changes in the setting times of cement pastes subjected to PUS were also reported.

The PSD data shows that applying PUS for up to 5 minutes marginally deagglomerates the coarse size fraction of PC particles in aqueous dispersion. However, ultrasound may not be able to effectively disaggregate the PC particles in normal pastes, even at longer exposure; particularly the finer size fractions (< 10 µm). Direct application of PUS to the PC paste does not alter the main types of PC hydration products but appreciably changes the pore solution composition and slightly affects the main hydrate proportions and kinetics. The study reveals for the first time, that applying PUS can potentially disturb the early formation of ettringite, whilst appreciably promoting the formation of amorphous aluminium hydroxide hydrate by considerably releasing aluminium ions into pore solutions of cement pastes at both w/c ratios of 0.50 and 0.80. Upon ultrasound exposure (particularly at longer times), noticeable changes were observed in Ca and Si concentrations denoting the influence of PUS on the dissolution of alite and/or aluminate phases due to the cavitation. Moreover, PUS was shown for the first time to be able to increase carbonates by intensifying the carbonation (ultrasound-assisted carbonation) in the PC pastes, particularly in the system with a higher water content.

In the next part of the study, the development of hydration under the exposure of ultrasound irradiation at various frequencies/power densities and durations was assessed. First, the effect of PUS on the extent of PC hydration was investigated by precisely measuring the chemical shrinkage, using a self-developed automated dilatometry method, to 14 days of hydration. To measure the evolution of chemical shrinkage, an automated vision inspection system was developed. Additionally, the mechanical performances of the PC mortars were evaluated at testing ages of 1, 3, 7, 28 and 91 days. Two different sonication procedures were adopted for the treatment of the fresh mortar mixes. This was to investigate the effect of applying ultrasound at various stages on the mechanical properties of mortars and the properties of the interface between the cement paste and the aggregates (interfacial transition zone, ITZ). In the first approach, ultrasound was applied to all the components of the freshly mixed mortar, i.e. water, PC and fine aggregates. In the second approach, PC slurry was first prepared using water and cement and ultrasonication was subsequently applied to the cement slurry. Finally, the fine aggregates were added during the final stages of mixing to obtain mortars with sonicated paste.

The results indicated an enhancement in the evolution of chemical shrinkage when both 26 and 132 kHz frequencies were applied to the cement paste for a duration of 2 minutes. Cement pastes sonicated at 26 kHz for 2 minutes showed a slightly higher rate of chemical shrinkage than those treated at 132 kHz for the same irradiation time. Similarly, the corresponding mortars yielded a higher rate of development for both compressive and flexural strengths when subjected to a higher acoustic intensity at 26 kHz over 91 days curing in water, than those treated by a gentler insonation at 132 kHz. The application of PUS to fresh mortar mixes reduced the strengths of hardened cement mortars at 1 day compared to the non-sonicated mortar. In this regard, the effect of ultrasound with a higher intensity at 26 kHz is more profound than PUS at 132 kHz. However, at later ages, the mortars treated at 26 kHz acquired a higher compressive and flexural strength than either those treated at 132 kHz or the control samples. Longer exposure of PUS at 26 kHz considerably enhanced 1-day strength that could be related to the deaeration effect of ultrasound on the partial removal of entrapped air in fresh mortar. The addition of aggregates to the ultrasonicated paste was found to lead to a considerably significant improvement in the flexural strength of the mortars, potentially indicating the modification of the bulk cement paste and the ITZ. These effects were supported by microstructural analyses of the hardened PC mortars fracture surfaces, using scanning electron microscopy (SEM) and energy dispersive X-ray spectroscopy (EDS) techniques.

The present research concludes that the application of PUS in general has positive effects on the extent of cement paste hydration and then mechanical properties of mortar when a higher power density is used. Furthermore, the observations made for the first time in this work strengthen the position that ultrasound could be a promising technique to enhance ternesite hydration in ternesite-rich belitic calcium sulphoaluminate cements, as a novel low-carbon binder and an alternative to PC. This will be further investigated in a post-doctoral programme.

Contents

List of Figures

List of Tables

Glossary

Abbreviations	Definition
PUS	Power ultrasound
PC	Portland Cement
SCM	Supplementary Cementitious Materials
w/c	water-to-cement ratio
w/s	water-to-solid ratio
Cement notation	
C	Calcium Oxide CaO
S	Silicon dioxide SiO_2
A	Aluminium oxide Al_2O_3
F	Iron oxide Fe_2O_3
H	Water H_2O
$	Sulphate SO_3
Cement phases	
C_3S	Tricalcium silicate
C_2S	Dicalcium silicate
C_3A	Tricalcium aluminate
C_4AF	Tetracalcium aluminoferrite
$CaSO_4.2H_2O$	Gypsum
Cement hydrates	
C-S-H	Calcium silicate hydrate
CH	Portlandite or Calcium hydroxide, $Ca(OH)_2$
AFt	Ettringite
AFm	Monosulfate (Ms)/carboaluminates (Mc & Hc); hydroxy-AFm
AH_3	Aluminium hydroxide
Mc	Monocarboaluminate/
Hc	Hemicarboaluminate
Methods and Techniques	
PSD	Particle Size Distribution
ICP-OES	Inductively Coupled Plasma Optical Emission Spectrometry
XRD	X Ray Diffraction
TGA	Thermogravimetry Analysis
DTG	Differential Thermogravimetry
FE-SEM	Field-Emission Scanning Electron Microscopy
EDS	Energy Dispersive X-ray Spectroscopy

1

Chapter 1: Introduction

1. Introduction

1.1. *Motivation*

Power ultrasound (PUS) has been propelled to the forefront in investigations of a wide variety of applications in material science; from surface cleaning and degassing, to particle dispersion and crystallisation. Sonochemistry was the umbrella title established since 1986 (Lindley and Mason, 1987; Lorimer and Mason, 1987) to cover the various strands of the application of PUS in the chemistry and material processing fields. The chemical and physical effects of PUS in a liquid medium have been acknowledged as the consequence of acoustic cavitation (Mason, 1999; Mason and Lorimer, 2002; Mason and Peters, 2002) and have already been extensively explored (Mason, 2003). There is a serious lack of knowledge, however, in understanding the effect of PUS in the field of cement-based systems. In recent years, a handful of research has been undertaken limited to the characterisation of ultrasonic dispersion of supplementary cementitious materials (SCMs) when used in a cementitious system. Ultrasound treatment was purported to be favourable to improve the efficiency of both densified silica fume (Martinez-Velandia et al., 2008; Martinez-Velandia et al., 2011; Rodriguez et al., 2012a; Rodriguez et al., 2012b) and natural pozzolans (Askarinejad et al., 2012). This was through the predominant mechanism of the enhanced dispersion of agglomerates which was identified to lead to better pozzolanic activities. Prior studies however, have failed to identify the effects of sonicated SCMs on hydration and more importantly, the effects of the direct application of ultrasound on the hydration of cementitious materials.

It is widely accepted that the Portland cement (PC) hydration process (which involves the transformation of anhydrous to hydrate phases) involves a complex dissolution-precipitation process (Taylor, H.F.W., 1997). Throughout hydration, the main constituents of PC react with water to form various hydrates such as calcium silicate hydrates (C-S-H), portlandite and appreciable amounts of AFt and AFm phases of which ettringite and calcium monosulphoaluminate or calcium monocarboaluminate are the most predominant phases (Juilland et al., 2010; Taylor, H.F.W., 1997). The elemental characterisation of the cement pore solution composition provides insight into hydration processes and understanding the associated nature of the assemblage of solid phases and their levels of saturation at various hydration times. Fundamentally, the quantification of the elements in cement pore solution is a powerful approach to understanding the thermodynamics and kinetics of cement hydration as well as predicting concrete durability (Hooton et al., 2010; Rothstein et al., 2002). Accordingly, the study of pore solution composition should have priority over other approaches to understand the underlying effects of insonation on cement hydration.

To address the present gap, the identification of underlying mechanisms in which ultrasound irradiation can affect the hydration kinetics of cementitious systems could be a priority. In this regard, it is important to understand the effects of PUS on the homogenising and dispersion of particles in cementitious materials and also the crystallisation and precipitation (nucleation and crystal growth) processes of different hydration phases in a cementitious system. Furthermore, the degassing effect of PUS could potentially remove the entrapped air voids, thus changing and controlling both the mechanical and transport properties of cementitious materials systems.

A substantial study of cement suspensions subjected to a direct application of ultrasound was reported by Peters (2017). However, this was limited to an inductively coupled plasma optical emission spectrometry (ICP-OES) analysis of the calcium and silicon ions concentration on diluted tricalcium silicate (C_3S). Her results indicated that PUS accelerates the kinetics of alite hydration but does not change the reaction path. Acoustic cavitation was the suggested mechanism by which PUS enhanced the hydration. It was hypothesised that the resulting increase in mass transfer and localised erosion effects improved the precipitation of very early C-S-H phases, providing unwrapped surfaces of C_3S grain and additional nucleation sites for more C-

S-H growth. In addition to undertaking the experiment on a simplified system of hydration, the analysis was carried out at one ultrasound power/frequency and over a few hydration times. Also, her research failed to report the details of the method used for the analysis and the proper accounting for the matrix effects. These together with a detailed analysis of the spectral wavelengths were not provided.

The effect of ultrasound on the compressive strength of mortars obtained from two different types of mix was also investigated by Peters (2017). The chosen mortars had a ratio of aggregate to cement of 1:1 which is lower than conventional mortar mixes (normally with ratio of 3:1). The PUS application was shown to increase the very early age compressive strength of the mortars (during the first 24 hours of curing) compared with the non-sonicated samples. The observed enhancements were referred to the acceleration of alite hydration plus the de-airing effect (Peters, 2017). However, that study failed to provide a comprehensive understanding of the underlying development of these mechanical properties for PC mortars at either early or long-term ages. Additionally, there was no explanation for the differences between the results of the two mixing procedures. In Peters' study (2017), the ultrasonic treatment was carried out at only one PUS power density/frequency in which the arrangement for the ultrasonic delivery was a probe-based set-up. This led to a significant rise in temperature in the high energy cavitation zone generated close to the tip of the probe of either the cement suspension or the mixed mortar.

1.2. *Methodology*

To address the present gap, this work provides a comprehensive investigation of the composition and development of the aqueous phase in cement pastes with two water-to-cement ratios (w/c) subjected to ultrasound irradiation just after mixing. With this regard, power ultrasound is applied to the fresh cement paste and mortar mixes, making it a direct treatment with acoustic sonication. To understand underlaying effects of ultrasound, this work mainly deals with examining the pure Portland cement systems rather than blended cementitious materials systems which can be more complex when there is still a serious lack of knowledge on interaction of ultrasound application in this field. The study presents a robust analysis method developed to quantify major elements in pore solutions of ultrasonicated PC pastes. Additionally, hydrate

assemblages were identified by XRD. A semi-quantification of important components was also performed using the data obtained by the thermogravimetric analysis (TGA/DTG), particularly for the identification of X-ray amorphous hydrates, such as aluminium hydroxide.. In this regard, this study outlines features that have not been previously examined. In addition, the setting characteristics are discussed of a PC system subjected to PUS.

The present work also explores the effects of ultrasonic treatment on the progress of cement paste hydration by an evaluation of chemical shrinkage and the compressive and flexural strength development of PC mortars. The evolution of chemical shrinkage was measured precisely with a self-developed automated vision inspection system. Mechanical properties were studied of both directly sonicated mortars and mortars obtained from sonicated cement pastes at two ultrasound intensities and irradiation times. The potential effects of ultrasound on the modification of cement paste and the interface between the bulk cement paste and the aggregates were also discussed and assessed by microstructural studies.

Overall, the lack of detailed understanding about the effects of ultrasound on the PC systems encouraged the researcher to extend the breath of our current knowledge on this promising topic.

2. Research aim and objectives

The work presented here aims to study the effects of power ultrasound on PC systems to obtain a generic understanding of the changes in particle size distribution, pore solution and kinetics of hydration when ultrasonic irradiation is directly applied into such systems. In this regard, the objectives are:

- To research into a comprehensive investigation on the composition and evolution of the aqueous phase in PC pastes subjected to ultrasound irradiation just after mixing, by the inductively coupled plasma optical emission spectrometry (ICP-OES) technique.
- To study the effects of three different ultrasonic frequency/power densities on two cement pastes with w/c of 0.50 and 0.80.

- To study a robust ICP-OES method properly developed to quantify Ca, K, Na, and S as the high-concentration analytes, and Al, Fe, Mg, and Si as the low-concentration analytes, with a high accuracy, in PC pore fluids extracted from pastes treated by ultrasound.
- To identify the hydrate assemblages by XRD and a semi quantification of feasible components is given using the data obtained by the thermogravimetric analysis (TGA/DTG).
- To examine the setting time of a PC system subjected to PUS.
- To evaluate the extent of hydration in PC paste (w/c = 0.50) subjected to ultrasound using a self-developed automated set-up to measure the chemical shrinkage of cement paste.
- To explore the mechanical performance of PC mortars treated by ultrasonic processing by measurement of the compressive and flexural strength development at an early age and long-term hydration.
- To examine microstructural analysis of sonicated hardened cement paste and the interface between the aggregates and the bulk cement paste using scanning electron microscopy and energy dispersive X-ray spectroscopy.

The main points to be elucidated in this study are:

- How does sonication change the particle size distribution of PC?
- Can ultrasound affect the PC pore solution compositions through early age and long-term cement hydration?
- Can ultrasound affect the hydration products and the extent of hydration in PC systems with different free water available for cement hydration?
- How are the mechanical properties of cement-based composites affected by the direct application of ultrasonic irradiation?

3. Thesis outline

The main scope of this thesis is understanding the effects of directly applying ultrasound to PC systems. The main focus is a pure PC system mixed at w/c = 0.50, of which the pore solution

compositions and hydration products are thoroughly examined. Then, the efficacy of ultrasound in a higher water to cement ratio (0.80) is investigated. The reason for studying such a high w/c (0.80) is to examine whether power ultrasound effects will be significantly changed when there is more free water available in the paste system for occurring ultrasonic cavitation. The progress of hydration in an ultrasonicated cement paste is the next topic to be explored. To obtain a deep understanding about the effects of ultrasound on the mechanical properties of the cement composites subjected to PUS, compressive and flexural strength development tests were carried out on the mortar samples. The results were further interpreted using the microstructural analysis of hardened cement paste and the interfacial transition zone between the aggregates and the bulk cement paste in mortars.

Chapter 2 reviews the fundamentals of power ultrasound and its applications, with an emphasis on the effects of acoustic cavitation on sonocrystallisation and its application in cement-based materials. Accordingly, some hypotheses are put forward to propose the mechanisms that ultrasound can affect the cement hydration. The most relevant researches in the field of cement-based materials are also surveyed. Furthermore, studies undertaken on the subject of ultrasound application to pure PC system and the SCMs used in cement-based systems are critically appraised. Finally, perspectives are suggested on the potential research needed to obtain a fundamental understanding of the power ultrasound interactions in cementitious materials.

Chapter 3 describes the methods, materials and the experimental set up used in this work. The details of the self-developed set-up for the measurement of chemical shrinkage as well as its accuracy and precision evaluation are given in this chapter.

Chapter 4 firstly reports the effects of sonication on the particle distribution of PC dispersed in both isopropanol and aqueous medium. Then, the effects of ultrasound on a pure PC system mixed at w/c = 0.5 and w/c = 0.80 are delineated and discussed by providing the evidence obtained from the study of the pore solution and the main hydrates. Changes in the setting times of the cement paste subjected to ultrasound are also reported.

Chapter 5 first outlines the extent of PC paste hydration after applying ultrasound at various power densities, which is investigated by the measurement of chemical shrinkage. Subsequently, the development of the mechanical properties of mortar specimens cast by two different methods

of ultrasonication is evaluated (the sonication of mortars and mortars made with sonicated paste) . The results of the compressive and flexural strengths at early age and long-term curing ages are provided. Finally, the microstructural studies of cement paste and mortar samples are featured.

Chapter 6 presents and discusses the main conclusions deduced from this research and suggests some lines of investigation.

4. References

Askarinejad, A., Pourkhorshidi, A. R., and Parhizkar, T. (2012). Evaluation the pozzolanic reactivity of sonochemically fabricated nano natural pozzolan. *Ultrasonics Sonochemistry*, 19(1):119–124.

Hooton, R., Thomas, M., and Ramlochan, T. (2010). Use of pore solution analysis in design for concrete durability. *Advances in Cement Research*, 22(4):203–210.

Juilland, P., Gallucci, E., Flatt, R., and Scrivener, K. (2010). Dissolution theory applied to the induction period in alite hydration. *Cement and Concrete Research*, 40(6):831–844.

Lindley, J. and Mason, T. J. (1987). Sonochemistry. Part 2-Synthetic applications. *Chemical Society Reviews*, 16:275–311.

Lorimer, J. P. and Mason, T. J. (1987). Sonochemistry. Part 1-The physical aspects. *Chemical Society Reviews*, 16:239–274.

Martinez-Velandia, D., Paya, J., Monzo, J., and Borrachero, M. V. (2008). Granulometric activation of densified silica fume (csf) by sonication. *Advances in Cement Research*, 20(3):129–135.

Martinez-Velandia, D., Paya, J., Monzo, J., and Borrachero, M. V. (2011). Effect of sonication on the reactivity of silica fume in Portland cement mortars. *Advances in Cement Research*, 23(1):23–31.

Mason, T. J. (1999). *Sonochemistry*. Oxford University Press.

Mason, T. J. (2003). Sonochemistry and sonoprocessing: the link, the trends and (probably) the future. *Ultrasonics Sonochemistry*, 10(4):175–179.

Mason, T. J. and Lorimer, J. P. (2002). *Applied Sonochemistry: Uses of Power Ultrasound in Chemistry and Processing*. Wiley-VCH.

Mason, T. J. and Peters, D. (2002). *Practical Sonochemistry, Power Ultrasound Uses and Applications*. Woodhead Publishing, 2nd edition.

Peters, S. (2017). *The Influence of Power Ultrasound on Setting and Strength Development of Cement Suspensions*. PhD thesis, Bauhaus-University Weimar.

Rodriguez, E. D., Bernal, S. A., Provis, J. L., Paya, J., Monzo, J. M., and Maria, V. B. (2012a). Structure of Portland cement pastes blended with sonicated silica fume. *Journal of Materials in Civil Engineering*, 24(10):1295–1304.

Rodriguez, E. D., Soriano, L., Paya, J., Borrachero, M. V., and Monzo, J. M. (2012b). Increase of the reactivity of densified silica fume by sonication treatment. *Ultrasonics Sonochemistry*, 19(5):1099–1107.

Rothstein, D., Thomas, J. J., Christensen, B. J., and Jennings, H. M. (2002). Solubility behavior of Ca-, S-, Al-, and Si-bearing solid phases in Portland cement pore solutions as a function of hydration time. *Cement and Concrete Research*, 32(10):1663 – 1671.

Taylor, H.F.W. (1997). *Cement chemistry, 2nd edition*. Thomas Telford Publishing, 2nd edition.

2

Chapter 2: Application of Power Ultrasound to Cementitious Materials: Advances, Issues and Perspectives

Synopsis [1]

A handful of studies have investigated the mechanisms by which ultrasound acts in cement-based systems, but little is known about this promising field. This chapter outlines the possible mechanisms involved in the effects of PUS as a method to promote the cement hydration kinetics of Portland cement and binary blends. It also reviews and analyses previous research conducted mostly on the dispersing effects of PUS on the enhancement of the pozzolanic reactivity of SCMs in cementitious systems. This review concludes with some perspectives on research needed to gain a fundamental understanding of this emerging field and explain which areas will be focused on in this work, then covered in the next chapters.

1. Introduction

Traditional Portland cement-based concrete has provided the foundation for the built environment for almost 200 years. The focus of modern concrete structures is high performance, design for long lifetime and to be aesthetically pleasing. According to the Mineral Products Association (MPA) cement fact sheet (Taylor, 2015), however, “the demands for sustainable development have placed a huge responsibility on the construction sector to continually improve existing processes, products and practices, and to innovate in order to reduce both energy used in service and embodied energy in products together with emission of greenhouse gases during manufacture”.

[1] **Main parts of this chapter have been published as**: Ganjian, E., Ehsani, A., Mason, T. J., Tyrer, M. (2018) Application of power ultrasound to cementitious materials: Advances, issues and perspectives. *Materials & Design*, 160:503-513

The kinetic mechanisms of ordinary Portland cement (OPC) hydration and the complex, interdependent chemical and microstructural phenomena which control the characterisation of cement hydration products have not been completely understood. However, major efforts have been made for both the sustainable use of OPC in cement-based composites and the enhancement of its perceived performance.

Replacing part of the Portland cement clinker represents a viable solution to reduce carbon footprint, either by using alternative supplementary cementitious materials (SCMs) like fly ash (PFA), ground granulated blast furnace slag (GGBS), silica fume (SF), calcined clays and natural pozzolans in blended cements, or by utilising SCMs separately as a partially substitute additive in mortar/concrete systems (Lothenbach et al., 2011). A few benefits have been investigated in cement-based materials incorporating SCMs, including an improvement in consistency and fresh concrete properties (Thomas, 2013a), decreased hydration heat evolution (Thomas, 2013b), improved mechanical/structural properties such as long-term strength development (Hassan et al., 2000), enhanced durability (Irassar et al., 1996; Papadakis, 2000; Xu et al., 1995) and reduced autogenous shrinkage (Akkaya et al., 2007). However, the use of SCMs often causes longer setting times (Edson et al., 2008), lower early strength development (Hassan et al., 2000) and an increase in drying shrinkage (Akkaya et al., 2007; Hu et al., 2017).

Several methodologies have been studied to overcome these drawbacks and improve the efficiency of OPC and SCMs in cementitious systems which include three main methods: thermal, mechanical, and chemical. The heat treatment i.e. thermal activation can be divided into calcination (Almenares et al., 2017; Alujas et al., 2015; Mielenz et al., 1950) and elevated temperature curing (Aldea et al., 2000). The former has been found highly contingent on limiting factors. These include the reactivity of the amorphous phases, the decrease of specific surface area and soluble fraction and also the increase of crystalline fraction. The latter often causes lower strength development in cementitious materials incorporating SCMs at later ages (Shi, 2001; Shi and Day, 2001).

Mechanical methods have been extensively utilised to enhance the pozzolanic activity of some types of SCMs by grinding them into ultrafine powders for a prolonged period of time. This decreases the particle size distribution and increases the dissolution rate of the pozzolans, which

accelerates the pozzolanic reaction rate and consequently the strength development of concrete containing SCMs. However, controversial results have also been obtained regarding the correlation between the fixed free portlandite (CH) and the pozzolans' surface areas as well as insignificant ultimate strength improvement (Alexander, 1960; Shi, 2001; Shi and Day, 2001; Walker and Pavia, 2011). Moreover, the finer the particles, the more chance of aggregation and agglomeration due to the interaction forces between the particles inside the matrix.

The utilisation of chemical accelerators (like $CaCl_2$) to accelerate early-age cement hydration has also been investigated. The chloride ions however, adversely interfere with various hydration products and could also cause the depassivation of the steel in reinforced concrete triggering corrosion and cracking (Angst et al., 2009). Other types of chemicals have also been identified that have shortcomings for the long-term strength and durability of cement-based composites (Lee et al., 2009; Prudencio, 1998). The surface treatment of GGBS with chemical activator(s) (Wang et al., 1995) changes the properties of their surface layers, which accelerates the rate of pozzolanic reactions, enhances the strength development rate, and increases the ultimate strength of cement-based composites. Nevertheless, some of the most effective chemicals such as caustic alkalis are not cost effective, user/eco-friendly nor practically feasible (Davidovits, 2008).

Furthermore, concretes subjected to high temperature curing at early ages attain higher early-age compressive and splitting tensile strengths but significantly lower long-term strengths and elastic modulus than those subjected to normal temperatures (Kim et al., 2002). Whilst the addition of heterogenous nucleation sites (with added synthetic C-S-H particles or limestone) were also found to be effective on cement hydration acceleration (Alizadeh et al., 2009), this approach is still very expensive and has limited practicality.

Power ultrasound has been used over a wide range of applications in materials science, from surface cleaning and degassing, to particle dispersion and the production of nanostructures. Although some of these applications have been investigated extensively, others are yet to be reviewed and hold new, exciting possibilities, such as the use of PUS to control the properties and performance of cementitious materials and enhance the properties of SCMs incorporating composites. Several ultrasound techniques have been used to characterise the setting and

hardening processes of cement pastes, mortar and concrete, providing an overall evaluation of mechanical strength, porosity, permeability and durability of cementitious composites (Salvador et al., 2017). A few studies have focused on the effects of power ultrasound on the performance of early age hydration reactions in cementitious matrices, as well as composites incorporating SCMs. This chapter presents a review of the literature on the effects of PUS on the early age hydration kinetics of PC and binary blends, together with some of the underlying mechanisms involved.

2. Ultrasonication

2.1. *Background*

The first reports on the chemical and biological effects of ultrasound were published in the early 20th century (Harvey, 1930; Harvey and Loomis, 1929; Richards and Loomis, 1927). However, it took many years for the industry to adopt ultrasound as a more general energy source to drive a range of chemical and processing operations. In 1972, Neppiras reviewed the main applications of power ultrasound (PUS) in industry; which at that time was referred to as macrosonics (1972). The major applications lay in cleaning, plastic and metal welding, wire and tube-drawing, ultrasonic machining, teeth descaling and the extraction of chemicals from plants. He also listed some “minor applications” which have since become rather more important. These included shaking and sieving (Newman et al., 1997), electrolytic processes (Yeager and Hovorka, 1953), crystallisation (Luque de Castro and Priego-Capote, 2007), emulsification (Gaikwad and Pandit, 2008), dispersion (Nguyen et al., 2014), depolymerisation (Kruus et al., 1988), degassing, the production of aerosols, drying, defoaming and sterilisation (Mason, 2003).

The various strands of the applications of power ultrasound in the chemistry and material processing fields were later to be brought together under the umbrella title of sonochemistry. The first ever international conference on sonochemistry was held at Warwick University in the UK in April 1986 and sonochemistry was further established as a subject in its own right with the publication of two major reviews (Lindley and Mason, 1987; Lorimer and Mason, 1987).

2.2. *Conventional power ultrasound*

Conventional power ultrasound is used in the frequency range between 20 kHz and 100 kHz (Fig. 2.1) and is able to generate acoustic cavitation in a liquid. Cavitation is the driving force for sonochemical reactions. PUS is generally at a lower frequency range than that used for diagnostic ultrasound, which is in the MHz range.

The most common way of generating ultrasound is by exposing a piezoelectric ceramic transducer to a high frequency alternating electric current. Under the influence of this electrical field the piezoelectric material expands and contracts producing a high frequency mechanical vibration. This vibrational motion can be transferred into and through any liquid medium, inducing cavitation and the associated physical and chemicals effects (Mason, 1999; Mason and Lorimer, 2002; Mason and Peters, 2002).

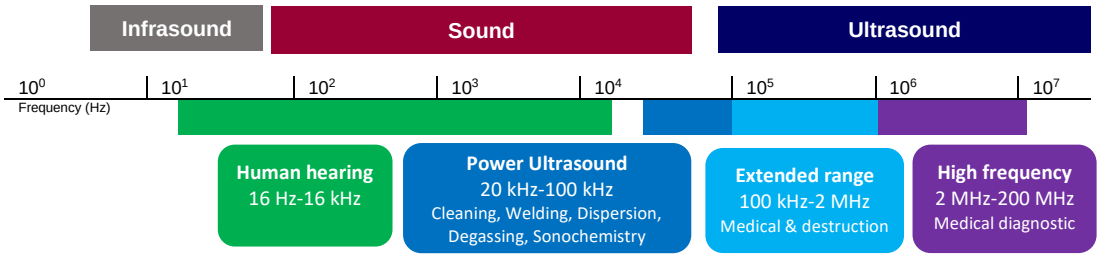

Fig. 2.1. Illustration of the frequency spectrum from infrasound to ultrasound

2.3. *Acoustic cavitation phenomena and cement-based materials*

The chemical and physical effects of PUS in a liquid medium have been universally acknowledged to be the consequences of acoustic cavitation. This is the formation, growth, and collapse of gaseous microbubbles in the liquid phase (Fig. 2.2). Ultrasound is transmitted through a material in the same way as any sound wave via a series of compression and rarefaction cycles. During rarefaction, provided that the negative pressure is strong enough to overcome the intermolecular forces binding the fluid, the fluid is literally torn apart producing tiny cavities (microbubbles) throughout the medium. In the succeeding compression cycle if cavities were enclosing a vacuum, they would collapse almost instantaneously. However, during cavity formation a small amount of gas or vapour is drawn in from the surrounding liquid. As a result, the succeeding compression cycle may not totally collapse the bubbles and so they will grow

slightly larger in the next rarefaction cycle with a further intake of gas and vapour. The process is known as rectified diffusion. The bubble will not grow indefinitely, there will be an equilibrium size for any bubble in an acoustic field (this depends on frequency). Some bubbles will continue to resonate in this stable state but many will become unstable and collapse, generating microspots of extreme conditions of temperature and pressure. Based on the theory which has been put forward to explain the energy release involved with cavitation, each cavitation bubble acts as a localised microreactor which generates instantaneous temperatures and pressures on collapse of several thousand degrees and over one thousand atmospheres respectively (Mason, 1999). This phenomenon has led to the most popular and widely accepted theory regarding the explanation of the effects of cavitation collapse the “hot spot” theory (Fitzgerald et al., 1956). The implosion of cavitation bubbles results in the formation of “shock waves” (strong pressure waves) and “jet streams” inducing a “microstreaming” effect, causing jets of liquid to be directed to the solid surface of any material suspended in the liquid and resulting in particle size reduction, particle collisions and surface activation/cleaning. The release of shock waves and the effect of microstreaming together may also cause intensive shear forces inside the liquid medium (Mason and Peters, 2002). It is these effects which make PUS attractive to the cement-based materials industry. Here, the systems are heterogeneous and material hydration is important during the transformation of a fluid suspension into a solid at room temperature with minimal bulk volume change.

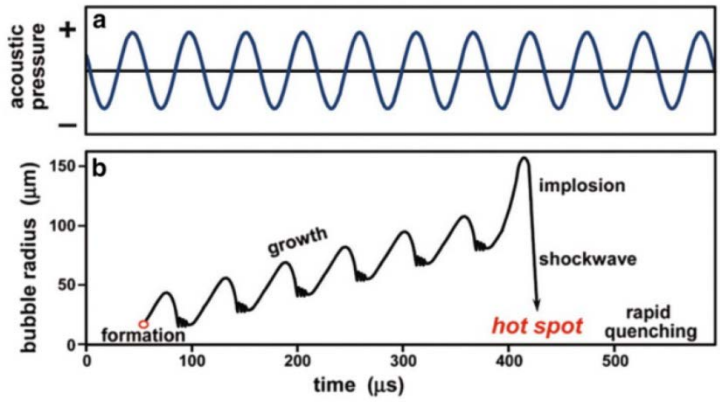

Fig. 2.2. Schematic illustration of the process of acoustic cavitation: the formation, growth and implosive collapse of bubbles in a liquid irradiated with high intensity ultrasound. Reproduced courtesy of Xu et al. (2013).

3. Mechanisms of Portland cement hydration

Many modelling and experimental works explain the phenomena occurring during cement clicker hydration and that of blended systems. It is universally hypothesised that the Portland cement hydration in which transformation of anhydrous to hydrate phases occurs is basically a dissolution-precipitation process (Scrivener and Nonat, 2011). It has been found that due to the congruently charge balanced dissolution of all the anhydrous phases, crystal structure would preclude the unrestricted dissolution of certain phases without others. So, during the hydration progress, the potential hydration products would intrinsically have a higher stability than the anhydrous phases (Garrault et al., 2006; Garrault et al., 2005; Scrivener and Nonat, 2011).

The hydration of tricalcium silicate (C_3S) referred to as alite, as the most important constituent of Portland cement clinker (accounting for 50-70% by mass) has been extensively investigated. Since its reaction kinetics mostly resemble those of Portland cement, alite is being considered to serve as a reliable model in studying Portland cement hydration (Damidot et al., 1990). The principal product of alite hydration is calcium-silicate-hydrates (C-S-H), a nearly amorphous phase, which primarily contributes to the strength and volume stability in cementitious materials (Taylor, 1997). Classical theories of hydration indicated that the surface of cement grains begins to be covered by nuclei of the C-S-H gel formed and grown within a few seconds after initially mixing with water. Remaining stable only in the induction period (which occurs because the size and number of growing regions are small); this impermeable metastable C-S-H phase has a greater solubility than C-S-H and a lower solubility than alite. Other researchers found two types of C-S-H during the initial stages of hydration including low density C-S-H and high density C-S-H (Singh et al., 2015; Taylor, 1997). However, according to the most leading theory known as the nucleation theory, it has been postulated that the induction period is controlled by the changes in ion concentration in the solution rather than the presence of inhibiting hydration layers formed on the surface of alite grains. Once the alite grains become covered with hydration products, the rate of hydration becomes controlled by the rate of diffusion through this layer and decreases slowly for weeks or months.

The theory proposed that the hydration of alite is mostly controlled by solution controlled dissolution/diffusion and nucleation with densifying growth mechanisms (Table 2.1). According to

the nucleation theory, the rate of hydration during the induction period is dominated by nucleation and growth of C-S-H formed at the early stage and this period ends when the growth of C-S-H starts. During early stages of hydration, the primary hydrates precipitate on the surface of alite, but not as a continuous membrane (Fig. 2.3) (Bullard et al., 2011; Kumar et al., 2012; Scrivener and Nonat, 2011; Singh et al., 2015; Thomas et al., 2009).

Table 2.1. Identified phenomena controlling early hydration kinetics, summarized from (Bullard et al., 2011; Kumar et al., 2012).

Mechanism	Overall kinetic behaviour	Reaction stage
Dissolution	dissolving alite grain and releasing ions into the pore solution	Up to the end of the induction period
Diffusion	transport of solution components through the pore volume of cement paste	
Nucleation	initiator of precipitation of solids heterogeneously on solid surface or homogenously in solution	Up to main heat evolution peak
Growth	surface attachment, incorporation of molecular units into the structure of crystalline or amorphous solids	

It has also been postulated that the nucleation/growth mechanism might be a continuous process, implying that existing C-S-H nanostructures stimulate the formation and expansion of new products outward from the original nucleation site (Thomas et al., 2009). Overall, it seems that crystallisation plays a significant role in cement-based materials hydration, controlling early and long-term properties of cementitious composites.

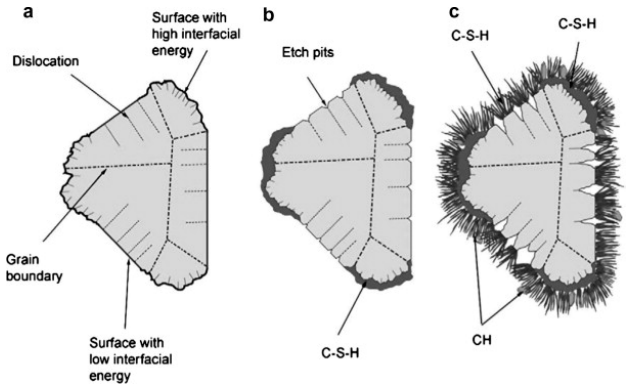

Fig. 2.3. Schematic representation of alite grain hydration at early stages (a) an anhydrous alite grain (b) the alite grain surface subjected to water with C-S-H formed, along with etch pits (dissolution voids) formation (c) finally stable nuclei of C-S-H and CH initiate growing, Reprinted courtesy of (Juilland et al., 2010)

4. Effect of PUS on crystallisation of inorganic materials

Power ultrasound has proved to be extremely useful in crystallisation processes. It serves a number of roles in the initiation of seeding and subsequent crystal formation and growth. This may be due to cavitation bubbles acting as nuclei for crystal growth or by the disruption of seeds/nuclei already present within the medium thus increasing the number of nuclei present in the solution. These effects have been examined in cementitious system by the addition of synthetic C-S-H (Alizadeh et al., 2009) or nanomaterials (Singh et al., 2016). The Insonation of gels formed from sodium aluminate and sodium silicate leads to increases in the nucleation and crystallisation rates for the formation of zeolites by up to 6-fold and 3-fold respectively at 85°C (Mason et al., 1989). The zeolite formed in the ultrasonic field shows reduced particle size and a narrower size distribution compared with those produced by conventional methodology. It was suggested that the reduction in particle size was due to an increase in the number of crystallisation nuclei and their dispersion by the acoustic field. The rate of nucleation was shown to increase with increasing irradiation intensity and this was also accompanied by a reduction in particle size (Askari et al., 2013; Mason et al., 1989).

One of the most relevant research findings relating to the effects of PUS on crystallisation involving cementitious materials is found in the studies carried out on the precipitation of calcium carbonate by Nishida (2004). He examined the influence of ultrasonic irradiation on the precipitation rate of a supersaturated solution of calcium carbonate ($CaCO_3$). He observed that PUS accelerated the precipitation of $CaCO_3$. He identified macrostreaming as a dominant factor of this phenomena rather than microstreaming which is generally known as one of major physical effects of cavitation. In a newer study, Boels et al. (2010) investigated the seeded crystallisation of calcite affected by the PUS. The measurement of volumetric crystal growth rate of calcite seed crystals showed that the ultrasonic irradiation considerably increased the crystallisation rate and surface area available for crystal growth and also caused disruption of conglomerates of single crystals.

Other experiments were carried out on salts like Barium sulphate ($BaSO_4$) (Guo et al., 2006a; Guo et al., 2006b) and Potassium sulphate (K_2SO_4) (Lyczko et al., 2002). Guo et al (2006a; 2006b) studied the effect of ultrasound on crystallisation and the homogeneous nucleation of

$BaSO_4$ and concluded that the induction time significantly decreased with increasing PUS energy due to the accelerated diffusion process. Likewise, the effect of ultrasound on primary nucleation of K_2SO_4 investigated by Lyczko et al. (2002) showed a significant reduction in induction time and accordingly the nucleation mechanism enhancement. Promotion of the dissolution-precipitation of the aluminium hydroxide-water system affected by the moderate sonication was documented by Enomoto et al. (1994). A study (Li et al., 2006) of the influence of PUS in controlling the supersaturation, nucleation and crystal growth during the acid–base reaction crystallisation showed the effectiveness of mixing, deagglomeration, reduction of both the induction period and metastable zone width of the crystallisation and also the modulation of the crystal size and size distribution. Similarly, the potential of PUS on controlling the crystallisation process of a type of antibiotics (roxithromycin) through the inducing accelerated nucleation, reduction of the induction time, suppressing agglomeration and changing crystal habit were investigated by Gou et al. (2005).

Overall, the studies completed on the effect of PUS on the precipitation of inorganic materials generally suggest that ultrasonication provides enhanced dissolution-precipitation, and consequently more nucleation sites and surface area for a more efficient growth of crystals. Therefore, this may be a promising approach for promoting the crystallisation properties of hydration products in cementitious materials.

5. Influence of PUS on cementitious systems

5.1. *Challenges in cement-based systems*

It has been recognised that aggregation or agglomeration can be induced between particles due to the interaction forces between particles of colloidal/suspension systems (including the electrical double layer, van der Waals, Born, hydration and steric forces) (Elimelech et al., 1995). During these processes, primary particles stick to each other, and spontaneously form irregular particle clusters, flocs, or aggregates held together by these weak forces that can be separated. So, large irregular agglomerates embedded in cement-based composites can significantly reduce the effectiveness of clinker cement and SCMs to participate in hydration as well as the pozzolanic reaction and consequently improve all those positive properties which pozzolans can bring to them. In terms of microstructural chemical reactions, the presence of SCM agglomerates leads to the formation of a C-S-H with a much higher calcium to silicate (Ca/Si) molar ratio than is usual in cementitious composites (Diamond et al., 2004; Rodriguez et al., 2012b). Generally, in cement chemistry and concrete technology, there are several challenges associated with the hydration of Portland cement and SCMs particles which might be approached by PUS application:

- Aggregation/agglomeration of cementitious materials; controlling packing density and hydration rate.
- Pore structure of hardened cement-based materials which significantly affects the mechanical properties and durability (Kumar and Bhattacharjee, 2003).
- Penetration/diffusion (dissolution) of anhydrous phases in the fluid suspension of cementitious materials during the hydration process occurs at the rapid slowdown in reaction stage at the beginning of hydration leading to a period of slow reaction known as induction time and continues through the growth process after the acceleration period; controlling early age and long term properties of cementitious materials (Scrivener and Nonat, 2011; Taylor, 1997).
- Hydration rate after acceleration period (growth of hydration products) appears to be even slower compared to crystalline hydrates, most probably due to the lack of available surface area and space for hydration; controlling the long-term properties of cementitious materials (Scrivener and Nonat, 2011).

- Hydration products can act as deposit/cover on the cement/SCMs particles and hinder further reactions (Scrivener and Nonat, 2011).
- Complex hydration kinetics; this appears to make each of the phases hydrate at a rate different from the others and are also affected in presence of each other (Scrivener and Nonat, 2011).

5.2. *Postulated mechanisms concerning the phenomenon*

It is thought that the most promising effects of PUS will relate to the homogenising and dispersion of cementitious particles through a colloidal cement system, leading to the deagglomeration of particle clusters. This will enhance the effectiveness of SCMs in the secondary hydration reactions. The intensity of cavitational effects which depends on the size and type of material presented in the medium, can lead to mechanical disaggregation and dispersion of loosely held clusters, the removal of surface coatings by abrasion, and enhance mass transfer to the surface.

Power ultrasound might also be influential on the crystallisation process of different hydration phases in a cementitious system. Furthermore, exfoliation of Portland cement and the anhydrous and hydrated phases of SCMs through the generation of surface damages triggered by the effects of cavitation bubble collapse might control the rate of hydration products and ultimately the properties of cementitious composites. The key mechanical effects of PUS offer an opportunity to overcome the types of challenges associated with cementitious materials outlined in Table 2.2.

In recent years, the application of ultrasonic treatment to disperse different types of powder and nanoparticles in an aqueous and non-aqueous solution as well as high viscosity polymer solution has been explored (Nguyen et al., 2014). Despite the limited efforts to characterise the ultrasonic dispersion of densified silica fume and apply it to cementitious systems (as well as one study carried out concerning the characterisation of the PUS effect on hydration and fluidity of cement/slag blended suspension), still relatively little is known about the effects of PUS on Portland cement and SCMs incorporated in cementitious systems. This review will focus on research carried out on the capability of PUS to improve the properties of cementitious materials. First, a discussion will be made on the potential beneficial effects of cavitation on cementitious materials, followed by some comments on the limited number of results published related to practical applications of PUS to Portland cement and SCMs.

Table 2.2. Proposed physical/mechanical effects of ultrasound cavitation tailored for cementitious materials

Systems	Postulated/investigated effects of PUS	Expected results in cementitious materials
Homogenous (*in absence of pre-existing crystal; liquid bulk*)	Enhanced mass and heat transfer from and onto the surface due to microstreaming (Luque de Castro and Priego-Capote, 2007; Mason and Peters, 2002; Riera et al., 2004)	Intensification/accelerated transportation of anhydrous cementitious materials and hydration phases/products
	Degassing of suspension (Mason and Peters, 2002)	Highly critical to pore structure of cement-based materials systems mainly air entrapped voids and air entrained voids (generated by air entrained agents) controlling both mechanical and transport properties
	Enhancing crystallization/precipitation (technically known as "sonocrystallisation") (Luque de Castro and Priego-Capote, 2007)	Reduction of the induction time Enhancing homogenous nucleation and growth of stable hydration products Reduction of metastable zone width
Heterogeneous (*in presence of wall or existing crystals; liquid-solid solution*)	Breaking up/erosion of the surface structure (surface damages) due to shock waves and/or jet streams (Amara et al., 2001; Luque de Castro and Priego-Capote, 2007; Mason and Peters, 2002)	Modifying the morphology of crystals/hydration products Allow penetration of phases entered in hydration reaction by affecting etch pits in the surface Release of hydration products from cementitious materials surfaces Allow penetration of particles already covered with hydration products by removal/release of formed hydration precipitates away
	Degradation of large solid particles due to shear forces induced by shock waves and microstreaming (Amara et al., 2001; Chatel and Colmenares, 2017; Luque de Castro and Priego-Capote, 2007; Mason, 1999; Mason and Peters, 2002)	Reduction of particle size and agglomeration Increase surface area of cement particles and SCMs Homogenising and Dispersion of anhydrous cementitious particles and hydrated phases
	High velocity collisions and accelerated motion of particles (Luque de Castro and Priego-Capote, 2007; Mason and Peters, 2002; Thompson and Doraiswamy, 2000)	More effective mass transfer, consequently intensification of those effects occur in homogenous systems
	Enhancing crystallization/precipitation (Luque de Castro and Priego-Capote, 2007)	Reduction of the induction time Enhancing heterogeneous nucleation and growth of stable hydration products Reduction of metastable zone width

5.3. *Parameters influencing the cavitation phenomena in cement-based materials*

It has been found that some external parameters have a great influence on cavitation as the most important phenomenon to induce sonochemical effects. Understanding these factors helps to provide condition in which the sonochemical effects are optimised. Some of the most influential factors affecting the sonochemical effects with regards to cement-based system are reviewed in Table 2.3.

Table 2.3. Review of some factors influencing the cavitation phenomena in cement-based materials

Parameters	Sonochemistry perspective	Cementitious materials perspective
Frequency	At higher frequencies, the rarefaction/compression cycle becomes shorter than the time required to permit the molecules to be pulled apart, making the cavitation difficult or impossible to achieve. Moreover, for a determined power level, the threshold in changing physical effects might be reached and so no further changes could be observed as a result of sonication. Frequencies usually opted for typical crystallisation fall in the range between 15 and 40 kHz which its variable was found to have the same influence on nucleation and growth (Richards and Loomis, 1927)	initiation of acoustic cavitation using combined low and high-frequency which might have substantial effects on the hydration crystallisation of cementitious materials.
Intensity (Power Input)	Whilst an increase in ultrasound intensity will provide an increase in the sonochemical effects, the barrier effect of larger and longer lived bubble formation to the transfer of acoustic energy, possibility of transducer material fracture and great loss in efficiency of power transfer from the source as a result of decoupling phenomena need to be considered (Luque de Castro and Priego-Capote, 2007; Richards and Loomis, 1927).	An increase in ultrasound power intensity is expected to cause heavier flow, enhanced mass transfer in the media and the driving force of crystallisation, leading to the higher the crystallisation rate.

Table 2.3. (Continued)

Temperature	Apart from a decrease in viscosity and surface tension, any increase in temperature will raise the vapour pressure of a medium and therefore will cause an easier cavitation with a less violent collapse. However, at higher temperatures, a large number of cavitation bubbles are generated because of the approaching solvent boiling point. Acting as a barrier to sound waves transmission, these will cushion the ultrasonic energy from the source	In the cementitious systems, the intensive increase and decrease in temperature will markedly accelerate and slow down the hydration rates, leading to a relatively fast and slow initial setting times, respectively, and adversely affected microstructure and hardening properties. Therefore, practical and technical considerations need to be taken when applying the PUS.
Gas bubbles	Dissolved gas and small gas bubbles in a fluid act as nuclei for cavitation, promoting cavitation and are then removed.	Degassing and defoaming characterisation of PUS is expected to be highly critical as the products of the hydration process consist of a pore system governing the properties of cement-based systems. The effect of PUS on the stability of entrained air bubbles has also needs to be understood.

6. Studies on the influence of PUS on cementitious materials

6.1. *Portland cement*

An experimental study performed by Rößler (2012) and Peters (2017) represents the first officially published experiment carried out on the influence of PUS on initial setting, hardening and hydration characterisation of Portland cement (CEM I 42.4R). In order to guarantee a uniformly continuous sonication until providing the required specific energy input, a flow-through cell sonication set-up equipped with a laboratory ultrasonic horn was utilised (UIP 1000hd, Hielscher, Germany). The set-up provided a constant frequency of 20 kHz and different amplitudes adjustable by a booster.

In the first part of the study, the research aimed to highlight the effect of PUS on setting and hardening of a cement suspension (with a w/c ratio of 0.37). The practical limitations regarding the use of PUS in concrete production, namely the initial setting time, temperature rise due to the ultrasound application and the minimal period of PUS treatment were considered. So, the optimal PUS parameters emerged to be 43µm (ultrasonic horn with front face diameter of 0.9 cm^2) and 75 J/mL for the PUS amplitude and specific energy input, respectively. The results of initial setting time demonstrated that ultrasound treatment shifts the initial setting time of cement paste to an earlier time. Moreover, the influence of PUS on cement hydration was evaluated by means of analysing the isothermal differential conduction calorimetry and the non-destructive ultrasonic P-wave velocity and microstructural study of cement suspension as well as the compressive strength development of mortars (Peters, 2017).

The results of isothermal heat release demonstrated that PUS accelerates the heat release rate limited to the hydration acceleration period, whereas the total heat release was unaffected by the PUS treatment (Fig. 2.4). Relying on the correlation between the P-wave velocity test results and the strength development of cementitious materials; it was deduced that an improved strength development of sonicated cement suspension limited to only the first 16 hours was most probably due to the accelerated cement hydration (Peters, 2017).

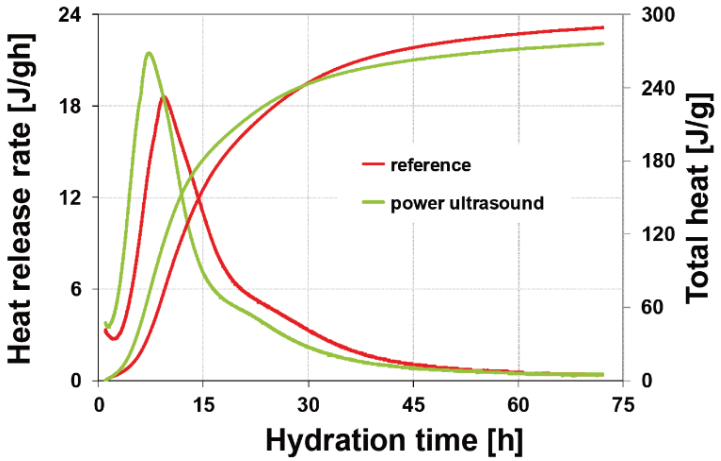

Fig. 2.4. Isothermal heat release rate and total heat of reference and sonicated cement suspension (w/c: 0.37 with 0.1 wt% SP) during first 72 hours of hydration, Reprinted courtesy of Peters (2017).

The enhanced compressive strength of mortars during the 24 hours of hydration as well as microstructure analysis of cement suspension (Fig. 2.5) underscored the PUS effectiveness on accelerating the cement hydration, confirming the results obtained from the hydration heat release and setting time examination (Peters, 2017).

Furthermore, in-depth investigations were performed on the characterisation of model substance hydration (synthesised alite) in order to evaluate primary (homogenous) and heterogeneous crystallisation and precipitation (nucleation and growth) of C-S-H phases. The former examination was conducted on clear Ca-Si solution and the latter was performed on diluted alite suspension. The results of electrical conductivity measurement and determination of Ca and Si ion concentration by the ICP-OES (Inductively Coupled Plasma-Optical Emission Spectroscopy) showed that PUS accelerates the kinetics of alite hydration but does not alter the reaction path. It was hypothesised that the mechanism of hydration acceleration facilitated by the ultrasound introduction would be dominated by the precipitation enhancement of very early C-S-H phases. Besides, it was postulated that the shock waves induced by the cavitation phenomenon is mostly responsible for increasing the particle collisions, leading to localised erosion effects and the removal of initial C-S-H precipitates away from alite surfaces. Consequently, not only do the alite grain surfaces remain unwrapped with C-S-H products, but also detached C-S-H precipitates provide additional sites for triggering more C-S-H phases growth. It was proposed that other PUS effects like hot spot and jet streams were accounted for a minor significance (Peters, 2017).

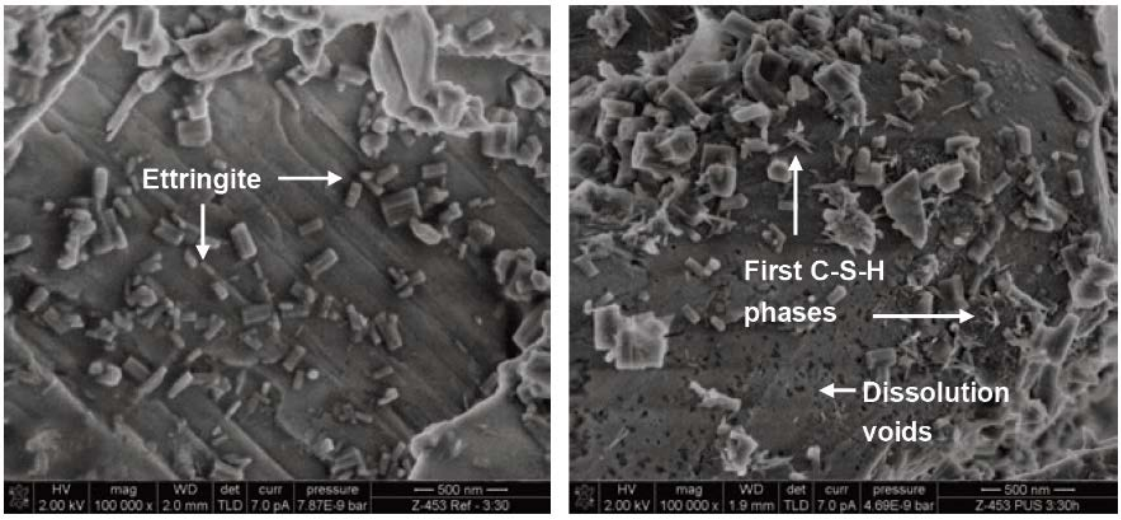

(a) 3 hours and 30 minutes hydration

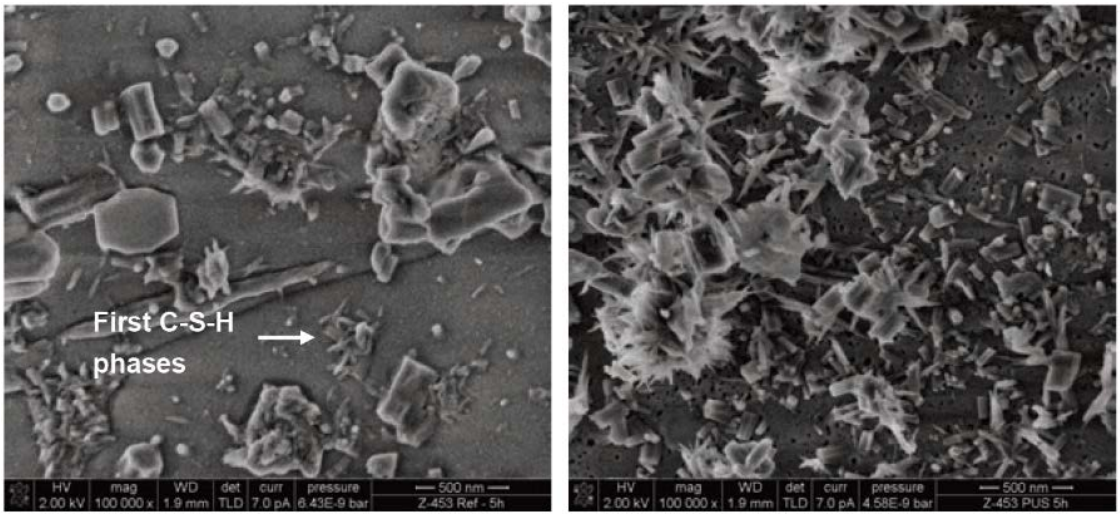

(b) 5 hours hydration

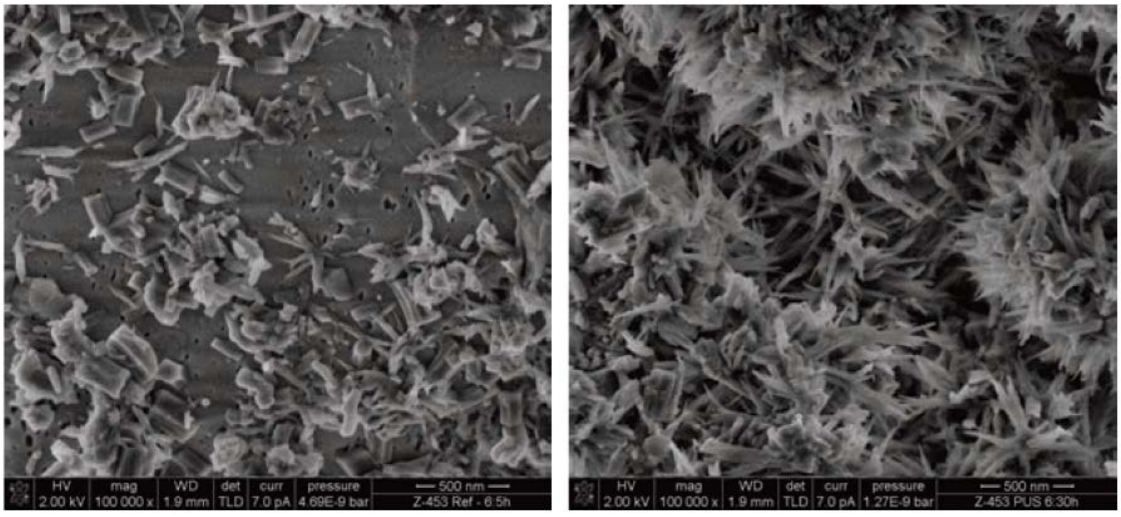

(c) 6 hours and 30 minutes hydration

Fig. 2.5. SEM micrographs of reference (left) and PUS treated (right) cement suspension microstructure (w/c: 0.37 with 0.1 wt% SP), Reprinted courtesy of Peters (2017).

The positive influence of PUS on fluidity and the generation of homogenous fresh cement paste was also confirmed by performing mini slump flow spreading time and V-funnel flow time examinations. Further observation was carried out to briefly characterise the hydration process of GGBS under the influence of PUS. Acceleration of GGBS blended cement hydration was deduced based on the initial setting time, compressive strength evaluation of mortars and isothermal heat release rate examination. Nevertheless, the isothermal heat calorimetry test on pure GGBS suspension incorporating CH showed that PUS application only slightly accelerates GGBS (Peters, 2017).

Recently, Resonance Acoustic mixing (RAM) technology that combines the principals of reciprocating movement agitator mixing and bubble acoustic micro-streaming mixing was employed by Vandenberg and Wille (2018) to evaluate its efficiency for mixing Ultra-high performance mortar. The results presented reduced flow and workability properties while improved mechanical properties in specimens mixed with RAM. Although an increase in hydration kinetics and change microstructural development of mixtures compared to a standard table paddle mixer were concluded, the study was not engaged to perform microstructural study and quantitative reasoning.

Overall, although some test results confirm the positive influence of PUS on cement hydration, some other examination results are not reflective of an entirely significant effect of hydration enhancement. More research, especially quantification of hydration is needed to gain a fundamental understanding about the mechanisms in which PUS affects cementitious systems.

6.2. *SCMs*

The mechanical effects of cavitation are already being used in generation of nanostructures and nanoparticles (Nguyen et al., 2014). These physical effects also have been postulated to provide a reduction in the size of densified or agglomerated particles by applying the forces of cavitation, breaking of agglomerates and aggregates. In this section, the studies performed to characterise the effects of PUS on SCMs have been overviewed.

It has been reported that silica fume as a SCM will significantly reduce both the interfacial transition zone between the aggregates and bulk cement paste and the deposition of a portlandite rim, resulting in improvement in fresh properties, mechanical strength and durability properties in

cement-based materials (Duval and Kadri, 1998; Nili and Ehsani, 2015; Nili et al., 2010; Toutanji and El-Korchi, 1995; Wong and Abdul Razak, 2005). However, the continuous interaction of individual spheres of silica fume particles promotes the formation of agglomerates. As in most silica-fume-bearing cementitious composites, the silica fume is introduced in its densified (agglomerated) form, and the agglomerates are likely to remain at least partly undispersed especially in normal concrete mixing (Diamond et al., 2004; Gapinski and Scanlon, 2006). This inhibits the complete transformation of silica rich gel into different morphological types of C-S-H through the pozzolanic reaction and consequently leaves a large number of unhydrated or partly reacted remnants of silica fume particles in the hardened cement paste (Sarkar and Aitcin, 1987). As for all SCMs, the un-reacted silica fume particles might reduce the effectiveness of pozzolanic reactions and adversely affect the positive contribution of them for improving mechanical and durability properties of cement-based composites (Martinez-Velandia et al., 2011).

Some studies (Table 2.4) have been carried out to deal with the dispersion of silica fume by utilizing the PUS approach, as an alternative to enhance its pozzolanic activity. Overall, it has been inferred that the sonication process generally shifts the particle size distribution towards smaller particle sizes, comparatively raising the volume content of sub-micrometric particles in the PUS treated silica fume suspension.

Gapinski and Scanlon (2006) recommended a sonication process to break and disperse the bonded silica fume agglomerates.

Table 2.4. Summary of PUS Studies on Silica fume

Author, Year	Testing Materials	Sonication approach	Test equipment & Conditions	Characterisation Approach
(Gapinski and Scanlon, 2006)	Densified silica fume (as received sample)	Built in 600 watt ultrasound	0.010% sodium pyro-phosphate solution as the surfactant	custom-built laser scattering particle size analyser with and a
(Martinez-Velandia et al., 2008)	3 types of densified silica fume with different granulometric distribution 1 type No-densifeid silica fume 1 type of Milled densified silica fume	Sonicator S-3000, Misonix Max. 600 watts; 20kHz Different sonication power: 141 (2.26 watt/g) and 168 (2.69 watt/g) (corresponding to 80 and 100 % of the maximum power of sonication probe) Different sonication time: 2, 4, 6, 8, 10, 12, 14, 16, 18, and 20 minutes.	600 ml precipitate beaker suspended in water Different SF/water ratio Temperature: 20-35 °C	Granulometric distribution curves analysis by calculation of mean particle diameters, 10, 50, and 90% percentiles and the volume of particles with a diameter lower than 1 µm (Submicrometric particles) Laser diffraction granulometric (LDG) analysis (Mastersizer 2000, Malvern Instruments); Specific surface area (SSA) measurement by BET method (Tristar 3000, Micromeritics)
(Martinez-Velandia et al., 2011)	1 type of densified silica fume (supplied by Ferroatlantica, Sabon, Spain) Sonicated silica fume by the procedure stated on the previous work Cement: CEM I-52.5R Superplasticizer Melment 240 (Bettor S.L)	Sonicator S-3000, Misonix Max. 600 watts; 20kHz Different sonication power, watts (watt/g): 60 (0.96), 81 (1.30), 111 (1.78), and 141 (2.26) Different sonication time: 5, 10, 15, 20, 25 minutes.	Preparation of cement mortars according to EN 196-1:1996 procedure: 5, 10 and 15% cement replacement by silica fume; Water/cm: 0.35; Curing time: 7 and 28 days; 600 ml precipitate beakers suspended in water (228.4 ml); Different SF/water ratio Temperature: 20-35 °C Mortars was ground in acetone and dried for 30 min at 60 °C	Laser diffraction granulometric (LDG) analysis SEM micrographs (JEOL JSM 6300) Calculation of the strength activity index (SAI) Study of fixation of hydrated lime by: TGA/DTG analysis (TGA Mettler-Toledo 850 thermobalance, 35-600 °C at 10 °C/min)

(Rodriguez et al., 2012b)	3 commercial densified silica fume 2 non-densified silica fume with different particle size distribution Cement paste: CEM-I 52.5R, silica fume sonicated suspension, Cement replacement 10%	Sonicator S-3000, Misonix Max. 600 watts; Output frequency: 20kHz Sonication time: 10 minutes	Aqueous dispersion: 5 g of SF and 20 g of water in a precipitate beaker of 50ml water/binder ratio: 0.4 Temperature kept steady at maximum 40 °C using an external cooling bath	PUS treated particles characterization by SEM micrographs, XRD analysis, laser diffraction analysis (DLA), zeta potential measurement and TEM micrographs, Microstructural characterization of cement paste samples affected by sonication treatment by TGA/DTG and SEM/EDS analyses
(Rodriguez et al., 2012a)	1 commercial densified silica fume (supplied by Elkem Silicon Materials, 940D) Cement: CEM I-52.5R	Sonicator S-3000, Misonix Max. 600 watts; Output frequency: 20kHz Sonication time: 15 minutes	Aqueous dispersion: solid to liquid ratio of 0.20 Temperature kept steady at maximum 40 °C using an external cooling bath 40 mm Cubic samples of mortar containing blended cements with 5, 10 and 20% cement replacement by densified and sonicated silica fume admixtures Water to binder ratio: 0.3 / Superplasticizer (Glenium ACE31, BASF)	PUS treated particles characterization by TEM micrographs Paste characterization on blended cement pastes with w/b:0.5 and 10 wt% substitution of silica fume for cement by XRD, TGA/DTG and MAS-NMR analysis Compressive strength development test (7, 28 and 60 days of curing) Pore size distribution of mortar specimens (28 days) by MIP, Microstructural characterization by SEM/EDS
(Hashem et al., 2015)	Commercial ultra-fine silica fume with particle size ranging from 625 nm to 48 nm Concrete mixture: 65% coarse aggregates and 35% fine aggregate Polycarboxylate admixture (Glenium C315 SCC)	Ultrasonication Bath (FALC Instruments) 150 watts, Frequencies 40 and 59 kHz Power set on 70 watts (according to 50% power) and 135 watts (100% power) Frequency set to 59 kHz Different sonication time: 7, 15, 60, 150 minutes.	600 ml precipitate beaker liquid/powder ratio: 1.5, 2.4, 6, 10 and 12 Mechanical homogenizer (rotor-stator) with working speeds of 9500, 13500 and 24000 rpm Temperature kept steady at maximum 40 °C using built-in heater Concrete mixtures, by 1, 5 and 10% untreated silica fume and 1% treated silica fume	Particle size analysis, calculating mean. Range, D50, D80, D20 and sub micrometre sizes. TEM micrographs of treated particles Zeta potential measurement (Zeta Sizer 2000, Malvern Instruments) Compressive strength measurement of concrete

Martinez-Velandia et al. studied the granulometric properties and deagglomeration of the different types of silica fume affected by PUS. The study confirmed the effectiveness of the PUS treatment on the granulometric distribution (2008).

In order to investigate the effectiveness of sonicated silica fume particles on the pozzolanic reactivity in cementitious system, Martinez-Velandia et al. (2011) introduced their optimised homogenous suspensions of silica fume treated by the means of the sonication process (Martinez-Velandia et al., 2008) to cement mortars. Sonicated silica fume incorporated mortars showed an increase of 10 to 15% in the compressive strength especially for longer sonication times and higher sonication power levels. The thermogravimetric study also confirmed the activation of the pozzolanic reactions (fixations of free portlandite) (Martinez-Velandia et al., 2011).

Rodriguez et al. (2012b) found that sonication treatment introduced to densified silica fume contributes to an increase in the volume of particles of smaller sizes and also the enhancement of its reactivity by a de-agglomeration mechanism, improving dispersion.

The effect of sonicated densified silica fume on the hydration products, performance and pore structures of blended cement based pastes was the topic for another study carried out by Rodriguez et al. (2012a). The results of the compressive strength development study showed that applying the sonicated silica fume promotes higher mechanical strength in cement mortar specimens so that a desirable mechanical performance can be achieved using a smaller content of SCMs. Moreover, the results of XRD, TGA/DTG analysis indicated that PUS treated silica fume shows higher pozzolanic reactivity, associated with higher consumption of portlandite through the hydration process compared with the densified silica fume admixture. Based on the results of MAS-NMR spectroscopy analysis, this causes the formation of an aluminium-rich C-S-H with a structure of longer chain length and lower Ca/Si ratio which is a more stable binding phase. The pore size distribution study of cement mortar specimens also showed that the incorporation of sonicated silica fume induces a significant decrease by more than 20% in the volume of large pores (with diameters larger than 10 μm) as well as a reduction in total porosity.

Hashem et al. (2015) studied the sonication process parameters for the preparation of nanoparticles of silica fume and used the optimum sample to investigate the pozzolanic reactivity

by introducing it to a concrete mixture. Based on the results obtained, the optimum sub-nanometric particle distributions of ultrasound treated silica fume correspond to the experimental condition: sonication power/frequency/process time: 135 watts/ 40 kHz/ 60 min; homogenizer speed of 24000 rpm and liquid/water ratio of 6. Introducing this optimised sample into cementitious system by 1% cement replacement; the sonicated silica fume incorporated concrete showed 10 and 20% enhancement in compressive strength compared to the reference silica fume and control mixtures, respectively. Sharobim et al. (2017) found that sonicated nano-silica enhances compressive strength of concrete and the microstructure of the cement matrix. As it is evident, all the reviewed studies have investigated the dispersion improvement of silica fume and nano-silica in the cementitious matrix whilst failing to address the kinetics of cement-based materials hydration under the effect of ultrasound.

Askarinejad et al. (2012) characterised the natural pozzolans' nanostructures affected by introducing the PUS irradiation to bulk natural pozzolans by SEM and XRD as well as studying the pozzolanic activity by TG/DTA analysis and mortar's compressive strength index. Similar to the results obtained from the studies carried out on the effect of PUS on densified silica fume, the results demonstrated that the pozzolanic reactivity of natural pozzolans was enhanced by applying PUS in optimised conditions.

Overall, It is evident that ultrasonic treatment has been shown to be a favourable alternative in enhancing the efficiency of densified silica fume and natural pozzolans in the following forms: improved dispersion of agglomerates (especially sub-micrometre particles leading to a much wider particle distribution and enhancing the pozzolanic activity associated with a lower amount of unreacted particles), and comparative mechanical performance using a lower dosage of SCMs replacing part of Portland cement. However, very little is known about the PUS influences on SCMs and extensive specific research is needed to clarify the mechanisms in which PUS influences Portland cement and SCMs hydration.

7. Conclusion and the focus of the present work

This review has surveyed existing research in the field of PUS applications in cementitious materials as well as the underlying mechanisms by which ultrasound irradiation can affect the hydration kinetics of cementitious systems. In addition to the known effects of disaggregation and the dispersion of particle clusters, it was postulated that PUS might firstly be influential on the homogenising and dispersion of cementitious materials particles and also on the crystallisation and precipitation processes (nucleation and crystal growth) of different hydration phases in a cementitious system. It was proposed that these effects were due to the acoustic cavitation leading to shock waves and jet streams that could result in enhanced mass transfer, erosion and exfoliation of anhydrous grains. Furthermore, the degassing effect of PUS was able to remove the air entrapped voids thus changing and controlling both the mechanical and transport properties of cementitious materials systems.

To address the present gap, some specific research areas have been identified, which are needed to make progress in both a fundamental understanding of such applications and to push forward the development and uses of ultrasound techniques for cement-based composites. Amongst these the author suggests the following lines of investigation:

- The effect of PUS on Portland cement hydration is not yet fully understood. More studies need to be conducted to confirm the effects of cavitation on cementitious materials, and at the same time to clarify its mechanisms. The only study undertaken has focused on a limited characterisation of alite hydration which is only considered as a binary system of Ca and Si ions in cement hydration. However, the effect of exposing PUS to complex systems of ternary compositions of $CaO\text{-}SiO_2\text{-}Al_2O_3$ need to be thoroughly investigated. Overall, the author believes that it is now time to expand the horizon of ultrasound-assisted crystallisation studies known as “sonocrystallisation” to cement hydration products. The aim should be to develop advanced theories regarding the homogenous and heterogeneous nucleation and the growth of cement hydration affected by ultrasound irradiation.
- The primary focus of nearly all studies carried out in the use of PUS to promote SCMs properties has been de-agglomeration and gaining an enhanced particle size distribution-. In addition, microstructural studies on cementitious composites have failed to reveal an in-depth

analysis of the hydration characterisation as well as mechanical and durability properties. Therefore, it is necessary to study the kinetics and mechanisms of PUS affected cementitious blended systems in which the hydraulic reactions of SCMs could lead to more complex hydration phases in combination with cavitational effects. The first step in fulfilling this objective may be to develop an analytical approach to qualify and quantify the reaction of SCMs independently of the cement clinker phases. Then, the intermixing levels of hydration phase compositions in blended systems (i.e. PC-silica fume, PC-slag, PC-PFA, PC-natural pozzolan) subjected to PUS should be investigated.

- The fresh state properties of cementitious materials markedly dominate the practical aspects of their usage in the field. In addition to the initial setting time, the characterisation of rheological parameters (i.e. yield stress and viscosity) of sonicated cement-based systems need to be well established.
- Expanding the practice of sonicated cement paste to concrete system should be pursued in future studies. It would require the development and manufacturing of ultrasound equipment tailored for concrete, and more notably, scaled up sonochemical processes.
- The influence of the degassing (de-airing or de-foaming) effects of PUS especially in present of air-entrained admixtures needs to be investigated.
- Studies on the influence of PUS on the crystallisation of hydration products in the presence of superplasticisers needs to be performed.
- A study needs to be carried out regarding the influence of high frequency as well as combined low and high frequency ultrasound exposure on the sonocrystallisation of cementitious materials hydration.
- The generated heat due to the cavitation phenomenon during PUS practice which could adversely affect the initial setting, needs to be addressed.

To address the priority research questions, this PhD work investigated the effect of ultrasound irradiation on PC systems, first with a focus on possible changes in the particle size distribution of PC. Then, pore solution compositions of PC paste subjected to ultrasound with various frequency/power densities at different hydration times were examined. In this regard, changes in

hydration products were also explored. Moreover, the present study surveyed the influence of ultrasound extent of hydration by the measurement of chemical shrinkage over 14 days hydration. Finally, the effects of PUS on the mechanical performance of PC mortar and the interface between the aggregates and the bulk cement paste were studied.

8. References

Akkaya, Y., Ouyang, C., and Shah, S. P. (2007). Effect of supplementary cementitious materials on shrinkage and crack development in concrete. *Cement and Concrete Composites*, 29(2):117 – 123.

Aldea, C.-M., Young, F., Wang, K., and Shah, S. P. (2000). Effects of curing conditions on properties of concrete using slag replacement. *Cement and Concrete Research*, 30(3):465 – 472.

Alexander, K. M. (1960). Reactivity of ultrafine powders produced from siliceous rocks. *Journal Proceedings*, 57(11).

Alizadeh, R., Raki, L., Makar, J. M., Beaudoin, J. J., and Moudrakovski, I. (2009). Hydration of tricalcium silicate in the presence of synthetic calcium-silicate-hydrate. *Journal of Materials Chemistry*, 19(42):7937–7946.

Almenares, R. S., Vizcaino, L. M., Damas, S., Mathieu, A., Alujas, A., and Martirena, F. (2017). Industrial calcination of kaolinitic clays to make reactive pozzolans. *Case Studies in Construction Materials*, 6:225–232.

Alujas, A., Fernandez, R., Quintana, R., Scrivener, K. L., and Martirena, F. (2015). Pozzolanic reactivity of low grade kaolinitic clays: Influence of calcination temperature and impact of calcination products on OPC hydration. *Applied Clay Science*, 108:94–101.

Amara, N., Ratsimba, B., Wilhelm, A.-M., and Delmas, H. (2001). Crystallization of potash alum: effect of power ultrasound. *Ultrasonics Sonochemistry*, 8(3):265–270.

Angst, U., Elsener, B., Larsen, C. K., and Vennesland, O. (2009). Critical chloride content in reinforced concrete - a review. *Cement and Concrete Research*, 39(12):1122–1138.

Askari, S., Alipour, S. M., Halladj, R., and Davood, A. F. (2013). Effects of ultrasound on the synthesis of zeolites: a review. *Journal of Porous Materials*, 20(1):285–302.

Askarinejad, A., Pourkhorshidi, A. R., and Parhizkar, T. (2012). Evaluation the pozzolanic reactivity of sonochemically fabricated nano natural pozzolan. *Ultrasonics Sonochemistry*, 19(1):119–124.

Boels, L., Wagterveld, R., Mayer, M., and Witkamp, G. (2010). Seeded calcite sonocrystallization. *Journal of Crystal Growth*, 312(7):961 – 966.

Bullard, J. W., Jennings, H. M., Livingston, R. A., Nonat, A., Scherer, G. W., Schweitzer, J. S., Scrivener, K. L., and Thomas, J. J. (2011). Mechanisms of cement hydration. *Cement and Concrete Research*, 41(12):1208–1223.

Chatel, G. and Colmenares, J. C. (2017). *Sonochemistry: From Basic Principles to Innovative Applications*. Springer International Publishing.

Damidot, D., Nonat, A., and Barret, P. (1990). Kinetics of tricalcium silicate hydration in diluted suspensions by microcalorimetric measurements. *Journal of the American Ceramic Society*, 73(11):3319–3322.

Davidovits, J. (2008). *Geopolymer Chemistry and Applications, 4th ed*. Geopolymer Institute.

Diamond, S., Sahu, S., and Thaulow, N. (2004). Reaction products of densified silica fume agglomerates in concrete. *Cement and Concrete Research*, 34(9):1625 – 1632.

Duval, R. and Kadri, E. (1998). Influence of silica fume on the workability and the compressive strength of high-performance concretes. *Cement and Concrete Research*, 28(4):533–547.

Edson, A., Fowler, D., Juenger, M., Suh, C., and Won, M. (2008). Effects of supplementary cementing materials on the setting time and early strength of concrete. Technical report, Center for Transportation Research, The University of Texas at Austin.

Elimelech, M., Gregory, J., Jia, X., and Williams, R. (1995). Chapter 1 - introduction. In *Particle Deposition and Aggregation*, pages 3–8. Butterworth-Heinemann.

Enomoto, N., Katsumoto, M., and e Nakagawa, Z. (1994). Effect of ultrasound on the dissolution-precipitation process in the aluminum hydroxide-water system. *Journal of the Ceramic Society of Japan*, 102(1192):1105–1110.

Fitzgerald, M. E., Griffing, V., and Sullivan, J. (1956). Chemical effects of ultrasonics-"hot spot" chemistry. *The Journal of chemical physics*, 25(5):926–933.

Gaikwad, S. G. and Pandit, A. B. (2008). Ultrasound emulsification: Effect of ultrasonic and physicochemical properties on dispersed phase volume and droplet size. *Ultrasonics Sonochemistry*, 15(4):554–563.

Gapinski, G. M. and Scanlon, J. (2006). Silica fume. *Norchem*.

Garrault, S., Behr, T., and Nonat, A. (2006). Formation of the C-S-H layer during early hydration of tricalcium silicate grains with different sizes. *The Journal of Physical Chemistry B*, 110(1):270–275.

Garrault, S., Finot, E., Lesniewska, E., and Nonat, A. (2005). Study of C-S-H growth on C3S surface during its early hydration. *Materials and Structures*, 38(4):435–442.

Guo, Z., Jones, A. G., and Li, N. (2006a). The effect of ultrasound on the homogeneous nucleation of baso4 during reactive crystallization. *Chemical Engineering Science*, 61(5):1617–1626.

Guo, Z., Jones, A. G., and Li, N. (2006b). Interpretation of the ultrasonic effect on induction time during baso4 homogeneous nucleation by a cluster coagulation model. *Journal of Colloid and Interface Science*, 297(1):190–198.

Guo, Z., Zhang, M., Li, H., Wang, J., and Kougoulos, E. (2005). Effect of ultrasound on anti-solvent crystallization process. *Journal of Crystal Growth*, 273(3):555–563.

Harvey, E. N. (1930). Biological aspects of ultrasonic waves, a general survey. *Biological Bulletin*, 59(3):306–325.

Harvey, E. N. and Loomis, A. L. (1929). The destruction of luminous bacteria by high frequency sound waves. *Journal of Bacteriology*, 17(5):373–376.

Hashem, M. M., Serag, M. I., El-Kady, H., and El-Feky, M. (2015). Increasing the reactivity of silica fume particles using indirect sonication: effect of process parameters. *International Journal of Modern Trends in Engineering and Research*, 2(7):537–557.

Hassan, K., Cabrera, J., and Maliehe, R. (2000). The effect of mineral admixtures on the properties of high-performance concrete. *Cement and Concrete Composites*, 22(4):267 – 271.

Hu, X., Shi, Z., Shi, C., Wu, Z., Tong, B., Ou, Z., and de Schutter, G. (2017). Drying shrinkage and cracking resistance of concrete made with ternary cementitious components. *Construction and Building Materials*, 149:406 – 415.

Irassar, E., Maio, A. D., and Batic, O. (1996). Sulfate attack on concrete with mineral admixtures. *Cement and Concrete Research*, 26(1):113 – 123.

Juilland, P., Gallucci, E., Flatt, R., and Scrivener, K. (2010). Dissolution theory applied to the induction period in alite hydration. *Cement and Concrete Research*, 40(6):831–844.

Kim, J.-K., Han, S. H., and Song, Y. C. (2002). Effect of temperature and aging on the mechanical properties of concrete: Part i. experimental results. *Cement and Concrete Research*, 32(7):1087 – 1094.

Kruus, P., Lawrie, J. A. G., and O'Neill, M. L. (1988). Polymerization and depolymerization by ultrasound. *Ultrasonics*, 26(6):352–355.

Kumar, A., Bishnoi, S., and Scrivener, K. L. (2012). Modelling early age hydration kinetics of alite. *Cement and Concrete Research*, 42(7):903–918.

Kumar, R. and Bhattacharjee, B. (2003). Porosity, pore size distribution and in situ strength of concrete. *Cement and Concrete Research*, 33(1):155–164.

Lee, S. T., Kim, D. G., and Jung, H. S. (2009). Sulfate attack of cement matrix containing inorganic alkali-free accelerator. *KSCE Journal of Civil Engineering*, 13(1):49–54.

Li, H., Li, H., Guo, Z., and Liu, Y. (2006). The application of power ultrasound to reaction crystallization. *Ultrasonics Sonochemistry*, 13(4):359–363.

Lindley, J. and Mason, T. J. (1987). Sonochemistry. Part 2-Synthetic applications. *Chemical Society Reviews*, 16:275–311.

Lorimer, J. P. and Mason, T. J. (1987). Sonochemistry. Part 1-The physical aspects. *Chemical Society Reviews*, 16:239–274.

Lothenbach, B., Scrivener, K., and Hooton, R. (2011). Supplementary cementitious materials. *Cement and Concrete Research*, 41(12):1244–1256.

Luque de Castro, M. D. and Priego-Capote, F. (2007). Ultrasound-assisted crystallization (sonocrystallization). *Ultrasonics sonochemistry*, 14(6):717–724.

Lyczko, N., Espitalier, F., Louisnard, O., and Schwartzentruber, J. (2002). Effect of ultrasound on the induction time and the metastable zone widths of potassium sulphate. *Chemical Engineering Journal*, 86(3):233–241.

Martinez-Velandia, D., Paya, J., Monzo, J., and Borrachero, M. V. (2008). Granulometric activation of densified silica fume (csf) by sonication. *Advances in Cement Research*, 20(3):129–135.

Martinez-Velandia, D., Paya, J., Monzo, J., and Borrachero, M. V. (2011). Effect of sonication on the reactivity of silica fume in Portland cement mortars. *Advances in Cement Research*, 23(1):23–31.

Mason, T. J. (1999). *Sonochemistry*. Oxford University Press.

Mason, T. J. (2003). Sonochemistry and sonoprocessing: the link, the trends and (probably) the future. *Ultrasonics Sonochemistry*, 10(4):175–179.

Mason, T. J., Lindley, J., Lorimer, J. P., Maan, R., and Roberts, C. W. (1989). The effects of ultrasound on the synthesis of zeolite naa.

Mason, T. J. and Lorimer, J. P. (2002). *Applied Sonochemistry: Uses of Power Ultrasound in Chemistry and Processing*. Wiley-VCH.

Mason, T. J. and Peters, D. (2002). *Practical Sonochemistry, Power Ultrasound Uses and Applications*. Woodhead Publishing, 2nd edition.

Mielenz, R., Witte, L., and Glantz, O. (1950). Effect of calcination on natural pozzolans. In *Symposium on Use of Pozzolanic Materials in Mortars and Concretes*, pages 43–92. ASTM International.

Neppiras, E. A. (1972). Macrosonics in industry 1. Introduction. *Ultrasonics*, 10(1):9–13.

Newman, A. P., Lorimer, J. P., Mason, T. J., and Hunt, K. R. (1997). An investigation into the ultrasonic treatment of polluted solids. *Ultrasonics sonochemistry*, 4(2):153–156.

Nguyen, V. S., Rouxel, D., and Vincent, B. (2014). Dispersion of nanoparticles: From organic solvents to polymer solutions. *Ultrasonics sonochemistry*, 21(1):149–153.

Nili, M. and Ehsani, A. (2015). Investigating the effect of the cement paste and transition zone on strength development of concrete containing nanosilica and silica fume. *Materials & Design*, 75:174–183.

Nili, M., Ehsani, A., and Shabani, K. (2010). Influence of nano-sio2 and microsilica on concrete performance. In *Proceedings Second International Conference on Sustainable Construction Materials and Technologies. SCMT2*, Universita Ploitecnica delle Marche, Ancona, Italy.

Nishida, I. (2004). Precipitation of calcium carbonate by ultrasonic irradiation. *Ultrasonics Sonochemistry*, 11(6):423–428.

Papadakis, V. G. (2000). Effect of supplementary cementing materials on concrete resistance against carbonation and chloride ingress. *Cement and Concrete Research*, 30(2):291 – 299.

Peters, S. (2017). *The Influence of Power Ultrasound on Setting and Strength Development of Cement Suspensions*. PhD thesis, Bauhaus-University Weimar.

Prudencio, L. R. (1998). Accelerating admixtures for shotcrete. *Cement and Concrete Composites*, 20(2):213 – 219.

Richards, W. T. and Loomis, A. L. (1927). The chemical effects of high frequency sound waves I. a preliminary survey. *Journal of the American Chemical Society*, 49(12):3086–3100.

Riera, E., Golas, Y., Blanco, A., Gallego, J. A., Blasco, M., and Mulet, A. (2004). Mass transfer enhancement in supercritical fluids extraction by means of power ultrasound. *Ultrasonics sonochemistry*, 11(3-4):241–244.

Rodriguez, E. D., Bernal, S. A., Provis, J. L., Paya, J., Monzo, J. M., and Maria, V. B. (2012a). Structure of Portland cement pastes blended with sonicated silica fume. *Journal of Materials in Civil Engineering*, 24(10):1295–1304.

Rodriguez, E. D., Soriano, L., Paya, J., Borrachero, M. V., and Monzo, J. M. (2012b). Increase of the reactivity of densified silica fume by sonication treatment. *Ultrasonics Sonochemistry*, 19(5):1099–1107.

Rößler, C., Peters, S., and Ludwig, H. M. (2012). Power ultrasound: An effective method to accelerate strength development of cementitious materials. *CPI-Concrete Plant International*, (3).

Salvador, R. P., Cavalaro, S. H. P., Segura, I., Hernandez, M. G., Ranz, J., and de Figueiredo, A. D. (2017). Relation between ultrasound measurements and phase evolution in accelerated cementitious matrices. *Materials & Design*, 113:341–352.

Sarkar, S. and Aitcin, P. (1987). Dissolution rate of silica fume in very high strength concrete. *Cement and Concrete Research*, 17(4):591 – 601.

Scrivener, K. L. and Nonat, A. (2011). Hydration of cementitious materials, present and future. *Cement and Concrete Research*, 41(7):651–665.

Sharobim, K. G., Hassan, M., Hanna, N. F., El-Feky, M. S., Khattab, E., and El-Tair, A. M. (2017). Optimizing sonication time and solid to liquid ratio of nano-silica in high strength concrete. *International Journal of Scientific & Engineering Research*, 8(8):6–16.

Shi, C. (2001). An overview on the activation of reactivity of natural pozzolans. *Canadian Journal of Civil Engineering*, 28(5):778–786.

Shi, C. and Day, R. L. (2001). Comparison of different methods for enhancing reactivity of pozzolans. *Cement and Concrete Research*, 31(5):813–818.

Singh, L., Bhattacharyya, S., Shah, S., Mishra, G., Ahalawat, S., and Sharma, U. (2015). Studies on early stage hydration of tricalcium silicate incorporating silica nanoparticles: Part I. *Construction and Building Materials*, 74:278 – 286.

Singh, L. P., Bhattacharyya, S. K., Shah, S. P., Mishra, G., and Sharma, U. (2016). Studies on early stage hydration of tricalcium silicate incorporating silica nanoparticles: Part II. *Construction and Building Materials*, 102:943–949.

Taylor, H. (1997). *Cement chemistry, 2nd edition*. Thomas Telford Publishing, 2nd edition.

Taylor, M. G. (2015). MPA Cement Fact Sheet 14b, Modern Cements (Bulk). Technical report, MPA Cement.

Thomas, J. J., Jennings, H. M., and Chen, J. J. (2009). Influence of nucleation seeding on the hydration mechanisms of tricalcium silicate and cement. *The Journal of Physical Chemistry C*, 113(11):4327–4334.

Thomas, M. (2013a). *Chapter 5: Properties of Fresh Concrete*, pages 57–67. Supplementary Cementing Materials in Concrete. CRC Press, Taylor & Francis Group.

Thomas, M. (2013b). *Chapter 6: Temperature rise and risk of thermal cracking*, pages 69–76. Supplementary Cementing Materials in Concrete. CRC Press, Taylor & Francis Group.

Thompson, L. H. and Doraiswamy, L. K. (2000). The rate enhancing effect of ultrasound by inducing supersaturation in a solid-liquid system. *Chemical Engineering Science*, 55(16):3085–3090.

Toutanji, H. A. and El-Korchi, T. (1995). The influence of silica fume on the compressive strength of cement paste and mortar. *Cement and Concrete Research*, 25(7):1591–1602.

Vandenberg, A. and Wille, K. (2018). Evaluation of resonance acoustic mixing technology using ultra high performance concrete. *Construction and Building Materials*, 164:716–730.

Walker, R. and Pavia, S. (2011). Physical properties and reactivity of pozzolans, and their influence on the properties of lime-pozzolan pastes. *Materials and Structures*, 44(6):1139–1150.

Wang, S.-D., Pu, X.-C., Scrivener, K. L., and Pratt, P. L. (1995). Alkali-activated slag cement and concrete: a review of properties and problems. *Advances in Cement Research*, 7(27):93–102.

Wong, H. and Abdul Razak, H. (2005). Efficiency of calcined kaolin and silica fume as cement replacement material for strength performance. *Cement and Concrete Research*, 35(4):696 – 702.

Xu, G. J., Watt, D. F., and Hudec, P. P. (1995). Effectiveness of mineral admixtures in reducing ASR expansion. *Cement and Concrete Research*, 25(6):1225 – 1236.

Xu, H., Zeiger, B. W., and Suslick, K. S. (2013). Sonochemical synthesis of nanomaterials. *Chemical Society Reviews*, 42(7):2555–2567.

Yeager, E. and Hovorka, F. (1953). Ultrasonic waves and electrochemistry. I. a survey of the electrochemical applications of ultrasonic waves. *The Journal of the Acoustical Society of America*, 25(3):443–455.

3

Chapter 3: Methods & Materials

1. Introduction

This chapter outlines the characterisation of the materials and the details of the methods used in this study. Sample preparation procedures for making cement paste and mortar specimens, analyses of pore solution compositions, measurement of chemical shrinkage, X-ray diffraction and thermogravimetric analysis, setting time, compressive and flexural strength tests and microstructural studies are also described. Moreover, the details of ultrasonic processing and the method for the calibration of ultrasonic devices used in this work are highlighted.

2. Raw materials

2.1. *Portland cement*

A fresh Portland cement (PC) CEM I 52.5 N (provided by Hanson, UK) used in this study. The content was kept in PP wide neck reagent bottles to limit possible changes in composition due to hydration and carbonation. Tables 3.1 and 3.2 show the chemical and mineralogical compositions and physical properties of the cement, respectively. The particle sizes shown in Table 3.2 were measured by the laser diffraction method (dispersed in Isopropanol) with a Malvern Mastersizer 2000 system with a Hydro 2000MU sampler (Malvern Instruments Ltd, Malvern, UK).

Table 3.1. Characteristics of the Portland cement

Chemical composition (%(w/w))		Mineralogical composition (%(w/w))	
CaO	63.1	C_3S	65.1
SiO_2	19.5	C_2S	14.3
Al_2O_3	4.6	C_3A	5.4
SO_3	3.4	C_4AF	7.8
Fe_2O_3	2.9		
MgO	1.1		
K_2O	0.7		
Na_2O	0.2		
LOI (%)	3.3		
Total	98.8		

Table 3.2. Physical Properties of the Portland cement

Properties	
Specific gravity (g/cm^3)	3.08
Specific surface area (BET) (m^2/kg)	375
D_{v10} (μm)	2.4
D_{v50} (μm)	12.3
D_{v90} (μm)	37.0

2.2. *Silica sand*

A natural siliceous standard sand with a silica content of more than 99% (supplied by Sibelco, France) was used to cast the mortar samples. Four different particle-size fractions were combined to reach to a sand with a particle size distribution resembling the CEN Reference sand according to the BS EN 196-1 (2016) requirements. The cumulative particle size distribution of the silica sand was determined through dry sieving and is shown in Fig. 3.1. The sand consisted mostly of uncrushed and rounded aggregates and its moisture content was measured less than 0.1% wt.

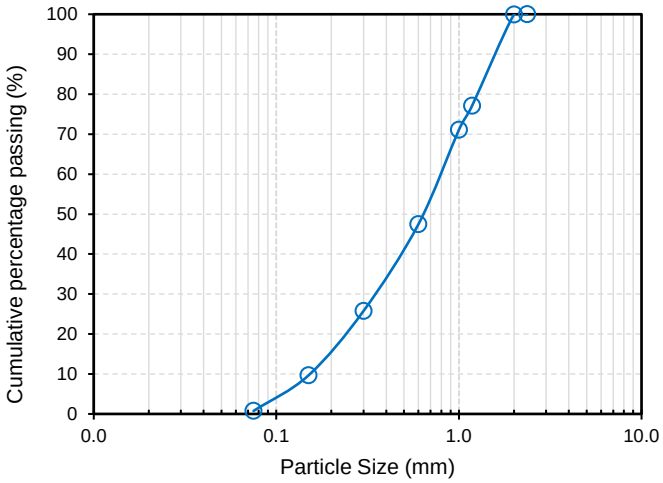

Fig. 3.1. Particle size distribution of the used silica sand

3. Ultrasonic instrumentation

Three ultrasonic frequencies/power densities were used to treat the cement paste and mortar mixes using an ultrasonic device. A large bespoke multi-frequency ultrasonic bath (Fig. 3.2) operating at frequencies of 26, 67 and 132 kHz (model FSD 450 MF) from Alphasonics (UK) was used to apply ultrasound directly to the fresh PC paste and the mortar mixes. These range of frequencies can be generally considered as low frequency (relatively higher sonication power) and high frequency (relatively less strict ultrasound intensity) and a mid-range ultrasound frequency (67 kHz). The ultrasonic bath was filled with 20 litres of pure distilled water (DI water) and maintained at 15 °C by immersing cooling coils attached to an ice bath to prevent overheating the samples during the sonication processing. A benchtop fixed frequency ultrasonic bath operating at 40 kHz (2.3 Litres, Langford Model 375TT) was also used to provide a higher power density for use in the study of the PC particle size distribution. The reason for choosing ultrasonic baths in this study instead of the set-up based on an ultrasonic horn (as used by Peters (2017)) is that in ultrasonic baths cavitation is more evenly distributed throughout the bath (Tudela et al., 2015). This is important to prevent the fast precipitation of cement particles in the paste/mortars and the re-agglomeration of cement particles in the high energy cavitation zone generated close to the tip of a probe. Initial trials with various ultrasound systems had confirmed that the application of high-power ultrasound was not appropriate for cementitious systems because it

produces significant temperature rise, accelerated setting time and loss of workability in the pastes. This was why only the 40 kHz benchtop ultrasonic bath (which provides a relatively higher power of acoustic energy compared to the larger bath) was used to study the distribution of particles in the cement. The Alphasonics bath also had the advantage that it could accommodate larger flasks containing greater volumes of fresh paste and mortar than was possible in the conventional laboratory ultrasound bath.

Fig. 3.2. The bespoke multi-frequency ultrasonic bath operating at frequencies of 26, 67 and 132 kHz (Alphasonics, UK)

3.1. *Sonochemical efficiency calibration of ultrasonic devices*

With respect to the reproducibility and reliability of the experiments, it is important to understand and correctly report data about the ultrasound equipment used including the amount of acoustic energy transferred into the medium. In this study, a simple method of calorimetry was undertaken in order to calibrate and evaluate the efficiency of the ultrasonic machines and obtain an estimation of the energy introduced to the system. The ultrasonic baths were calibrated using the calorimetry method (Koda et al., 2003) with DI water. The method adopted involved the measurement of the rise in temperature (T) of DI water with a specific volume (200 ml) in a 400

ml glass beaker over a period of time (t) after starting the ultrasound irradiation. Acoustic energy dissipated into the system is absorbed by the liquid inside the beaker and produces heat.

Calorimetry experiments were undertaken on the Alphasonics multi-frequency ultrasonic machine at three frequencies; 26 kHz, 67 kHz and 132 kHz; and the fixed frequency ultrasonic cleaning device at 40 kHz. Temperature was measured by a K-type thermocouple (Fluke) connected to a data logger (Extech Thermometer Datalogger) at intervals of 3 seconds. The thermocouple was suspended in the centre of the DI water (in the beaker) and did not touch the inner walls. The experiment was repeated in triplicate for each frequency and the following plots of each run were created for each ultrasonic system. The ultrasonic power actually entering the system was obtained according to Eq. (1):

$$\text{Power} = \left(\frac{dT}{dt}\right) C_p M \qquad \text{Eq. (1)}$$

where c_p is the heat capacity of the solvent (here water which is 4200 J/kg$^{\circ}$C) and M is the mass of solvent used inside the vessel. The value of (dT/dt) represents the gradient of the curve of T vs t (Fig. 3.3(a)-(d)) at time zero and was estimated by constructing a tangent to the curve at time zero. The power density dissipated into the system is given by Eq. (2):

$$\text{Power density} = \textit{Power} / \textit{volume of solution in the vessel} \qquad \text{Eq. (2)}$$

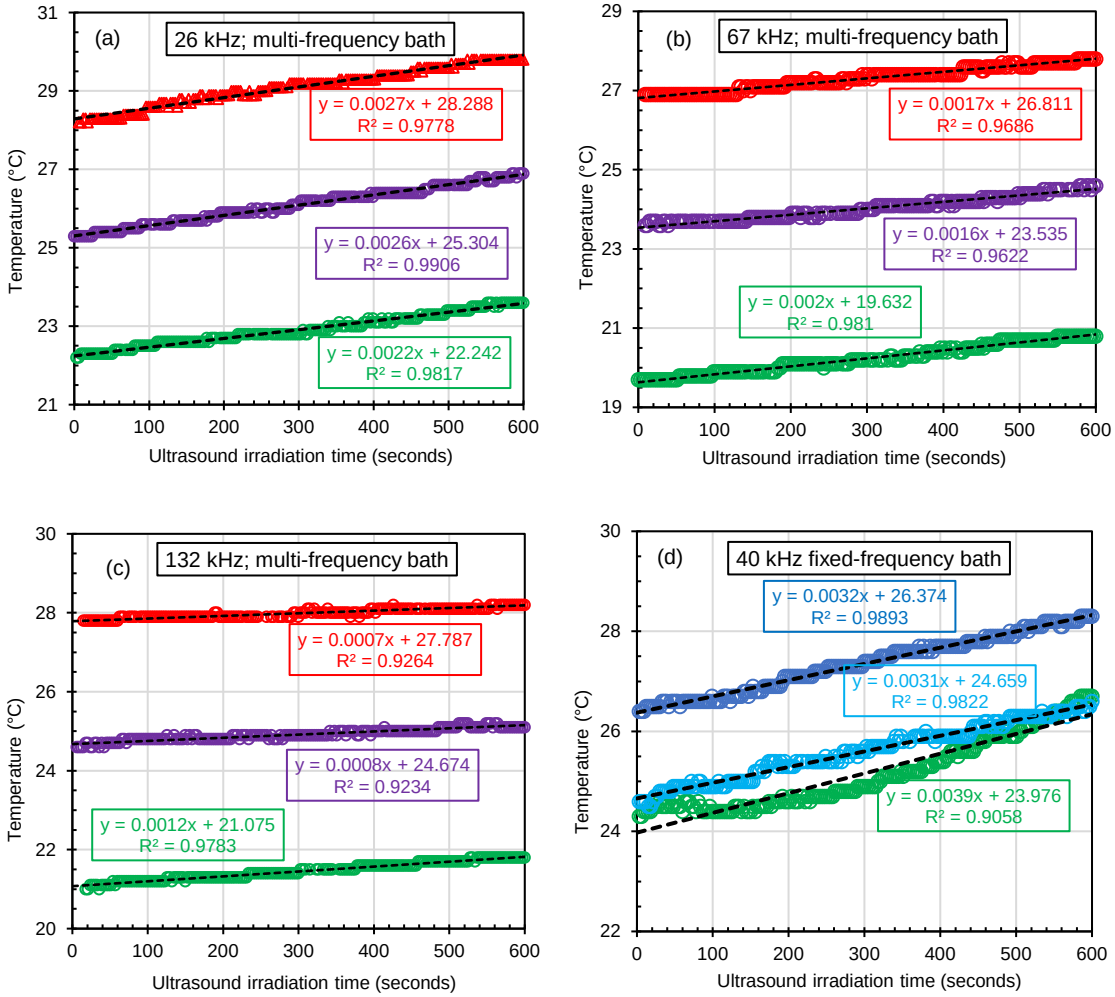

Fig. 3.3. Linear curve fitting of the data collected from the temperature rise versus time for the calibration of different ultrasonic devices used in this study based on the calorimetry method; (a)-(c): 26, 67 and 132 kHz frequencies of the large multi-frequency ultrasonic bath and (d): the 40 kHz fixed frequency ultrasonic bath

Using the data given in Fig. 3.3 an estimation of the actual ultrasonic power dissipated into the baths as well as the values for the power densities were determined and summarised in Table 3.3. The working electrical power of equipment at each frequency was measured by a plug-in power meter (Prodigit Electronics, model 2000MU). It should be noted that this is only an estimate, as neither the sonochemical degradation of the liquid nor the erosion of the emitting surface were taken into account (Mason, 2016).

Table 3.3. Frequencies and power of ultrasonic devices used in the experiment

Ultrasonic device	Frequency (kHz)	Electrical power (W)	Measured ultrasonic power (W)	Power density (W/cm^3)
Multi frequency ultrasonic bath	26	593 ± 20	2.10 ± 0.2	0.011 ± 0.001
	67	548 ± 8	1.48 ± 0.2	0.007 ± 0.001
	132	541 ± 14	0.63 ± 0.2	0.003 ± 0.001
Fixed frequency ultrasonic bath	40	81 ± 1	2.86 ± 0.4	0.014 ± 0.002

As shown in Table 3.3, the order of ultrasound power input at each frequency used in this work was 40 kHz > 26 kHz > 67 kHz > 132 kHz. Given the higher ultrasound power dissipated by the 40 kHz bath and its smaller capacity, this device was used only for studying the changes caused by the PUS to the particle size distribution of cement particles dispersed in the aqueous medium.

4. Particle size distribution measurement

Changes in particle size distribution (PSD) of the PC subjected to ultrasound were determined based on the wet dispersion method and the data processed from the laser diffraction (LD) technique (Arvaniti et al., 2015). The measurements were performed in both isopropanol (IPA) and DI water dispersants using a Mastersizer 2000 optical instrument coupled to a Hydro 2000MU wet dispersion accessory (Malvern Instruments Ltd, UK). The optimum operating conditions for dispersion were selected through a series of experiments. The background spectrum was measured according to the manufacturer's instructions by loading the dispersion unit with IPA or DI water. Then, stock suspension (20 wt.% in either IPA or DI water) was added drop-wise to the circulating dispersant liquid (at a pump speed of 1400 RPM) until the recommended obscuration level was achieved (based on a method adopted from Hackley et al (Hackley et al., 2004)), after which the LD analysis was started. The obscuration levels were kept approximately constant for all measurements (at a range of 10-15%). The refractive indexes used in the Mie analysis for the PC were set at n = 1.73 with k = 0.1, and the values for IPA and water were assigned 1.378 and 1.33, respectively (Cyr and Tagnit-Hamou, 2001; Malvern MAN 0396, 2007). The beaker used for the ultrasonic treatment was the same beaker that was attached to the particle size analyser (dispersant unit's beaker). This contained the powder mixture made up to a constant obscuration level and placed at an identical depth and position in the 40kHz ultrasonic bath for separate treatment periods of up to 10 minutes. An ice bath and copper coil were used to prevent overheating the samples. Three measurements per aliquot were taken before and after sonication at 2, 5, 7, and 10 min. The process was carried out for both IPA and aqueous suspensions. To estimate the state of changes due to the ultrasound treatment, some important parameters were calculated based on the PSD data normalised on the total volume of particles (volume distribution). The span was determined using volume-weighted percentiles D_{v10}, D_{v50} (median) and D_{v90} which are the respective diameters below which 10%, 50% and 90% by volume of the total particles are found. In addition, an indirect estimation of specific surface area ($SSA_{PSD\text{-}LD}$) based on the LD method (Frias et al., 1991) was calculated using the surface area mean diameter or the surface weighted mean (D[3, 2]) and the density of PC (ρ), in accordance with Eq. (3):

$$SSA_{PSD-LD} = \frac{6}{\rho . D[3,2]} \quad \text{Eq. (3)}$$

The change in the morphology of the PC particles affected by ultrasound on the IPA dispersed sample was also examined by a scanning electron microscope (FE-SEM, Zeiss Sigma 500 VP).

5. Study of pore solution

5.1. *Preparation of cement paste mixtures*

Portland cement pastes mixed at water-to-cement ratios (w/c) of 0.50 and 0.80 were made using the same mixing procedure are that adopted from ASTM C305-14 (2014). 2 kg of PC was sampled from three containers then swirled and turned upside down several times to ensure homogeneity. 200 g of cement was mixed with 100 g of DI water (w/c ratio: 0.50) or 160 g of DI water (w/c ratio: 0.80) by adding the powder to the liquid and allowing 30s for the absorption of the water. Subsequently, the suspension was stirred at 800 rpm for 30s and then at 1200 rpm for another 30s with a Ministar 20 control overhead stirrer equipped with a 4-blade propeller stirrer (both by IKA). After letting it stand for 90s, the mix was stirred at 1200 r/min for 60s.

5.2. *Ultrasonic treatment*

For the PUS treated samples, ultrasonic irradiation was applied directly to the fresh cement paste mixes (inside a 400 ml beaker) with the multi-frequency ultrasonic bath at frequencies of 26, 67 and 132 kHz. For the treatment of all the samples, the bath was filled up to the same level of water (20 cm) and the beakers containing the paste slurry were positioned in the centre of the ultrasonic tank and their bottom were fixed at the same distance (7 cm) from the ultrasound transducers. 1 % (v/v) Decon solution was added to the water in the tank, to maintain the reproducibility of the tests. This is due to producing a much better coupling between the ultrasonically reverberating base of the tanks and the liquid medium inside.

To study the effect of ultrasound energy, the durations of sonication treatment in this study were opted to be 2 and 10 minutes. These treatment durations were selected as two relatively low and high ultrasonication times, considering the limitation of temperature rise in cementitious materials that increases the chance of quick setting. Generally, the 10 minutes sonication can be considered as a relatively long processing time for ultrasound application in materials science. To

avoid the effect of temperature on hydration, the produced heat by the ultrasonic irradiation (especially during 10 minutes treatment) was kept controlled in the paste samples using a cooling coil immersed inside the system tank. In this regard, the maximum temperature increment in the samples due to the sonication was measured as about 1.0 °C and 4.5 °C respectively for 26 kHz ultrasound (having the highest power density) treatment during 2 and 10 minutes. These temperature rises were understood to be negligible to lead a significant changes in samples. The sonication power per grams (W/g) of fresh pastes was also kept steady during the whole experiment.

5.3. *Pore fluid sample preparation*

A pore solution study was performed on the paste samples filtered at 15 min, 6 h, 1, 7 and 28 days hydration times. For the 15 min samples (before the initial setting time), just after the sonication treatment (if any) of the fresh paste, the pore solution was extracted using vacuum filtration. For the rest of the curing ages, just after the mixing and applying of the ultrasonic treatment, the fresh paste was cast into 180 ml PP securitainers, sealed and cured at a temperature of 21±1°C.

The pore solutions of the hardened samples (6 h, 1, 7 and 28 days) were extracted after the steel-die method as outlined by Barneyback and Diamond (1981). The expression of pore fluid at these curing ages was undertaken under maximum pressure of 250 MPa and a loading rate of 2.5 kN/s. It has been reported that at higher pressures than 250 MPa, the pore solution compositions may vary considerably due to the changes affected on the solubility of solids (Vollpracht et al., 2016).

After extraction, the resulting liquid was immediately filtered using a plastic syringe connected to 0.45 µm PTFE disposable 25mm syringe filters (Fisherbrand). To prevent the precipitation of hydration in the solid phases, a sample preparation involved two stages of dilution processes immediately after the filtration of the pore solution: 1:10 for quantifying high-concentration elements (Ca, K, Na, S) and afterwards a further dilution 1:20 resulting in a final dilution of 1:200 for quantifying low-concentration elements (Al, Fe, Mg, Si). All dilutions were prepared with 2% (v/v) nitric acid in di-water. The diluted solutions were immediately put into sealed HDPE

containers and stored in a fridge. The ICP-OES analyses were undertaken within two weeks of the pore solution extraction. Hydroxide concentrations were determined with a pH-electrode (HI1043, Hanna Instruments Ltd.) connected to a Benchtop pH Meter Fisherbrand Accumet AE150, Fisher Scientific) in an undiluted pore solution.

5.4. *ICP-OES analysis*

The total concentrations of analytes were determined using a PerkinElmer Optima 8300 ICP-OES (PerkinElmer, Inc. USA). The ICP-OES operating conditions for the analyses are shown in Table 3.4.

In this study, the expected concentration values for the calibration solutions were taken from the work carried out by Caruso et al. (2017). In contrast to their work, however, the author developed this analysis method considering the 4 points calibration curves and the same calibration range for all the low concentration elements. Afterwards, by examining the concentrations obtained from the trail analysis, the compositions of the multi-element working calibration solutions (detailed in Table 3.5) were adjusted to ensure that they covered the concentration range of several elements in the samples.

Table 3.4. Operating conditions for the analysis with Optima 8300 ICP-OES

Operating conditions	Values/type
Nebuliser	Cross Flow
Spectral range	165-782 nm,
Detector system and shear gas	Dual view/Argon
RF Power	1500 W
Pump flow rate	1.5 mL/min
Plasma gas flow	8 L/min
Auxiliary gas flow	0.2 L/min
Nebulizer gas flow	0.7 L/min
Replicates per sample	3
Flush time	45s

As indicted in Table 3.5, two groups of matrix-matched multi-element working calibration solution and a group of individual standards for the analysis of silicon were prepared. 1000 ppm AAS single-element primary standard metal solutions of calcium, potassium, sodium and sulphur (from Fisher Scientific) were used for making working standard solutions related to the analysis of high concentration elements. With respect to the analysis of low concentration elements, 10 mg/L fully traceable single-element primary standard solutions of aluminium, iron, magnesium and silicon (form Inorganic Ventures) were used to prepare multi-element working calibration solutions containing Al, Fe and Mg as well as individual working standards of Si. The nitric acid (Analytical reagent grade, 65%) for the preparation of all the solutions and sample dilutions was purchased from Fisher Scientific. An independent periodic table mix for ICP (TraceCERT) was

supplied from Sigma-Aldrich (Sigma-Aldrich Ltd.) and used for checking the accuracy of the ICP method developed in this study. The range of recoveries for all analyses were kept within 100±5%. The reason for preparing individual solutions of silicon is to enhance the accuracy and tackle the difficulty of the analysis of the silicon by ICP-OES. Therefore, daily fresh individual solutions of silicon were prepared prior to performing the analysis. Despite keeping all the solutions inside the sealed plastic containers, however, the use of the non-glass volumetric flasks for the silicon calibration solutions were one of the limitations in this study. Pore solution samples were prepared and analysed in triplicate. The plasma viewing for analysing Na and K was radial, whilst the axial view was set for all the other spectral lines.

Table 3.5. Composition of the 4-points working calibration solutions used in this study for the analysis of high- and low-concentration analytes by ICP-OES (mg/L).

Elements	Multi-element solutions for high-concentration elements				Multi-element solutions for low-concentration elements				Individual solution for Silicon			
	Mix 1	Mix 2	Mix 3	Mix 4	Mix 5	Mix 6	Mix 7	Mix 8	Si 0.25	Si 0.50	Si 0.75	Si 1.00
Ca	2.5	5.0	7.5	10.0	-	-	-	-	-	-	-	-
K	50	100	150	200	-	-	-	-	-	-	-	-
Na	10	20	30	40	-	-	-	-	-	-	-	-
S	25	50	75	100	-	-	-	-	-	-	-	-
Al	-	-	-	-	0.25	0.50	0.75	1.00	-	-	-	-
Fe	-	-	-	-	0.25	0.50	0.75	1.00	-	-	-	-
Mg	-	-	-	-	0.25	0.50	0.75	1.00	-	-	-	-
Si	-	-	-	-	-	-	-	-	0.25	0.50	0.75	1.00

The blank used for all analyses is nitric acid 2% (v/v) in DI water.

6. Study of hydrates

Portland cement hydrate assemblages were identified by X-ray diffraction (XRD) analysis. Also, a semi-quantification of important components was performed using the data obtained by the thermogravimetric analysis (TGA/DTG).

6.1. *Sample preparation*

Portions of fresh cement paste made for the pore solution study (following the mixing procedure described in section 5.1 and the ultrasonication method detailed in section 5.2) were used for both the XRD measurements and the TGA/DTG analysis. Ultrasonic treatment was made according to the same procedure for the pore fluid compositions study as described in section 5.2. Fresh pastes were cast into 20 ml HDPE containers, sealed with plastic paraffin film and cured at 21±1°C. Analyses were carried out on a dried, finely crushed hardened cement paste that was cut into small pieces after specific hydration ages. A solvent exchange technique was used to stop the hydration of small paste slides of the cement paste. The method of drying the samples involved the displacement of water with isopropanol (99% ACS) to stop hydration followed by the evaporation of the solvent at 40 °C inside an oven. This approach has been shown (Zhang and Scherer, 2011) to have a minimal effect on the chemical composition of hydrates and is the best known method for preserving the pastes' microstructure. The crushed pieces of pastes were immersed during 48 h in a container filled with isopropanol (the volume of the solvent was at least 50 times that of the paste). The solvent was exchanged twice during the first 24 h. Special care was taken during the sample preparation to avoid carbonation and prepare a representative sample for analysis.

6.2. *X-ray diffraction analysis*

XRD analysis was performed on the powdered samples of hardened pastes cured at 7 and 28 days using a X'Pert-Pro diffractometer (PANalytical, Malvern Panalytical (applying CuKα radiation (λ=1.54Å). The samples were scanned between 7° and 70° 2θ, with a step size of 0.017° 2θ and a dwell time of 5s per step.

6.3. *Thermogravimetric analysis (TGA/DTG)*

The TGA analysis was performed using the Simultaneous Thermogravimetry – Differential Scanning Calorimetry instrument, model STA 449 F5 Jupiter (NETZSCH-Gerätebau GmbH, Germany). The dynamic heating ramp varied between room temperature and 980 °C. The heating rate was 20 °C/min and the crucibles used were made of alumina. The test was conducted under nitrogen atmosphere. All the tests were performed by using approximately 40 mg of dried finely ground PC paste samples. The method used for drying the samples involved the immersion of crushed pieces of hardened pastes in a container filled with IPA (99% ACS) over 48 hours to stop hydration followed by evaporation of the solvent at 40 °C inside a desiccator overnight (the volume of solvent was at least 50 times that of the paste and exchanged twice). This approach was shown by Zhang and Scherer (2011) to have a minimal effect on the chemical composition of hydrates and is the best known method for preserving the pastes' microstructure.

The methodology used for the semi-quantification of chemically bound water, calcium hydroxide (portlandite) and calcium carbonates was adopted from the approach proposed by De Weerdt et al. (2011). The method is defined based on the various regions of weight losses attributed to dehydration, dehydroxylation and decarbonation of corresponding hydrated compounds (Monteagudo et al., 2014). The temperature ranges for the various decomposition regions were chosen as follows: 40-550 °C for dehydration and dehydroxylation, and 600-980 °C for decarbonation. These regions were in compliance with the observed regions in the derivative TG curves of the paste samples in this study. The reason for taking 40 °C as the reference temperature (rather than higher temperatures like 105 °C) was to avoid missing the weight loss that corresponds to hydrates like C-S-H, and the AFt and AFm phases which lose part of their combined water below 105 °C.

For determination of the chemically bound water, the difference between the weight after solvent exchange (using the mass at 40 °C) and the weight after drying at 550 °C was calculated and expressed as a percentage of the dry sample weight at 550 °C, based on the TGA measurement (Eq. (4)):

$$\text{Bound water (wt.\%)} = \frac{W_{40} - W_{550}}{W_{550}} \times 100 \qquad \text{Eq. (4)}$$

where W_{40} and W_{550} represent the mass of sample at 40 °C and 550 °C temperatures, respectively.

With respect to the semi-quantification of portlandite, an approximate decomposition region with a temperature between 410 °C and 530 °C was considered. An approach known as the tangential method (Scrivener et al., 2016) was used (linked to the integration of the peak area) to calculate the mass loss related to the portlandite deconvolution in the derivative TG plot. The reason for using this method rather than the stepwise method was to exclude the weight loss of the C-S-H and any other hydrate whose mass loss overlapped within this temperature boundary with the weight loss of the portlandite. It is worth mentioning that the tangential method assumes the linearity of the weight change related to the C-S-H or other phases is present before and after the portlandite deconvolution. The fraction of 74/18 was applied to convert the portlandite bound water into the portlandite mass, using the molecular masses of portlandite (74 g/mol) and water (18 g/mol). Like the hydrate water calculation, the amount of portlandite was expressed as a percentage of the dry sample weight at 550 °C based on TGA data (Eq. (5)):

$$\text{Portlandite (wt.\%)} = \frac{WL_{CH}}{W_{550}} \times \frac{74}{18} \times 100 \qquad \text{Eq. (5)}$$

where WL_{CH} represents the weight difference corresponding to the portlandite peak determined using the tangential method.

The weight loss in the temperature region between 600 °C and 980 °C was used to estimate the amount of calcium carbonates present in the hydrated pastes, assuming no carbonation was permitted during the cement hydration. A conversion factor of 100/44 was inserted to consider the CO_2 derived from the calcium carbonate, using the molecular masses of $CaCO_3$ (100 g/mol) and CO_2 (44 g/mol). The values were expressed as a percentage of the fully decarbonated sample weight at 980 °C based on the TGA measurement (Eq. (6)):

$$\text{Carbonates (wt.\%)} = \frac{W_{600}\text{-}W_{980}}{W_{980}} \times \frac{100}{44} \times 100 \qquad \text{Eq. (6)}$$

where W_{600} and W_{980} represent the mass of sample at 600 and 980 °C temperatures, respectively.

The calculated values for the carbonates, in this study, represent the total amount of carbonates in which the amount of carbonated portlandite after manufacture of the specimens (plus ultrasonication) and the carbonation of the anhydrous materials were both intrinsically

included into the estimation. One approach to be considered would be applying a correction to take the carbonation of anhydrous materials into account. However, this causes an error in the calculations as it is not possible to differentiate the amount of anhydrous materials in the various samples under the effect of several characteristic PUS. Besides, the correction for the portlandite decarbonation would be dismissed considering that not all the weight loss measured in the decarbonation region is due to the portlandite carbonation.

Aluminium hydroxide (AH_3) which is an X-ray amorphous hydrate decomposition occurs in the temperature range of 260-320 °C due to its dehydroxylation (Scrivener et al., 2016). This weight loss was used for the semi-quantification of the amount of AH_3 present, using the molecular masses of $Al(OH)_3$ (78 g/mol) and water (18 g/mol) as the conversion factor (Eq. (7)). Similar to the bound water and portlandite calculation, the amount of AH_3 was expressed as a percentage of the dry sample weight at the end of the dehydration and dehydroxylation boundaries which was 550 °C.

$$AH_3\ (\text{wt.\%}) = \frac{W_{260} - W_{320}}{W_{550}} \times \frac{78}{18} \times 100 \qquad \text{Eq. (7)}$$

where W_{260} and W_{320} represent the mass of the sample at temperatures of 260 °C and 320 °C, respectively.

7. Setting time

Initial and final setting times of the cement pastes were determined using the Vicat apparatus according to the ASTM C191-19 (2019) standard procedure (Method A: Manual Vicat Needle Apparatus). First, the mixing water required for the normal consistency of PC was measured, following the procedure described in ASTM C187-16 (2016). Then, the setting time tests were undertaken on PC pastes with slightly higher water-to-cement ratios than in the standard consistency to ensure that ultrasound cavitation would be present which would be less likely in the normal mix containing less free water. The mixing procedure for the preparation and ultrasonication of fresh paste mixes were chosen as detailed in sections 5.1 and 5.2, respectively.

8. Measurement of chemical shrinkage

The Measurement of chemical shrinkage (Geiker and Knudsen, 1982; Tazawa et al., 1995) (also known as hardening shrinkage) has been widely used as a relatively cheap and simple indirect method (Parrott et al., 1990) to evaluate the extent of cement hydration, the amount of voids formed within a cement paste and the susceptibility to self-desiccation (Lura et al., 2010). Satisfactory correlations (Parrott et al., 1990) were found between the hydration directly assessed by quantitative X-ray diffraction analysis and the indirect methods e.g. heat of hydration by isothermal calorimetry (Lura et al., 2010) and non-evaporable water by thermal analysis.

In this work, the measurement of chemical shrinkage was carried out to determine the effect of PUS on the progress of the cement paste hydration. Precise measurements of chemical shrinkage of the PC pastes were performed using the dilatometry method adopted from Geiker (1983) and the ASTM C1608-17 (2017) procedure.

The cement pastes were prepared with w/c = 0.50 according to the procedure described in section 5.1. Ultrasound was directly applied following the same method detailed in section 5.2. Immediately after mixing (and the ultrasonic treatment), paste quantities of approximately 12.5 ± 0.5 g each were placed in borosilicate glass vials (27 mm diameter and 55 mm height). The vial was gently tapped 10 times on a soft surface to avoid entrapped air bubbles. The remainder of the vial was filled with the DI water. A graduated 1.0 mL borosilicate pipette was used as a capillary tube and fitted through a one-hole plastic stopper and placed tightly into the top of the vial so that the water would rise into the pipette to an initial level. This was carried out carefully to avoid disturbing the paste and to minimise the likelihood of any air bubble entrapment. The colour indicating paraffin oil (pale red in colour) was then placed by using a syringe above the water level inside the capillary tube, to minimise the water evaporation from inside of the tube and facilitate the detection of the amount of liquid in the pipette during the testing period. The prepared specimens were placed inside a thermostatic water bath to maintain isothermal conditions at 23.0 ± 0.5 °C. Over the course of time, the water level through the capillary tube decreased due to the chemical shrinkage of the cement paste inside the vial. The time and the level of the dyed oil, followed by the water level, were periodically recorded in this work using an automated test set-

up developed by the author and following advice from Dr Olivier Hass, who is an image processing specialist (Fig. 3.4).

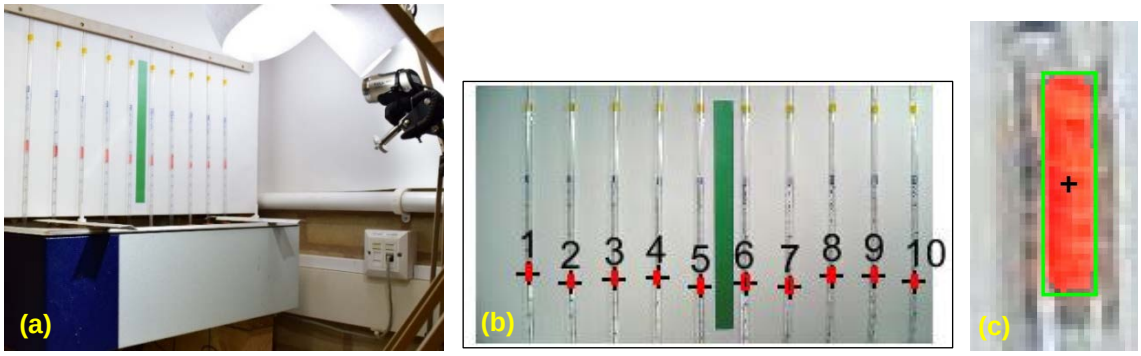

Fig. 3.4. Images of (a) automated dilatometry set-up; (b) an example of dye detected inside the capillary tubes together with a 250mm-high green rectangle bar used for calibration and the relative measurement of the position of the dye in the capillary tube; (c) zoomed version of the colour thresholding (red pixels) with the resulting bounding box (green pixels) and the centroid (black + sign) calculated by the software developed in this study for the measurement of chemical shrinkages

A high resolution (12 Megapixels) colour digital camera (TeckNet C108 1080p HD Webcam) was used to capture images of the capillary tubes at 5 minutes intervals for a total period of 14 days. Each image was saved as an RGB image, where R, G and B refer to the colours Red, Green and Blue, respectively. The image acquisition as well as the processing was implemented using MATLAB® and the Image Processing Toolbox™.

The volume of water absorbed by the cement paste was calculated based on the localisation of the paraffin oil within each capillary tube referred to as the region of interest (ROI), according to the following method:

i) To use colour thresholding to convert the RGB image into a binary image based on the relationship specifically developed to identify the colour of the dye using (Eq. (8)):

$$g(x,y)=\begin{cases}1 & \text{if } f_G(x,y)+f_B(x,y)<1.4f_R(x,y)\\ 0 & \text{otherwise}\end{cases} \qquad \text{Eq. (8)}$$

where $g(x,y)$ is the resulting binary image with x and y being the pixel coordinates along the horizontal and vertical directions, respectively; with the subscripts f_R, f_G and f_B representing the original image colour maps for Red, Green and Blue, respectively.

ii) To apply mathematical morphology to extract the shape of the ROI in each capillary tube, first using a closing operator with a disk structuring element with a radius of 5 pixels to fill holes within the ROI and create a smoothed contour.

iii) To use 8 connectivity to connect the neighbouring pixels, that represent the dye present in each capillary tube, within the binary image in order to identify the ROIs representing each of the 10 different capillary tubes.

iv) It is likely that more than 10 ROIs will be detected. This step rejects ROIs that do not belong to the capillary tube and selects the ROI that is the lowest in the capillary tube in the unlikely case should the dye split or mark the capillary tube. Thus, to check the validity of the detected ROIs using mathematical morphology operators:

    a. Calculate the bounding box, the centroid and the area of each candidate ROI.
    b. Remove all candidate ROIs that have very small or very large areas as they are not in the typical range of areas for the ROIs representing the dye.
    c. Remove all candidate ROIs that are outside the bounding box for the expected location of the dye in the image.
    d. Check the relative position of each candidate ROI. If the candidate ROIs have a similar horizontal location, meaning that they are located in the same capillary tube, select the one that occupies the lowest location within the capillary tube as on rare occasions, the volume of dye on top of the water could split.

v) To perform spatial calibration for each image to convert the position of the ROI from pixel to mm and then to mL.

    a. Use colour thresholding to extract the green rectangle template (Eq. (9)):

$$\text{GreenTemplate}(x,y)=\begin{cases}1 & \text{if } f_R(x,y)+f_B(x,y)<1.3f_G(x,y)\\ 0 & \text{otherwise}\end{cases} \qquad \text{Eq. (9)}$$

    b. Apply closing to remove the unlikely presence of holes and irregularities in the boundaries of the green rectangle.
    c. Remove small green areas less than 10000 pixels.
    d. Calculate the bounding box coordinates.
    e. Deduce the height of the bounding box which is also the height of the green rectangle.

f. Convert the ROI positions in pixels into positions in mm. It was found that the vertical calibration was sufficient given the high resolution of the camera, the relative position of the camera and the capillary tubes, the negligible impact of optical distortion and the relatively large variation of measurements made along the vertical axis.

vi) To convert the change in position of each dye in the capillary tube from mm to mL based on each capillary tube graduation.

The accuracy of the software was visually evaluated to the order of 1 to 2 pixels for the bounding box, due to outliers. This corresponded to 0.8mm and 0.0044 ml. A blank sample vial filled with DI water was covered with dye as for the other samples and placed at the corner of the set-up. This was used as a reference sample against which to assess the measurements' accuracy. Fig. 3.5 shows the results of changes in water level detected in the blank sample in comparison with the vial filled with the cement paste at w/c = 0.5 for up to 14 days. As can be seen in the enlarged area of the horizontal axis, the maximum error in the measurement of the water level for the blank sample was ±0.0040 mL. This was only 1.5% of the relative measurement of the water level in the capillary tube fitted to the vial with the cement paste at 24 hours (Fig. 3.5). To further reduce this error, the centroid of the threshold area corresponding to the presence of dye in the capillary tube was used for the calculations. Additionally, measures were taken to ensure constant light conditions throughout the testing period.

The volume of the water uptake by the cement paste hydration was calculated and hence the evolution of the chemical shrinkage was determined. The calculations set in the software were made in accordance to Procedure A described in ASTM C 1608-17 (2017). The automation of this experiment as well as the development of an image processing code were carried out at Coventry University to be used in the present work. Triplicate measurements were taken for each mix to evaluate and check the precision of the method.

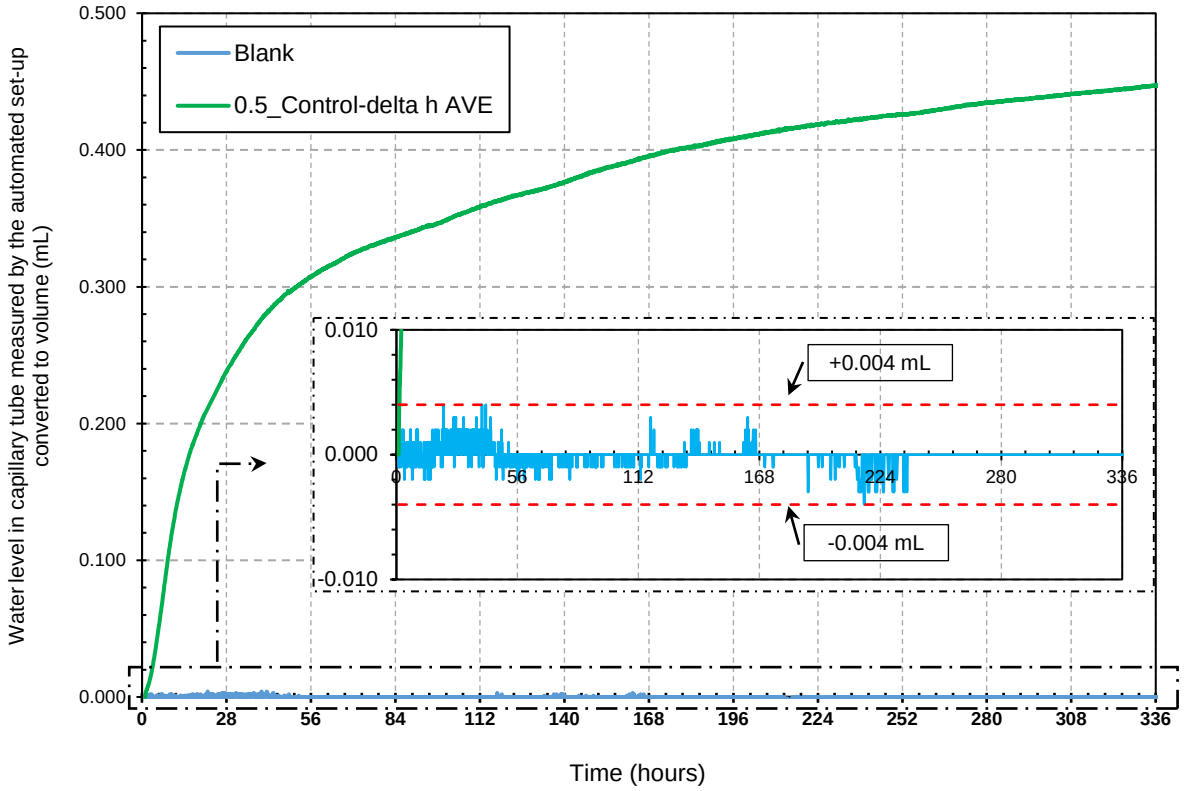

Fig. 3.5. Relative measurement of changes in water levels (mL) in the capillary tubes for the blank sample (vial filled with DI water) compared to the vial filled with cement paste at w/c = 0.5.

9. Characterisation of mechanical performance

The effects of PUS on the mechanical performance of cement mortars were examined by assessing the development of compressive and flexural strengths. Two different mixing procedures were adopted to prepare the mortar mixes. This was to investigate the effect of applying ultrasound at various stages on the mechanical properties of the mortars and the properties of the interface between the cement paste and the aggregates. In the first approach, ultrasound was applied at once to the fresh mortar when the mixing procedure was carried out, using all the components of the mortar mixes i.e. water, PC and fine aggregates. This group of mixes is called “sonicated mortars”. In the case of the second group of specimens, PC slurry was first prepared using water and cement. Afterwards, ultrasonication was applied to the cement slurry (paste). Finally, the fine aggregates were added during the final stage of mixing to obtain mortars with sonicated pastes labelled “paste-sonicated mortars”. It should be noted that the total volume of materials to be treated kept constant for both two mixing approaches. The mixing

procedure was carried out in accordance with BS EN 196-1 (2016). For proportioning the mortar mixes, the water/cement ratios for all mixes were kept at 0.50 (similar to the chemical shrinkage test for the cement slurry pastes). The aggregate-to-cement ratio was 2.75. Three test specimens of 40 mm × 40 mm × 160 mm prisms, were cast for each testing age of 1, 3, 7, 28 and 91 days from each batch of fresh mortar. Moulded specimens were vibrated for 15s by the vibration table and then covered and stored at 21.0 ± 1 °C. After 24 hours, the specimens were demoulded, tested or cured in water at 21.0 ± 1 °C. For both mixing approaches, the compressive and flexural strength tests were performed on the prismatic hardened mortar specimens according to BS EN 196-1 (2016). For a better comparison between the various mortars treated by different PUS frequencies and irradiation times, relative compressive and flexural strength indices were calculated in percentages (%) compared to the strengths of the non-sonicated (Control) sample.

10. Microstructural analysis

The interface between the aggregates and the bulk cement paste (the interfacial transition zone, ITZ) were examined using a Field-Emission Scanning Electron Microscope (FE-SEM, Zeiss Sigma 500 VP) coupled with an energy dispersive X-ray spectroscopy detector (EDS, Oxford Instruments X-Max 80). The qualitative analyses were performed in regions of fracture with samples selected after the mechanical strength testing. Prior to the analysis, specimens were dried following the same procedure used to prepare the samples for the XRD and TG analyses (described in section 6.1).

11. References

Arvaniti, E. C., Juenger, M. C. G., Bernal, S. A., Duchesne, J., Courard, L., Leroy, S., Provis, J. L., Klemm, A., and De Belie, N. (2015). Physical characterization methods for supplementary cementitious materials. *Materials and Structures*, 48(11):3675–3686.

ASTM C1608-17 (2017). *Standard Test Method for Chemical Shrinkage of Hydraulic Cement Paste*. ASTM International, West Conshohocken, PA.

ASTM C187-16 (2016). *Standard Test Method for Amount of Water Required for Normal Consistency of Hydraulic Cement Paste*. ASTM International, West Conshohocken, PA.

ASTM C191-19 (2019). *Standard Test Methods for Time of Setting of Hydraulic Cement by Vicat Needle*. ASTM International, West Conshohocken, PA.

ASTM C305-14 (2014). *Standard Practice for Mechanical Mixing of Hydraulic Cement Pastes and Mortars of Plastic Consistency*. ASTM International, West Conshohocken, PA.

Barneyback, R. and Diamond, S. (1981). Expression and analysis of pore fluids from hardened cement pastes and mortars. *Cement and Concrete Research*, 11(2):279 – 285.

BS EN 196-1 (2016). *Methods of testing cement. Determination of strength*. British Standards Institution.

Caruso, F., Mantellato, S., Palacios, M., and Flatt, R. J. (2017). ICP-OES method for the characterization of cement pore solutions and their modification by polycarboxylate-based superplasticizers. *Cement and Concrete Research*, 91:52 – 60.

Cyr, M. and Tagnit-Hamou, A. (2001). Particle size distribution of fine powders by laser diffraction spectrometry. Case of cementitious materials. *Materials and Structures*, 34:342–350.

Frias, M., de Rojas, M. S., Luxan, M., and Garcia, N. (1991). Determination of specific surface area by the laser diffraction technique. comparison with the blaine permeability method. *Cement and Concrete Research*, 21(5):709 – 717.

Geiker, M. (1983). *Studies of Portland cement hydration: measurements of chemical shrinkage and a systematic evaluation of hydration curves by means of the dispersion model*. PhD thesis, Technical University of Denmark.

Geiker, M. and Knudsen, T. (1982). Chemical shrinkage of Portland cement pastes. *Cement and Concrete Research*, 12(5):603 – 610.

Hackley, V., Lum, L.-S., Gintautas, V., and Ferraris, C. (2004). Particle size analysis by laser diffraction spectrometry: Application to cementitious powders. Technical report, NIST Interagency/Internal Report (NISTIR).

Koda, S., Kimura, T., Kondo, T., and Mitome, H. (2003). A standard method to calibrate sonochemical efficiency of an individual reaction system. *Ultrasonics Sonochemistry*, 10(3):149 – 156.

Lura, P., Winnefeld, F., and Klemm, S. (2010). Simultaneous measurements of heat of hydration and chemical shrinkage on hardening cement pastes. *Journal of Thermal Analysis and Calorimetry*, 101(3):925–932.

Malvern MAN 0396 (2007). Sample dispersion and refractive index guide Mastersizer 2000. Technical report, Malvern Instruments Ltd. Available from: http://cfile223.uf.daum.net/attach/12667E044948653F1F7F4B.

Mason, T. J. (2016). Ultrasonic cleaning: An historical perspective. *Ultrasonics Sonochemistry*, 29:519 – 523.

Monteagudo, S., Moragues, A., Galvez, J., Casati, M., and Reyes, E. (2014). The degree of hydration assessment of blended cement pastes by differential thermal and thermogravimetric analysis. morphological evolution of the solid phases. *Thermochimica Acta*, 592:37 – 51.

Parrott, L., Geiker, M., Gutteridge, W., and Killoh, D. (1990). Monitoring Portland cement hydration: comparison of methods. *Cement and Concrete Research*.

Peters, S. (2017). *The Influence of Power Ultrasound on Setting and Strength Development of Cement Suspensions*. PhD thesis, Bauhaus-University Weimar.

Scrivener, K., Snellings, R., and Lothenbach, B. (2016). *A Practical Guide to Microstructural Analysis of Cementitious Materials*. CRC Press US. Taylor & Francis Group.

Tazawa, E., Miyazawa, S., and Kasai, T. (1995). Chemical shrinkage and autogenous shrinkage of hydrating cement paste. *Cement and Concrete Research*, 25(2):288 – 292.

Tudela, I., Zhang, Y., Pal, M., Kerr, I., Mason, T. J., and Cobley, A. J. (2015). Ultrasound-assisted electrodeposition of nickel: Effect of ultrasonic power on the characteristics of thin coatings. *Surface and Coatings Technology*, 264:49 – 59.

Vollpracht, A., Lothenbach, B., Snellings, R., and Haufe, J. (2016). The pore solution of blended cements: a review. *Materials and Structures*, 49(8):3341–3367.Weerdt, K. D., Haha, M. B., Saout, G. L., Kjellsen, K., Justnes, H., and Lothenbach, B. (2011). Hydration mechanisms of ternary Portland cements containing limestone powder and fly ash. *Cement and Concrete Research*, 41(3):279 – 291.

Zhang, J. and Scherer, G. W. (2011). Comparison of methods for arresting hydration of cement. *Cement and Concrete Research*, 41(10):1024 – 1036.

4

Chapter 4: Effect of power ultrasound on the pore solution of Portland cement pastes

1. Introduction [1]

First, this chapter, provides the results of changes in the particle distribution of Portland cement (PC) when treated by ultrasound at 40 kHz. Then, there is a detailed investigation of the influence of the direct application of power ultrasound (PUS) at several frequencies and power densities on the pore solution of Portland cement (PC) pastes. Two PC pastes at water-to-cement ratios of 0.50 and 0.80 were studied. This study presents a robust method of analysis developed to quantify important high-concentration and low-concentration analytes present in PC paste pore solutions. The composition of the pore solutions and hydrates, after introducing PUS irradiation for various periods, were examined using inductively coupled plasma optical emission spectroscopy (ICP-OES), X-ray diffraction (XRD) and thermogravimetric analysis (TGA) techniques. In addition, the setting characteristics of PC system subjected to the PUS is reported.

2. Particle size distribution

The measurements of frequency by volume PSD and cumulative by volume PSD of the PC before and after ultrasound treatment at 40 kHz for 2, 5, 7 and 10 min are illustrated in Fig. 4.1. The important parameters calculated from the PSD data are also reported in Table 4.1.

There were significant observations regarding the PSD data measured in both the IPA and water. First, the aqueous PSD was quite a bit coarser in comparison with the IPA. In particular,

[1] A paper titled "*Insights into the positive effects of power ultrasound on the pore solution of Portland cement pastes*", based on the results discussed in this chapter, has been submitted to the "Cement and Concrete Composite" journal.

the particle sizes less than 10 µm were clearly underestimated in the PSD measured in the aqueous medium. Whilst apparently being marginally effective to disaggregate the larger particles, ultrasonication failed to properly disperse the size fraction below 10 µm in the aqueous sample. This could be due to some initial hydration in which the colloidal phase formed around the cement grains upon contact with the water (Hackley et al., 2004). Apparently, the formation of the colloidal gel layer is considerably enhanced within the finer particles, as this fineness can lead to accelerating the dissolution rate of the clinker phases (Taylor, 1997).

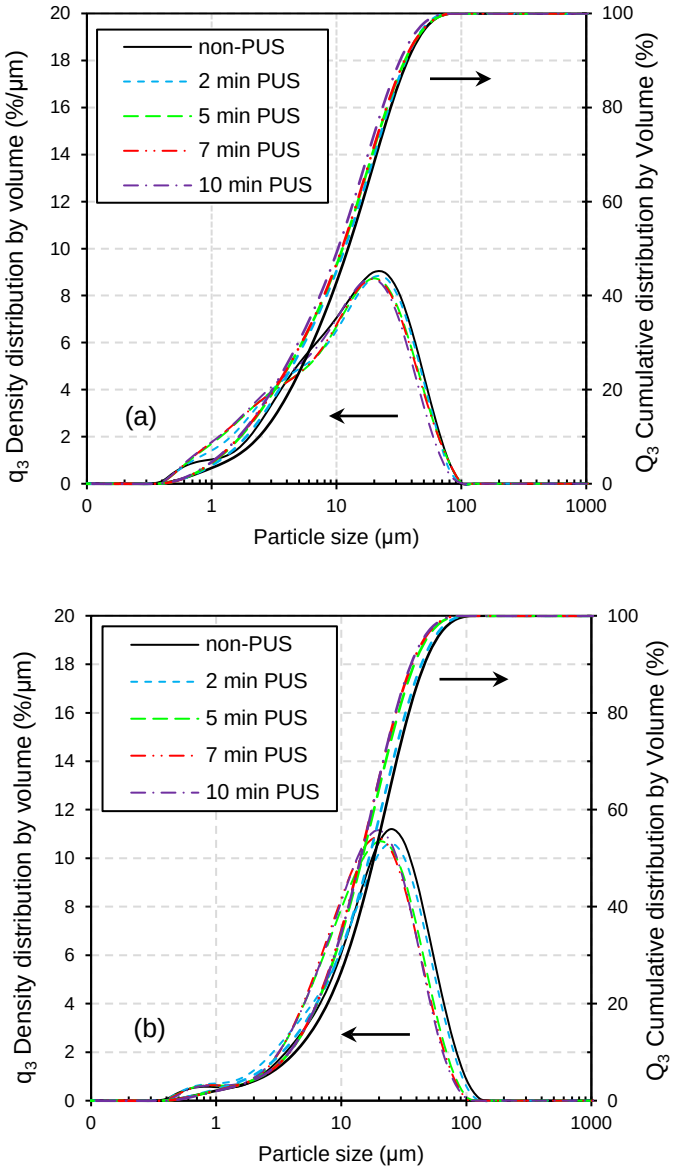

Fig. 4.1. Effect of ultrasound at 40 kHz for 2, 5, 7 and 10 min on the frequency particle size distribution and cumulative particle size distribution curves of the PC dispersed in (a) IPA and (b) DI water

The PSD results are consistent with the findings reported by Hackley et al. (Hackley et al., 2004) who used a probe system (Sonifier 450 from Branson Ultrasonics) and indicates that ultrasound did not disaggregate the fine size fraction. From the perspective of the PC's PSD report, it is evident that there is no advantage over using a water dispersant but the main point here is to examine how PUS can affect the PC's PSD within a medium closely analogous to real PC hydration as it is in the scope of this study.

Furthermore, the values for the main parameters of PSD (as given in Table 4.1) signify an insubstantial shift towards finer PSD at the expense of coarser sizes and an increase in SSA in both IPA and aqueous dispersion due to ultrasonic treatment. The limited change in the overall morphology of PC upon sonication at 40 kHz for 5 min can also be seen from the SEM micrographs shown in Fig. 4.2. The effect, however, appeared to saturate above 2 min and 5 min sonication for IPA and aqueous dispersion, respectively. Although the longest PUS treatment (10 min) still slightly shifted the size fractions in the IPA dispersion to a finer PSD, PC dispersed in an aqueous medium showed some re-agglomeration but mainly in the medium size fraction (see D_{v50} and D[3, 2]) at 10 min sonication. Only a very limited decrease in coarser sizes was observed. The SSA steadily increased upon sonication in the presence of IPA, whilst in the aqueous medium, the SSA did not change above 2 min of ultrasonication. This can be related to the observation that the finer size fraction is not affected by ultrasound in the aqueous suspension, or else it is underestimated (Malvern Ltd, 2015). Considering a substantially higher number of particles in a normal PC system (having a lower water-to-solid ratio or more than 40% v/v anhydrous PC in paste, as studied in this work), compared to the massively diluted suspension typically used for the wet PSD analysis, these findings highlight that ultrasound, even at longer irradiation to the normal PC paste, may not be very effective in the disaggregation of particles particularly the finer size fraction.

Table 4.1. Parameters for PSD measurement (based on the LD method) of the PC treated by ultrasound at 40 kHz dispersed in IPA and DI water for several durations

	D_{v10} (µm)	D_{v50} (µm)	D_{v90} (µm)	Span (D_{V10} - D_{V90} /D_{V50})	D [3, 2] (µm)	SSA_{PSD-LD} (m^2/g)
IPA dispersed						
non-PUS	2.39	12.34	37.04	2.81	5.31	0.367
2 min PUS	1.89	11.61	35.79	2.92	4.72	0.413
5 min PUS	1.70	11.15	35.24	3.01	4.46	0.436
7 min PUS	1.67	11.02	34.97	3.02	4.41	0.442
10 min PUS	1.65	10.27	32.25	2.98	4.28	0.456
DI water dispersed						
non-PUS	4.28	18.25	46.24	2.30	8.04	0.242
2 min PUS	3.37	16.68	43.71	2.42	7.03	0.277
5 min PUS	3.87	14.70	38.34	2.35	7.23	0.269
7 min PUS	3.87	14.16	36.72	2.32	7.17	0.272
10 min PUS	3.84	14.27	36.08	2.26	7.25	0.269

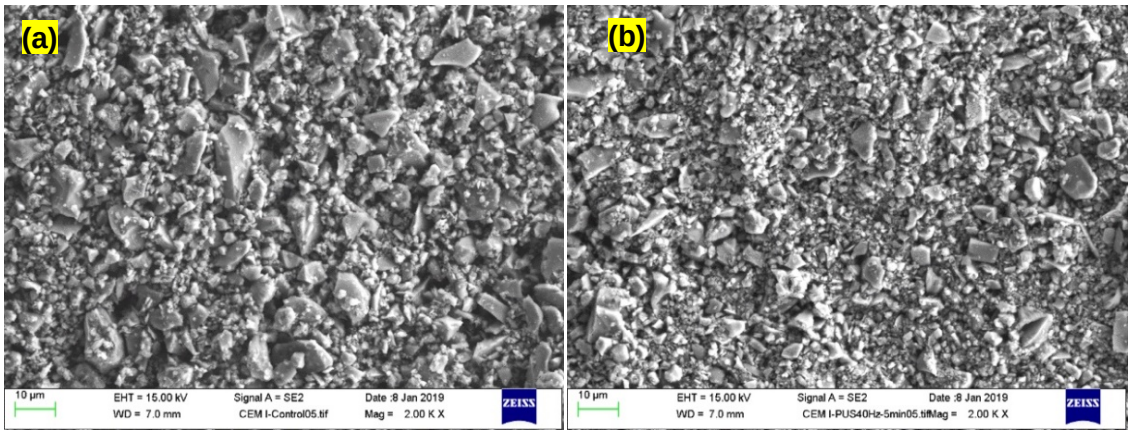

Fig. 4.2. SEM micrographs showing the effect of ultrasound treatment on the morphology of PC dispersed in IPA; (a) non-treated sample (b) sonicated at 40 kHz for 5 min

3. Accuracy of the ICP-OES method

The accuracy of the method used in this study was evaluated by calculating the closeness of agreement between measured concentrations and the accepted reference value of concentration (TraceCERT periodic table mix for ICP) for each spectral line. The certified values (at 20°C) of the reference ICP mix were declared to be 9.48 mg/L with expected uncertainty values of 10 mg/L for all the elements analysed in this study. Table 4.2 shows the closeness to the agreement values for the selected spectral lines investigated in this study. The recovery ratios were considered better than 100±5% for the whole analysis.

The limits of detection (LOD) and the limits of quantification (LOQ) or the low-concentration elements obtained from the method developed for the ICP-OES analysis are given in Table 4.3. Fifteen independently prepared blanks (with respect to the Al, Fe, Mg and Si) containing 10 mg/L of Ca, 200 mg/L of K, 40 mg/L of Na and 100 mg/L of S (all as interferences) in nitric acid 2% (v/v) were analysed. Their LOD and LOQ values were calculated as three and ten times the standard deviation of the mean analytes concentrations.

Table 4.2. Percentage deviation of analytes concertation from the expected value for the TraceCERT ICP reference

Analyte/Spectral line (nm)	Closeness agreement (%)
Ca 317.937	4.0
K 766.505	1.6
Na 588.998	2.7
S 181.976	1.9
Al 396.160	2.2
Fe 259.946	2.5
Mg 279.559	1.0
Si 251.611	4.6

Overall, the results indicate that the method used for the ICP-OES analysis in this study presents an acceptable level of trueness, offering satisfactory reliability and sensitivity in the analysis of the PC pore solution which is known to be a very complicated matrix. As discussed before, the only concern is the results for Si which show relatively poor accuracy (4.6 % closeness of agreement) and can be considered as one of the limitations in this study that corresponds to the usage of the borosilicate glassware in preparing both the standards and the samples.

Table 4.3. LOD and LOQ values for the low-concentration analytes

Analyte	Selected wavelength (nm)	LOD		LOQ	
		µg/L	µmol/L	µg/L	µmol/L
Al	396.160	13.6	0.50	45.4	1.68
Fe	259.940	20.3	0.36	88.9	1.59
Mg	279.559	4.2	0.17	14.1	0.58
Si	251.611	12.7	0.45	42.4	1.51

4. PC pastes with w/c = 0.50

The first system to be analysed was the PC paste mixed at a moderate water-to-cement ratio of 0.50. This section delves into the changes in the composition of the pore solution resident in the pores, as well as the hydrates subsequent to the application of ultrasonic irradiation to such a system.

4.1. *Pore solution composition*

The pore solutions of several PC pastes were analysed, mixed at w/c = 0.50 and immediately treated by PUS at 26, 67, and 132 kHz frequencies for both 2 and 10 min after mixing. The pore fluids extracted from the pastes after 15 min of sealed hydration (to study early hydration); then 6 hours and 1 day (to study the middle period of hydration), and 7 and 28 days (to study late hydration). The total concentrations of the various compositions are illustrated in Fig. 4.3 and Fig. 4.4 as a function of time up to 28 days. The overall trends manifested in the non-sonicated sample (Control) were consistent with the data reported by others (Lothenbach and Winnefeld, 2006; Taylor, 1997; Vollpracht et al., 2016). There were however, some important, although quite small, differences in the samples subjected to ultrasound. Generally, within the first 6 hours of hydration, the pore solution composition was dominated by Ca, S, K, Na and OH^- ions in all samples which is evident in Fig. 4.3((a)-(d)) and Fig. 4. The rapid dissolution of alkali metal sulphates after only a few minutes contributed a significant concentration of K, Na and S. Smaller proportions of S were expected from the dissolution of gypsum and anhydrite present in the PC as the concentration of S appeared to be about 5 times higher than that of Ca, signifying the role of alkali

sulphates present in the clinker to supply sulphate ions (Locher, 2006; Taylor, 1997). Initially, Ca is supplied in the solution mainly by the dissolution of C_3A and gypsum (present as an additive) considering the high reactivity of C_3A and relatively high solubility of gypsum. Only small proportions of C_3A and C_3S are dissolved during the early stages of hydration (Locher, 2006).

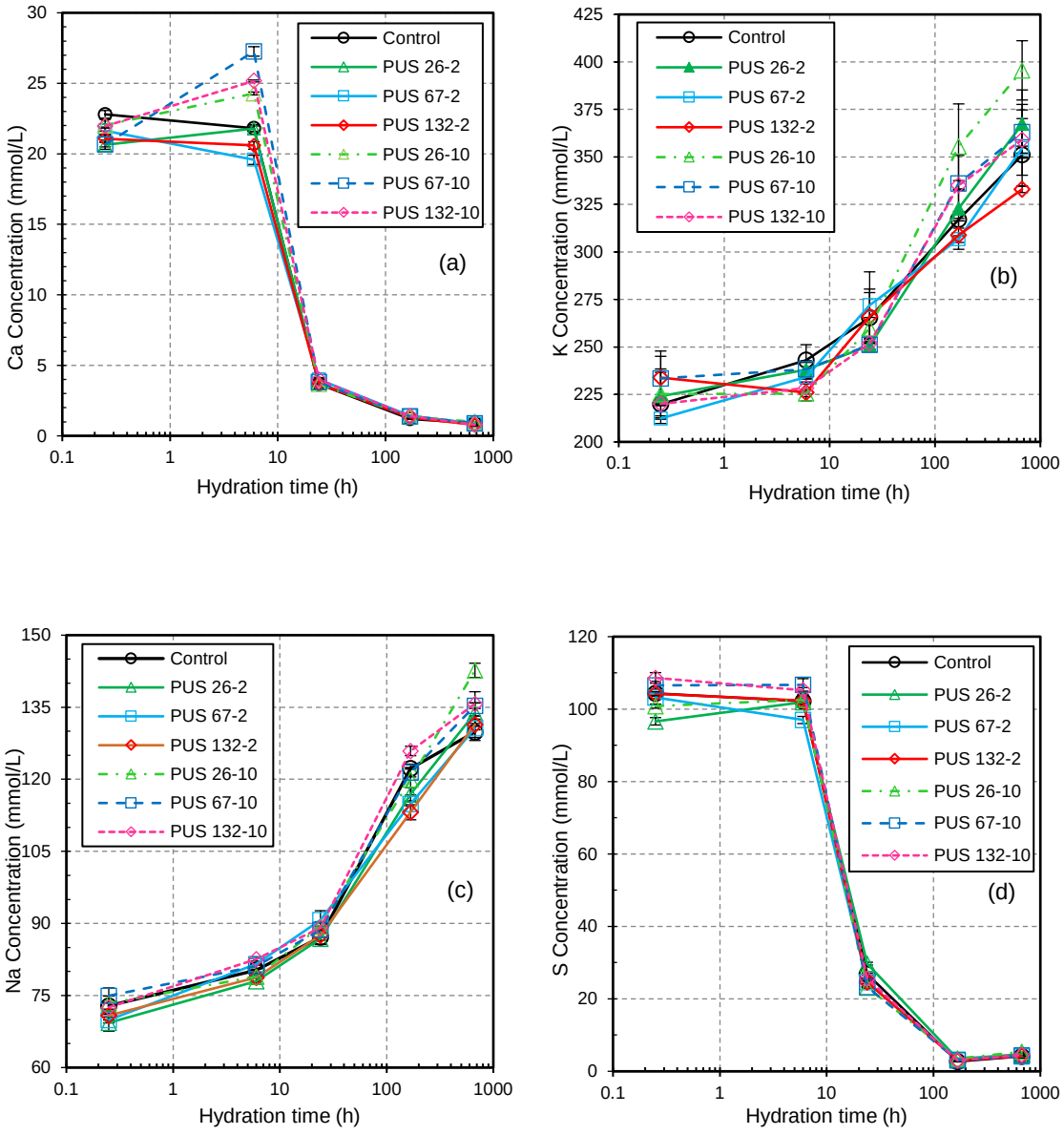

Fig. 4.3. ICP-OES measurement of the total concentrations of elements ((a) to (h)) in the pore solution expressed from the PC pastes, mixes subjected to PUS at 26, 67 and 132 kHz for duration of 2 and 10 min compared to the untreated mixes (Control); all mixed at w/c = 0.50.

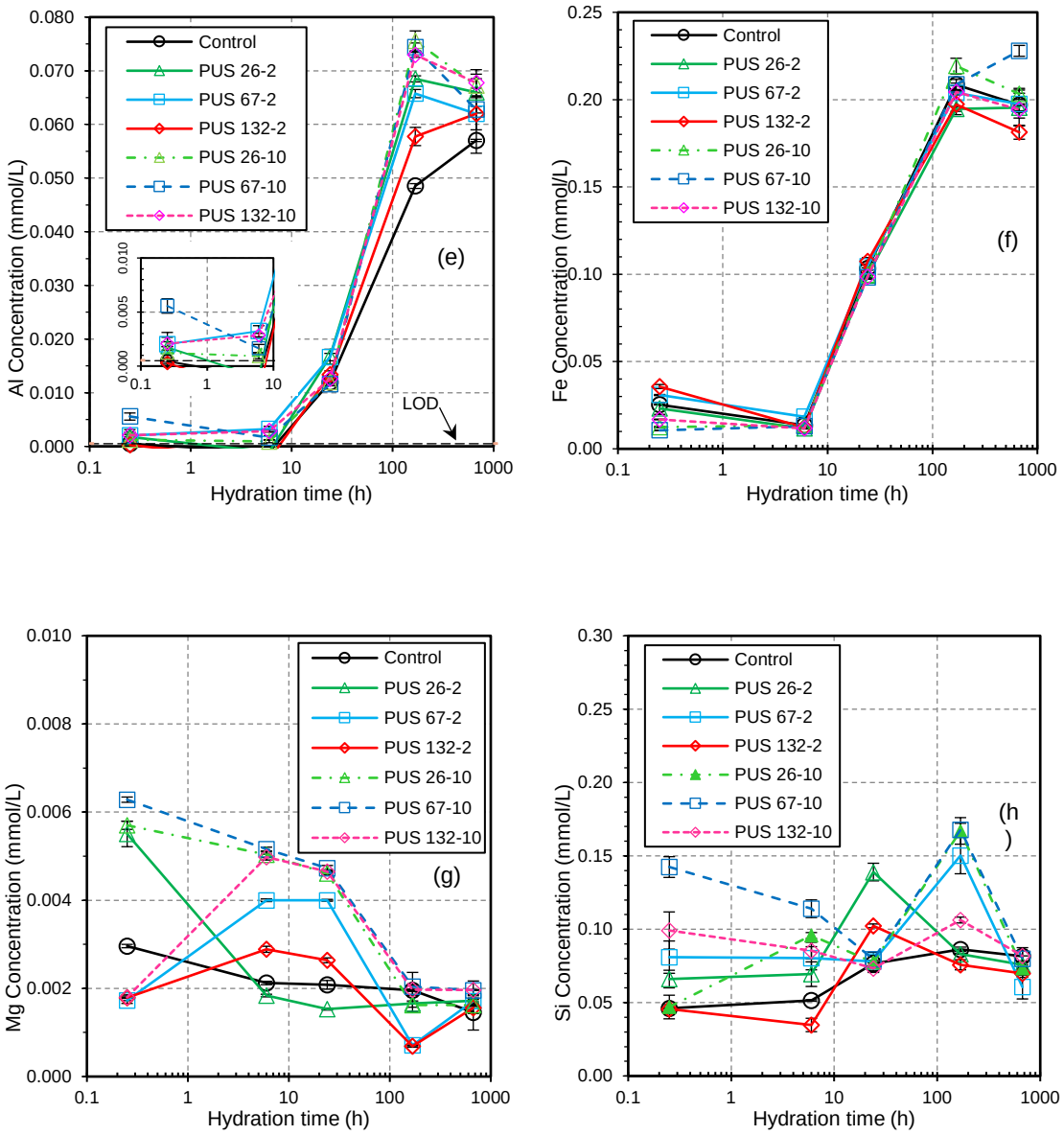

Fig. 4.3. (Continued) ICP-OES measurement of the total concentrations of elements ((a) to (h)) in the pore solution expressed from the PC pastes, the mixes subjected to PUS at 26, 67 and 132 kHz for duration of 2 and 10 min compared to the untreated mixes (Control); all mixed at w/c = 0.50.

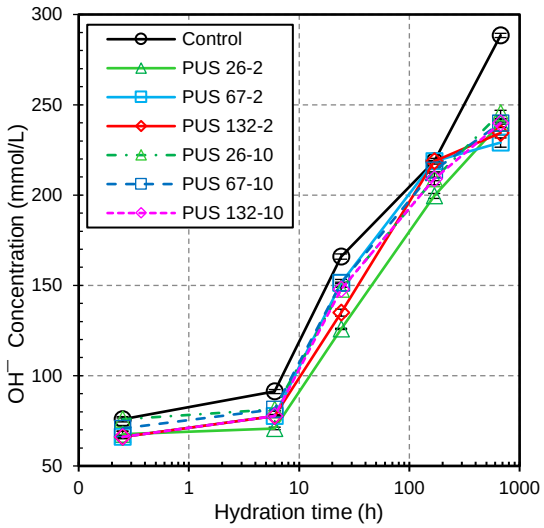

Fig. 4.4. Concentration of hydroxide ions by pH measurement of the pore solution immediately after extraction using a calibrated electrode

The change in the concentrations of Ca, S and OH^- remained rather consistent during the first 6 hours of hydration as confirmed by B. Lothenbach and F. Winnefeld (2006), implying that there is an approximate balance between the ongoing dissolution of anhydrous phases and the precipitation of hydrates during the induction period of hydration (Taylor, 1997). For the sonicated samples, however, appreciable changes were detected. Immediately after mixing, the concentration of Ca in all the sonicated pastes was lower than the control sample, whilst longer exposure to ultrasound (for 10 min) at all frequencies increased that which was measured at 6 hours (see Fig. 4.3(a)). For instance, PUS at 26 and 67 kHz enhances the release of Ca into the pore solution by 11% and 25% compared to the untreated sample, respectively. The slightly lower initial Ca resulting from the ultrasound treatment, could be the result of either a higher rate of ettringite formation or ultrasound-induced precipitation, crystallisation of the portlandite out of the supersaturated pore solution could also adversely affect the early ettringite formation. Considering the decrease in the hydroxide ions in all the sonicated samples compared to the non-sonicated paste illustrated in Fig. 4.4 (this will be discussed further in this section in page 73), the latter is more probable, but needs more investigation.

As observed by D. Rothstein et al (2002) and B. Lothenbach and F. Winnefeld (2006), similar to Ca, the concentration of S (Fig. 4.3(d)) in the PC system remained unchanging during early

hydration. There are roughly analogues trends in the PUS treated sample but with different levels of concentrations compared to the Control. Upon ultrasonication at 26 kHz for 10 min and at the other frequencies for 2 min, the concentrations of S during the first 6 hours of hydration exhibited lower values than that of the control sample. Similarly, this leads to the conclusion that PUS (mostly at a more gentle acoustic power) may enhance ettringite formation at early hydration by increasing the rate of sulphate precipitation, as reported by L. A. Davies et al (2015) in a fairly similar but not equivalent system. Considering the rise in hydroxides during the first 6 hours, it was discernible that that the rate of dissolution of the sulphates either from the clinker sulphates or the gypsum had been slightly increased by a longer irradiation of ultrasound at 67 or 132 kHz. Also, the frequency dependences of changes could be deduced in the concentrations of Ca and S introduced by ultrasound during the early period of hydration.

The concentration of K immediately after mixing was slightly raised by PUS, whereas the rate of increase in the concentration of K more or less slowed down in the ultrasonic treated samples during the first 6 hours of hydration (see Fig. 4.3(b)). Consequently, at 6 hours, the whole of the samples with ultrasonication demonstrated a reduced value of K concentration next to that of the control paste. A similar observation could be made in Na development in the pore solution (as per Fig. 4.3(c)) where the early concentration of the majority of pastes did not yield a rise in comparison to the control sample upon ultrasonication. The perceived slower rate of increase in alkali concentration under the influence of ultrasonic treatment could be associated with two conditions based on observations in the PC system (Lothenbach and Winnefeld, 2006). There is a slower decrease in pore solutions in which lower amount of hydrates are formed with relatively high bound water (e.g. ettringite) that consume a high proportion of pore fluid (as chemically bound water). In addition, the failure of PUS to intensify the release of alkali trapped in the gradually hydrating clinker phases could be another explanation. The occurrence of the latter effect can be unlikely, as degradation of the solid particles of anhydrous clinker would be expected, due to the shock waves and shear forces induced by the ultrasonic cavitation. Also, looking into the composition of other elements and hydrates may shed light on the mechanisms by which ultrasound affects hydration.

At the beginning of hydration, the concentration of Al in the control sample together with the sample treated by the PUS with the lowest acoustic energy (132 kHz) fell below the LOD as detailed in Fig. 4.3(e). The remaining sonicated samples, however, showed higher concentrations so they exhibited values above the LOD. Fe (Fig. 4.3(f)) started with a slight increase in concentration due to the shorter sonication at a lower acoustic power associated with the higher frequencies, then marginally dropped during the first 6 hours due to the appreciable suppression of ferrite phases hydration. As can be deduced from Fig. 4.3(g), ultrasonic processing at a relatively higher acoustic power dissipation (either 26 kHz for 2 and 10 min or 67 kHz for 10 min) increases the Mg concentrations just after mixing, while more gentle treatment is not very effective. At the same time, the Si concentrations were elevated in most samples upon ultrasonication, representing that PUS might be able to degradate the silicon bearing solid phases of anhydrous PC clinker (e.g. C_3S and/or C_2S) due to the shock waves and shear stresses of micro- or macrostreaming generated by the ultrasonic cavitation. The Si concentration in the pore solutions continued to be higher for all the ultrasonic treated pastes compared to the control sample during the first 6 hours of hydration. The exception was 132 kHz, associated with the lowest ultrasound energy density in this study.

Following the next 18 hours and up to 7 days, considerable changes in the composition of the pore solution could be seen. The concentrations of Ca and S dropped substantially where the system was continuously depleted from its sulphates. This can be attributed predominantly to the continuous precipitation of ettringite and the appreciable growth of C-S-H on the ettringite network (Lothenbach and Winnefeld, 2006; Taylor, 1997). The concentrations of alkalis and OH^-, however, continued to gradually increase until later ages, so that the PC hydration proceeded in a pore solution mainly of alkali hydroxides (Bye et al., 2011; Locher, 2006). Except at 132 kHz (linked to the minimum ultrasound power in this study), the pore solution finished 28 days hydration with a higher concentration of K and Na released into the solution due to the ultrasonic irradiation at various intensities. The maximum release corresponded to the 26 kHz ultrasound for 10 min irradiation which dissipated the highest energy density of PUS into the system. This observation along with other results (particularly the Al trends), can support the hypothesis that

ultrasound cavitation may be influential in breaking up and eroding the solid clinker particles, leading to an increased dissolution rate of the clinker phases.

From the first day onwards, the Ca concentrations were measured at exactly the same concentration for all mixes. In contrast, there were subtle differences in the concentrations of S measured at 7 days, indicating negligible various levels of sulphate depletion in the system at some points of hydration. It can be inferred from these findings that marginally dissimilar amounts of ettringite might be formed in each sample. Nevertheless, the results yielded the same concentration of S in all samples analysed for the rest of the hydration evolution. The observed trends signify that the ultrasonic frequency and power are independent of the changes introduced by PUS to the composition of the pore solution with respect to the consumption of Ca and S (i.e. AFt/AFm formation), at later ages of hydration. Moreover, this indicates that any considerable changes in properties of the resultant hydrates could be primarily related to the changes in early age hydration in which ultrasound is responsible for slightly different compositions of pore solution for precipitation and the formation of hydrates.

Among the trace elements, the concentrations of Al and Fe (Fig. 3(e) and (f)) were also drastically increased from 6 hours up to 7 days of hydration which was in agreement with other studies (Lothenbach et al., 2007; Rothstein et al., 2002). Interestingly, following the trends from very early hydration, the comparison of Al concentrations between the control and the sonicated pastes proved for the first time that ultrasound irradiation leads to a consistent increase in the release of Al into the solution as the pore solution continues to develop. The observed effect was markedly conspicuous at 7 days and 28 days of hydration where the minimum increases in the Al concentration measured in the sonicated samples at 132 kHz were measured by 18% and 11% as compared to the control mix, respectively. As can be seen in Fig. 3(e), the higher the acoustic power (associated with the frequencies at the energy density order of 26 > 67 > 132 kHz in this study), the higher the content of Al released into the pore solution at 7 days of hydration. Likewise, the pore solution development shows a higher amount of Al attributed to all the sonicated samples at 28 days. The findings provide enough evidence that a PC pore solution, under the effects of ultrasound processing, would be subjected to a higher degree of saturation with Al, regardless of frequencies/acoustic power. Additionally, alongside the evidence from Ca, S, Si and the alkali

trends, the influence of ultrasound on the hydration of clinker phases (particularly C_3A) can be inferred.

The Mg concentration remained high for up to 1 day and then start to drop gradually to the same levels as all the other samples at 28 days. For the Si, although a longer exposure of ultrasonication (at all frequencies for a duration of 10 min) kept the concentrations higher than the control sample at 7 days, all reached lower values (but with negligible differences) compared to the Control at 28 days. It should be noted that the rather incongruent data for Si (e.g. analysis at 1 day) could be related to the limitations of the samples/working standards preparation in this study, with respect to the silicon interference which was linked to the usage of borosilicate glass volumetric flasks instead of the potential use of polymethylpentene flasks. Even though, in addition to developing a detailed method (as discussed in the section 2.5) for the ICP-OES analysis, the highest care was taken to provide high accuracy and precision during the sample preparation and in performing the analyses.

Similar to the trends detected for the Ca and S concentrations, Mg and Si in the pore solution finished the 28 days hydration at roughly at the same levels of concentrations among the sonicated and the control samples, denoting the characteristic ultrasonic independency on the changes introduced to the pore solution composition at this age of hydration.

4.2. *Hydration products*

4.2.1. XRD analysis

The XRD patterns of the hardened pastes treated by PUS at frequencies of 26, 67 and 132 kHz for 2 and 10 min are shows in Fig. 4.5. The identified phases have been determined based on the crystallography database and labelled at characteristic diffraction peaks of each phase. The main hydrates detected by XRD were portlandite, ettringite and AFm phases, including mainly hydroxy-AFm (C_4AH_{13}, a broad peak that possibly corresponds to a solid solution of hemicarboaluminate and hydroxide substituted monosulphate) (Matschei et al., 2007) and monocarboaluminate (with a small peak). The formation of carboaluminate phases in the paste system can be indicative of a small addition of calcite to the clinker used in this study. This favours and conditions the formation of hemicarboaluminate which converts to monocarboaluminate as hydration proceeds (Fernandez et al., 2018; Ipavec et al., 2011; Zajac et al., 2014). The peaks corresponding to the anhydrous phases of C_3S, C_2S and C_4AF were also visible in all the samples. Overall, the qualitative phase analysis of the XRD scans showed similar hydration products and no significant changes in the peak positions and the intensities of corresponding crystalline phases between the control sample and all the other sonicated pastes. This indicates that the characteristic power and frequency of PUS employed in this study did not alter the reaction path (in agreement with the findings of Peters (2017), using different materials and arrangements for the ultrasound delivery). Nor did it change the main hydration products of the PC paste system mixed at w/c = 0.50 after 7 days of hydration. The crystalline products and the corresponding intensities detected by the XRD scan were found to be roughly identical to those of the sonicated products at various frequencies. Slight differences in the intensities of the AFt and AFm phases could be due to a higher sensitivity of these phases to the sample preparation than the AH_3 and portlandite (Scrivener et al., 2016). Despite the formation of similar crystalline hydrates detected by XRD, more investigation is needed to get an insight into the amorphous hydrates using a different technique, as the ICP-OES revealed appreciable changes in the available ionic species in the pore solution among the samples.

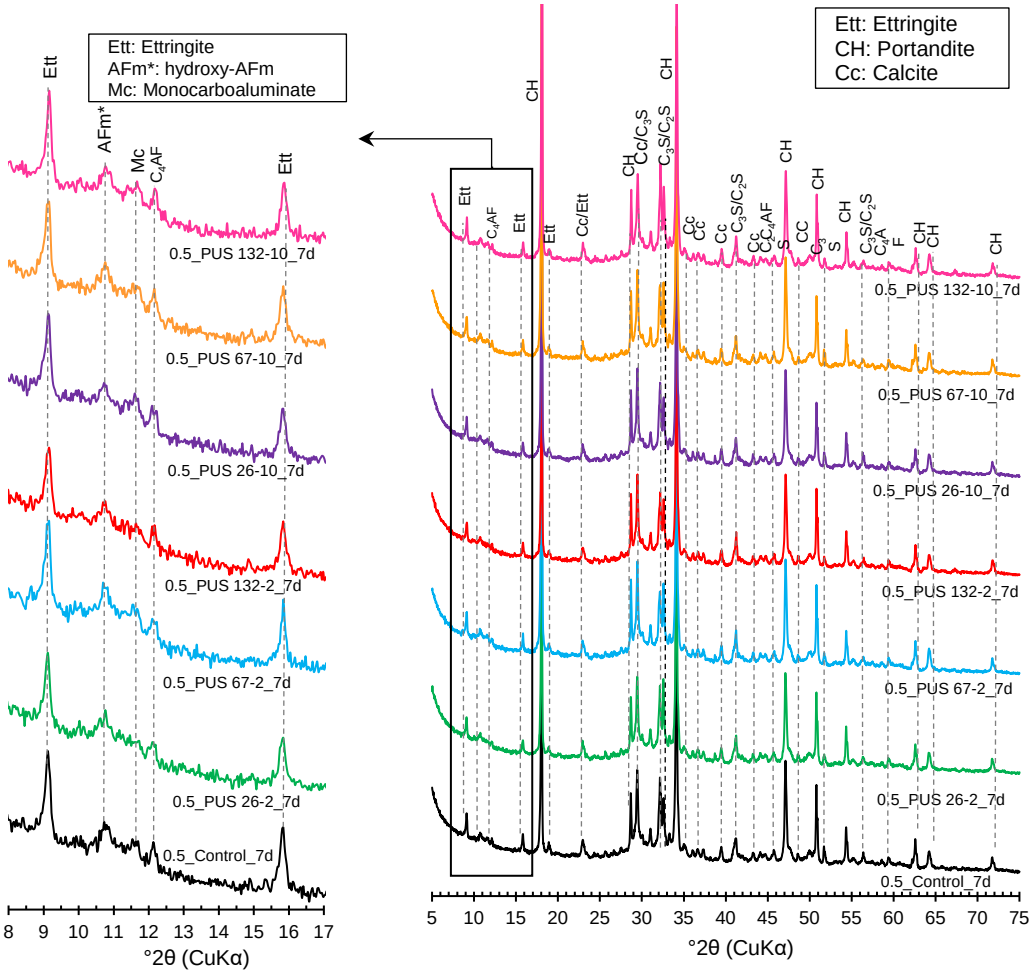

Fig. 4.5. XRD-patterns for the hardened PC pastes, mixes treated by ultrasound at 26, 67 and 132 kHz for durations of 2 and 10 min; all mixed at w/c = 0.50 after 7 days of sealed hydration. The main peaks of hydrates and anhydrous phases are indicated, and the details of low angles are shown.

4.2.2. TG/DTG analysis

Fig. 4.6 presents the TGA weight loss and the corresponding derivative (DTG) curves for the hardened pastes subjected to PUS at frequencies of 26, 67 and 132 kHz, treated for 2 and 10 min, all with w/c = 0.50 and sealed hydrated for 7 days. As with the previous analyses, one control sample without sonication treatment was compared to the others. The TGA/DTG spectra showed similar hydration products to the XRD analysis including ettringite, C–S–H, portlandite, and calcite for all the samples. Also, a mass loss at around 150 °C (clarified in Fig. 6) indicated the presence of AFm phases for all the pastes corresponding to monocarboaluminate/hemicarboaluminate as observed in the XRD patterns. From the TGA data, however, the mass losses in the various

samples looked slightly different, indicating marginal differences in the amount of some hydrates. Therefore, the weight loss values of the decomposition regions that correspond to the hydrated compounds were calculated and used to perform a semi-quantification of the amounts of bound water, amorphous aluminium hydroxide, portlandite and carbonates in various samples using the methods explained in chapter 3 (section 6.3). The results of the semi-quantification are depicted in Fig. 4.7.

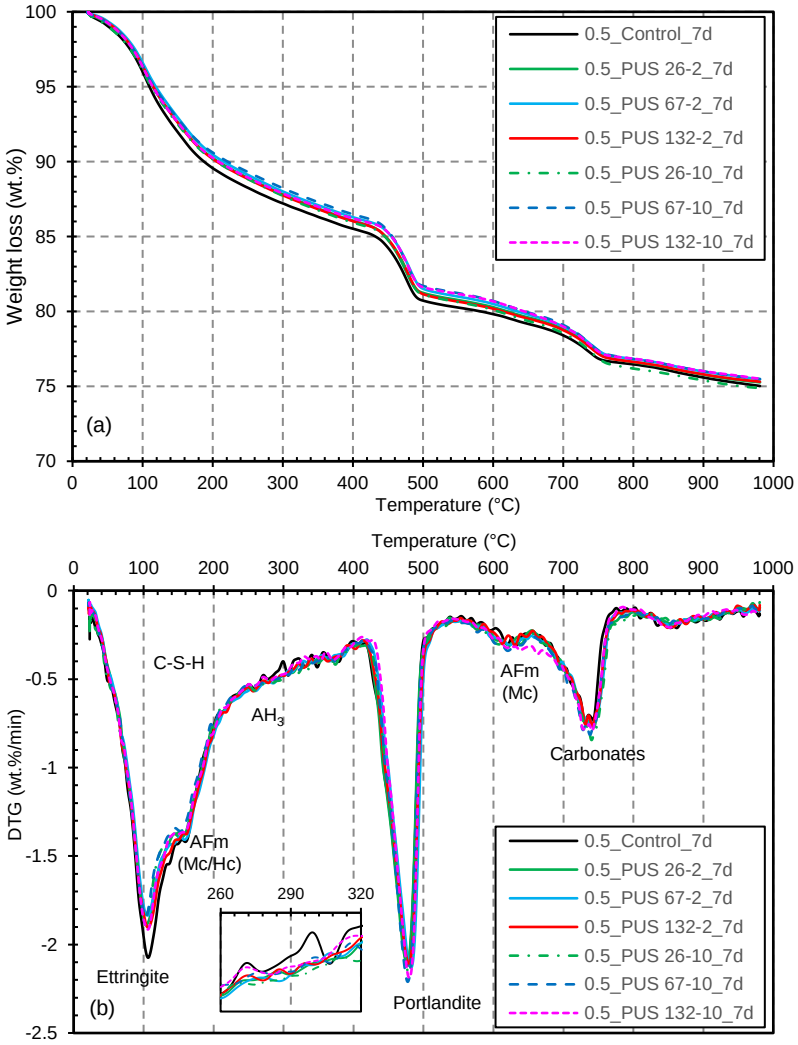

Fig. 4.6. TGA curves (a) and derivative of TGA (DTG) curves (b) of the hardened PC pastes, mixes treated by PUS at 26 , 67 and 132 kHz for 2 and 10 minutes compared to the untreated mix (Control); all mixed at w/c = 0.50 after 7 days of sealed hydration.

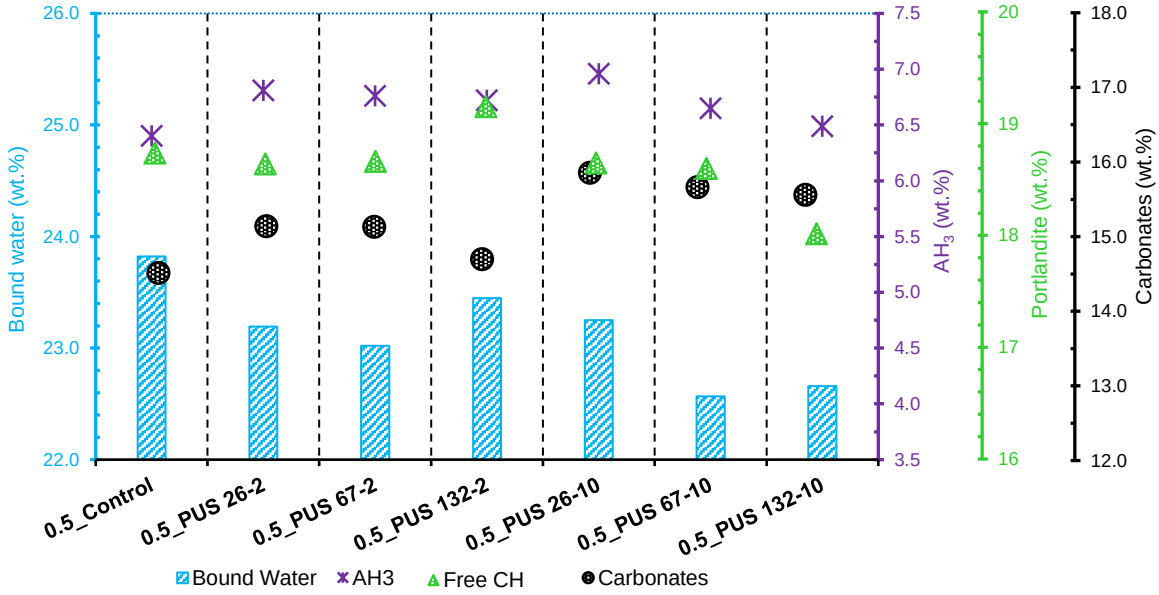

Fig. 4.7. Semi-quantification of bound water, aluminium hydroxide (AH_3), portlandite and carbonates obtained from the TGA/DTG data for hardened PC pastes, mixes treated by PUS at 26, 67 and 132 kHz for 2 and 10 min compared to the untreated mix (Control); all mixed at w/c = 0.50 after 7 days of sealed hydration.

As noted in chapter 3 (section 6.3), amorphous aluminium hydroxide (AH_3) in hydrated PC systems decomposes between 260 °C and 320 °C. The dehydroxylation temperature of AH_3, however, is reported to match that of calcium aluminate hydrates in katoite (C_3AH_6), some AFm phases and ettringite (Scrivener et al., 2016). From the XRD patterns (Fig. 4.5), we know that there was no characteristic peak visible with respect to hydrogarnet or its family endmembers like katoite. Also, the main weight loss of ettringite due to the dehydration was observed at around 100 °C (see Fig. 4.6), while showing only a negligible mass loss due to the dehydroxylation of the aluminium hydroxide between 200 °C and 400 °C (Lothenbach et al., 2008). The presence of hydroxy-AFm and monocarboaluminate (not monosulfoaluminate) as AFm phases were approximately identical by very weak peaks in the XRD analysis in all samples. For the monocarbonate ($4CaO{\cdot}Al_2O_3{\cdot}CO_3{\cdot}11H_2O$) or hemicarbonate ($4CaO{\cdot}Al_2O_3{\cdot}0.5CO_3{\cdot}12H_2O$) the interlayer water (five molecules) removes at temperatures between 60 °C and 200 °C and the loss of the octahedral layer water (six molecules) occurs at a temperature between 200 °C and

300 °C (Scrivener et al., 2016). Therefore, to make a qualitative evaluation in this study, we could, with a good level of confidence, conservatively attribute the temperature region between 260 °C and 320 °C in all the TGA/DTG spectra mainly due to the dehydroxylation of AH_3. Hence the corresponding mass loss was used for the semi-quantification of the amount of amorphous AH_3.

The bound water content at 7 days of hydration (demonstrated by bar chart in Fig. 4.7) decreased in all the samples treated by PUS, in both the short and long exposure times. Alongside the visual comparison of the deconvolution of DTG curves corresponding to the ettringite (designated in Fig. 4.6), it can be hypothesised that the application of characteristic PUS in this study can interfere slightly with the formation and stabilisation of the early hydrates which contain a relatively high quantity of bound water in their structures (Taylor, 1997). In particular, fully hydrated ettringite ($3CaO{\cdot}Al_2O_3{\cdot}3CaSO_4{\cdot}32H_2O$) with a molecular weight of 1255 g/mol, loses 576 g/mol water which is the highest value amongst common hydration products of PC systems (Scrivener et al., 2016). Having the least effect of interference, the samples treated by ultrasound at 132 kHz for 2 min exhibited the highest bound water, whilst the lowest bound water was obtained for the pastes subjected to PUS at 67 and 132 kHz for 10 min (about 5.3% and 4.9% lower than the control, respectively). Not all the samples subjected to the longer exposure of PUS achieved a low bound water, where 26 kHz ranked the second highest content.

On the other hand, the amount of amorphous AH_3 increased in all the pastes when ultrasound was introduced compared to the Control, which was in agreement with the results of Al concentrations at 7 days of hydration discussed in section 4.1. As presented in Fig. 4.7, PUS at 26 kHz leads to the highest quantities of AH_3 formation in both 2 and 10 min of sonication at around 6% and 9%, respectively. 132 kHz at the same exposure durations is responsible for the lowest AH_3 content by 5% and 1.5% individually, for 2 and 10 min ultrasonication, all compared to the control. These findings underpin the influence of ultrasound power density on the formation of amorphous AH_3 hydrate where the higher the ultrasound power dissipated to the PC system; the more AH_3 hydrate is formed. Combined with the discussion made in section 4.1, these results support the proposition that ultrasound irradiation can increase the dissolution rate of aluminate in PC clinker.

Except for the frequency of 132 kHz, the absolute portlandite quantities did not vary significantly between the untreated paste and the samples subjected to other characteristic ultrasonication. As shown in Fig. 4.7, paste under sonication at 132 kHz for 2 minutes has a slightly higher bound water content compared to other ultrasound treated samples along with an increase in portlandite content. This observation supports the hypothesis that short irradiation of a higher frequency ultrasound (here at 132 kHz) moderately promotes the precipitation of portlandite, whilst longer acoustic irradiation at the same frequency adversely affects the formation of portlandite, where the bound water is also significantly lower than the untreated sample.

Fig. 4.7 also shows the results of the weight losses corresponding to the decarbonation region (600-980 °C) expressed as percentages of the sample weight at 980 °C for samples hydrated at 7 days. The deconvolution of carbonates shown in Fig. 4.6 could be related to the limestone filler on the cement and also denoting that the samples have undergone carbonation but at slightly different levels. Assuming negligible carbonation was allowed during the hydration and grinding of sample for analysis, an explanation for observing the detected carbonation is related to the method employed in this study for stopping hydration. As described in chapter 3 (section 6.1), IPA was used for the solvent exchange. Subsequent gentle drying at 40 °C inside a desiccator was performed to remove the excess water from the capillary pores prior to performing TGA. Taylor (1997) reported that unless taking an extreme drying procedure (e.g. heating at 105 °C), organic liquids cannot be thoroughly removed from cement pastes and react with C-S-H to produce CO_2, affecting the mass losses in TGA with respect to the carbonates. A very gentle approach, however, was adopted in this study, to limit the decomposition and alteration of hydrates, particularly ettringite.

The higher the power of ultrasonication and/or the longer the duration of exposure, the higher the degree of carbonation (see the hatched circles in Fig. 4.7). The lowest energy of ultrasound associated with 132 kHz (for 2 min), resulted in carbonates that were nearly the same as the Control. The highest ultrasound power (26 kHz for 10 min) delivered the highest level of carbonation (about 9.2%) and also showed the highest amount of AH_3.

5. PC pastes with w/c = 0.80

Following the examination of a normal PC paste subjected to ultrasonic irradiation, it is necessary to understand whether the efficiency of acoustic cavitation in the PC system is dependent on the water content in the system. Therefore, this section investigates the influence of higher amounts of “free water” available in the large capillaries, before it is physically absorbed onto the surface or held in small capillary and gel pores, to induce effective ultrasonic cavitation. Similar to the previous part, the study first delves into the analysis of the pore solution composition together with the semi-quantification of some hydrates at 7 and 28 days using TGA/DTG techniques in pastes with w/c ratios of 0.80. The XRD analysis on samples with w/c = 0.50 (section 4.2.1) concluded with the formation of identical hydrates assemblages among the untreated and sonicated hardened pastes at all frequencies. Accordingly, including the XRD data for w/c = 0.80 system is considered dispensable. To be even more concise, the results of only 2 min ultrasonic processing at 26 kHz are presented in this section.

5.1. *Pore solution composition*

Fig. 4.8(a)-(h) and Fig. 9 present the total concentrations of Ca, K, Na, S, Al, Fe, Mg and Si ionic species by ICP-OES and hydroxide by pH measurement in the pore solutions of PC pastes mixed at w/c = 0.80, as a function of time up to 28 days. The results of the untreated mix (labelled as 0.8_Control) were compared with the mix immediately treated by PUS at 26 kHz for 2 min and plotted in graphs with the control paste at w/c = 0.50. Overall, similar trends were observed in Ca and S concentrations at the higher w/c, compared to the system with w/c = 0.50. Likewise, the pore solution here is still dominated by Ca, S, K, Na and hydroxide. However, there are some differences in later hydration particularly at 28 days.

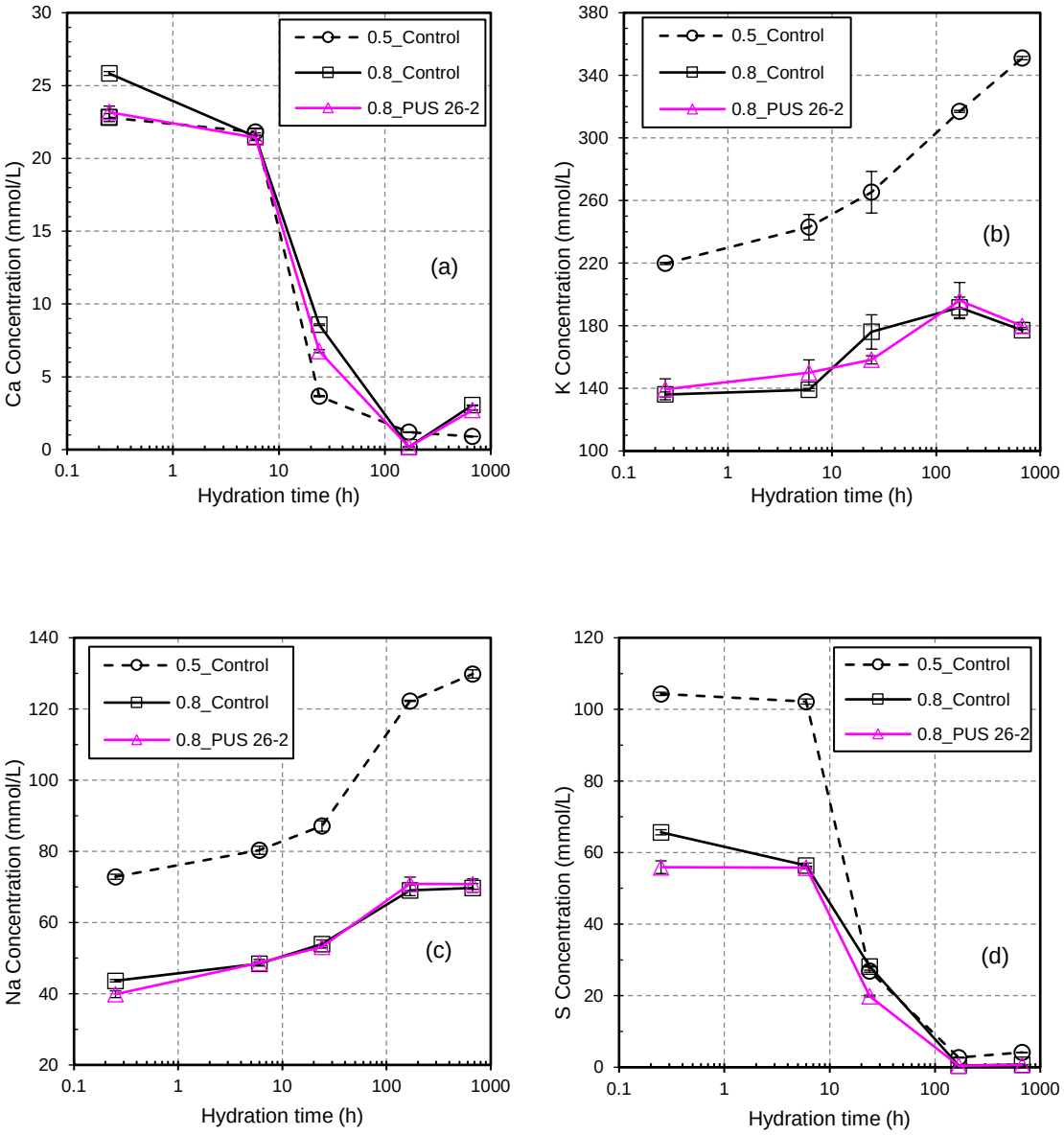

Fig. 4.8. ICP-OES measurement of total concentrations of elements ((a) to (h)) in the pore solution expressed from the PC pastes, mix with w/c = 0.80 subjected to PUS at 26 kHz for a duration of 2 min compared to untreated mixes at w/c = 0.50 and 0.80 (0.5_Control and 0.8_Control).

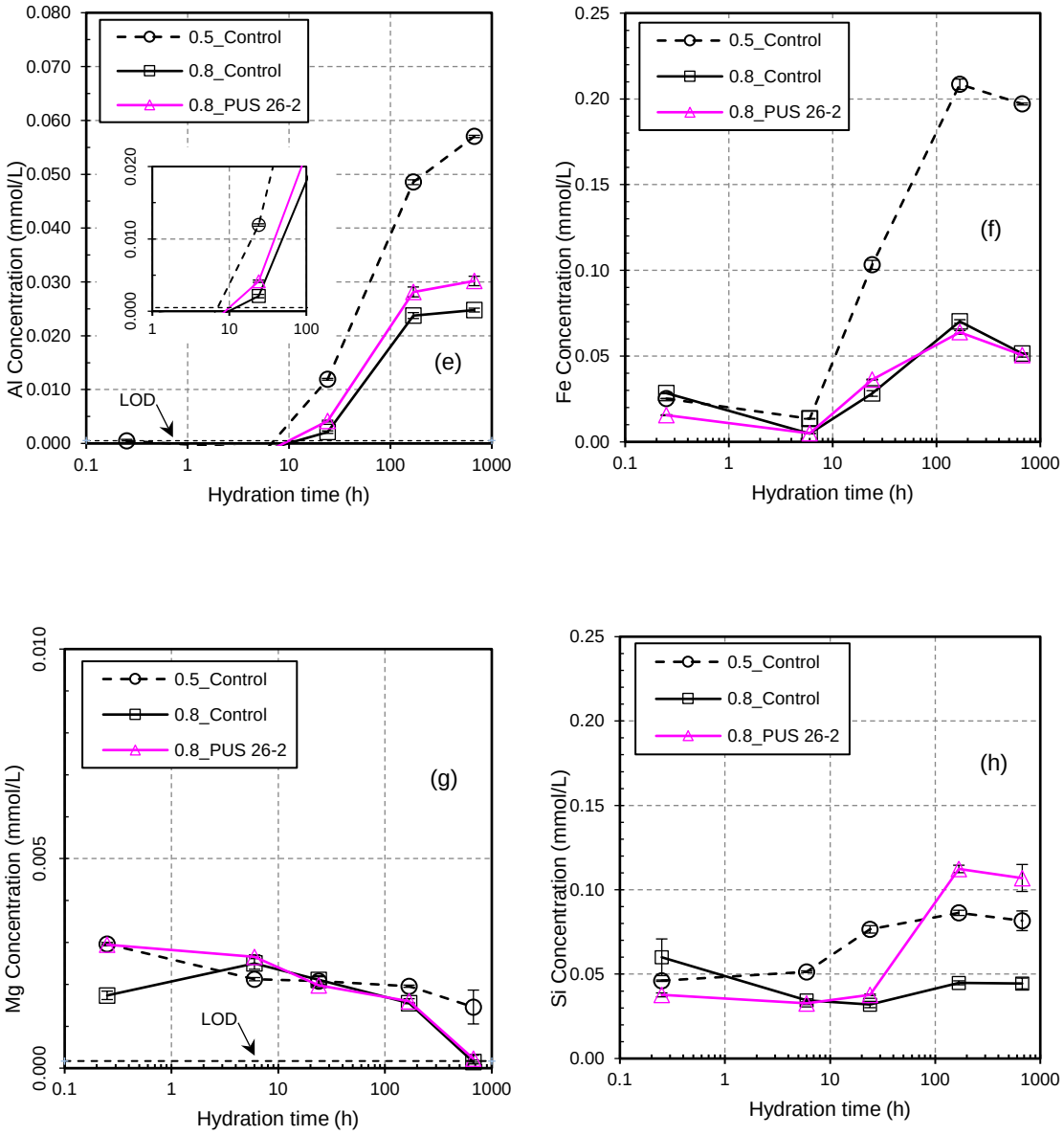

Fig. 4.8. (Continued) ICP-OES measurement of total concentrations of elements ((a) to (h)) in the pore solution expressed from the PC pastes, mix with w/c = 0.80 subjected to PUS at 26 kHz for a duration of 2 min compared to untreated mixes at w/c = 0.50 and 0.80 (0.5_Control and 0.8_Control).

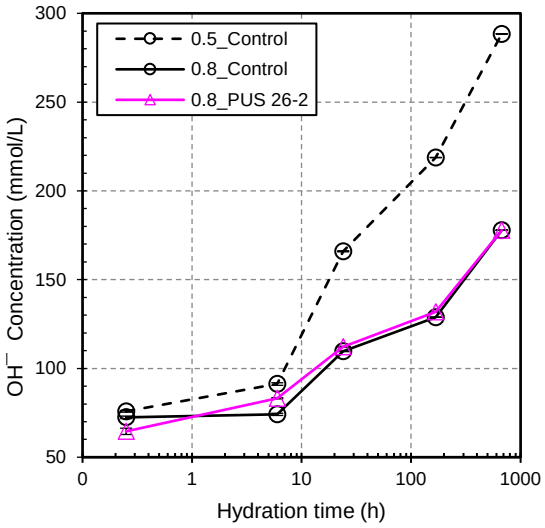

Fig. 4.9. Concentration of hydroxide ions by pH measurement of pore solution immediately after extraction using a calibrated electrode

Consist with the observations made in the lower w/c system, Ca concentration was initially subsided by ultrasonic irradiation at 26 kHz, compared to the control sample immediately after mixing and ultrasonication. The extent of the decrease in Ca concentration detected in w/c = 0.80 at this time signified a marked drop (about 10%) which was more than that of in w/c = 0.50 (Fig. 4.8(a)). This suggests that perhaps the acoustic cavitation in the paste system with higher free water is generated more effectively. In addition, OH^- began the pore solution development in sonicated paste with a lower concentration compared to that of the untreated sample (see Fig 4.9). As commented in section 4.1, these observations together may link to the effect of ultrasound on the limited intensification of early portlandite precipitation out of supersaturated pore fluid with calcium hydroxide. As can be deduced from Fig. 4.8(d), a similar effect is also present for S at the beginning of hydration. Both highlight that the degree of saturation of the solution with respect to Ca and S can be adversely affected by PUS at very early hydration, disturbing the favourable conditions for the formation of ettringite during very early hydration.

The concentration of S in higher w/c, although significantly lower during 6 hours of hydration (due to the dilution effect), suddenly overlapped with that of w/c = 0.50 at 1 and 7 days, finally ending after 28 days hydration, again at a slightly lower concentration. Under the influence of ultrasound at 26 kHz, a decrease in the S concentration was evidenced in samples with higher

w/c at 1 day, which suggests that more ettringite might be precipitated during the middle period of hydration versus the control paste.

The dilution effect (more free water available to be consumed by hydration products) led to a lower concentration of alkalis in the pore solutions of samples at a higher w/c ratio in comparison to that of the lower w/c (as per Fig. 4.8(b) and (c)). In the sonicated samples, the concentrations of alkalis did not appear to be appreciably different from the non-sonicated samples. The concentrations of alkalis in samples with a higher w/c rose at a broadly slower rate compared to the trends detected in the lower w/c mixes. The other contradiction between the alkali trends observed in two w/c ratios was observed between 7 and 28 days where no change and a drop were detected individually for Na and K. This could be due to more uptake of alkali by C-S-H hydrates during the later age hydration of pastes with higher w/c ratios in which the proportion of residual unhydrated PC decreased due to a higher degree of hydration. Additionally, through the hydration in the system containing higher water, alkalis incorporated in aluminate and silicate phases dissolved at a lower rate and more capillary water was available to be consumed by various hydrates, both of which lead to a lower rate of increase in alkali concentration. Therefore, no notable sign of ultrasound interaction on alkalis was observed in pastes with w/c = 0.80.

Similar to the results of w/c = 0.50, the Al concentration during early hydration was below the LOD as the amount of Al released from the dissolution of aluminates was consumed to nucleate and precipitate the network of ettringite. Upon further hydration of the aluminates, more Al was produced and continues to increase in both systems. The rate of increase, however, was slower in the high w/c system due to the dilution effect. Consistent with the findings for the pastes with lower w/c ratios (section 4.1), the ultrasonic irradiation causes persistent enhancement of the release of Al into the pore solution in comparison with the control pore solution (see Fig. 4.8(e)). This can be linked to the effect of PUS on the dissolution rate of aluminate.

The fairly consistent trends derived from the results of Fe during early hydration (Fig. 4.8(f)) suggests minimum change in aluminate ferrite hydration in both systems under the effects of dilution. The remaining hydration, however, proceeded with different amounts of Fe concentration but at a lower rate for the system with higher w/c ratios, which is likely connected to the dilution effect.

Due to the dilution effect, the Mg concentrations (shown in Fig. 4.8(g)) did not exhibit much difference through the pore solution development, even though all the values were still detectable above the LOD. The positive effect of PUS to improve the release of Mg into the pore solution was evidenced at the beginning of hydration which is in agreement with the data obtained for w/c = 0.50.

As can be seen in Fig. 4.8(h), samples subjected to ultrasound yield less Si in the pore solution, whereas Si reaches a higher concentration at a later age of hydration compared to both the untreated pastes mixed at w/c = 0.50 and 0.80. This condition may favour the formation of C-S-H with a higher Si/Ca ratio in the system effected by PUS.

5.2. *TG/DTG analysis*

To follow the effects of PUS on reactions in the PC system with w/c = 0.80, TG analyses were performed on pastes treated by PUS at 26 kHz for 2 min and cured at 7 and 28 days. The corresponding curves of TGA/DTG are individually presented in Fig. 4.10 and Fig. 4.11. On a par with the previous analyses, one control sample without sonication treatment was compared to the others. Likewise, the results of semi-quantification of the bound water, AH_3, portlandite and carbonates in various samples using the methods explained in chapter 3 (section 6.3) are illustrated in Fig. 4.12.

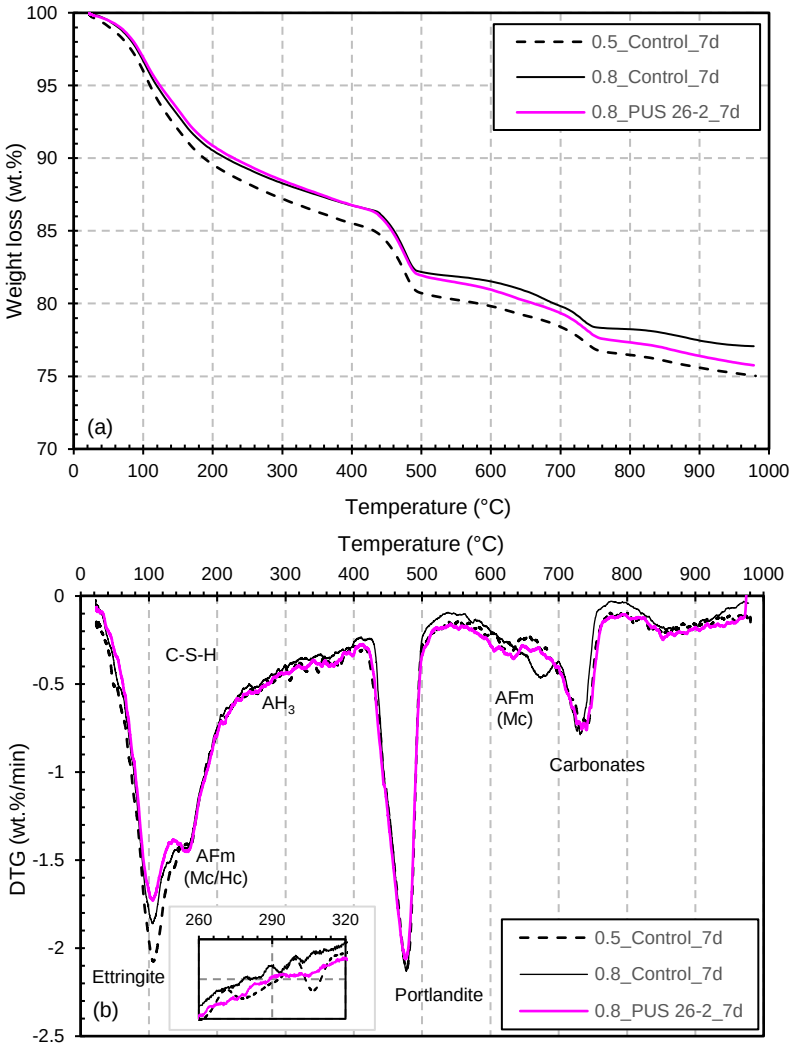

Fig. 4.10. TGA curves (a) and derivatives of TGA (DTG) curves (b) of the hardened PC pastes mixed at w/c = 0.80 and subjected to PUS at 26 kHz for 2 min compared to untreated mixes (Control) at w/c = 0.50 and 0.80, all after 7 days of sealed hydration.

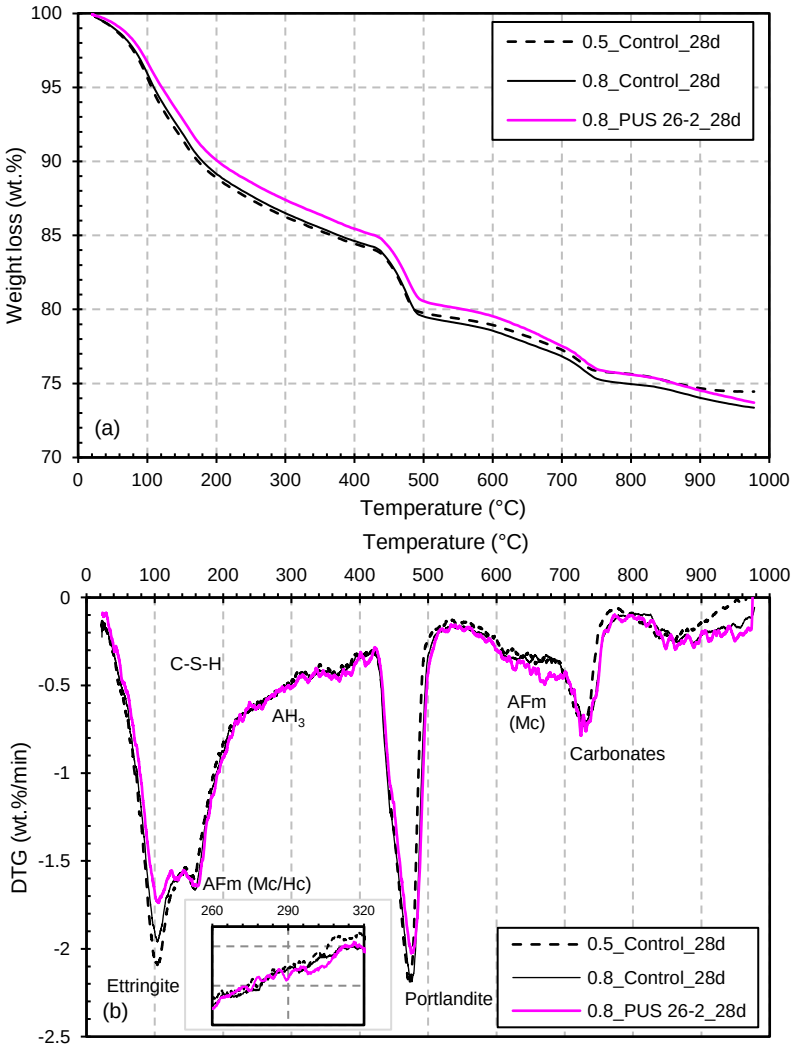

Fig. 4.11. TGA curves (a) and derivatives of TGA (DTG) curves (b) of the hardened PC pastes mixed at w/c = 0.80 and subjected to PUS at 26 kHz for 2 min compared to untreated mixes (Control) at w/c = 0.50 and 0.80, all after 28 days of sealed hydration.

From the TGA/DTG plots, it is clear that ettringite formation has been slightly supressed when ultrasound was applied at 26 kHz as shown in the results of both 7 and 28 days hydration. The total amount of hydrates deduced from the estimation of bound water (Fig. 4.12), however, appears not to have been affected at an early age (7 days) where the bound water was marginally higher than the Control (w/c = 0.80). In parallel, the AH_3 quantity also increased as was expected, based on the rise in Al concentration in the pore solution (shown in Fig. 4.8(e)). It is noted that the higher bound water of paste with w/c = 0.8 at 28 days could be related to the fact that higher w/c cement paste generally exhibit a higher degree of hydration than lower w/c paste as there is

more space available for the dissolution of reactant and the nucleation/precipitation of hydration products (Bentz, 2006).

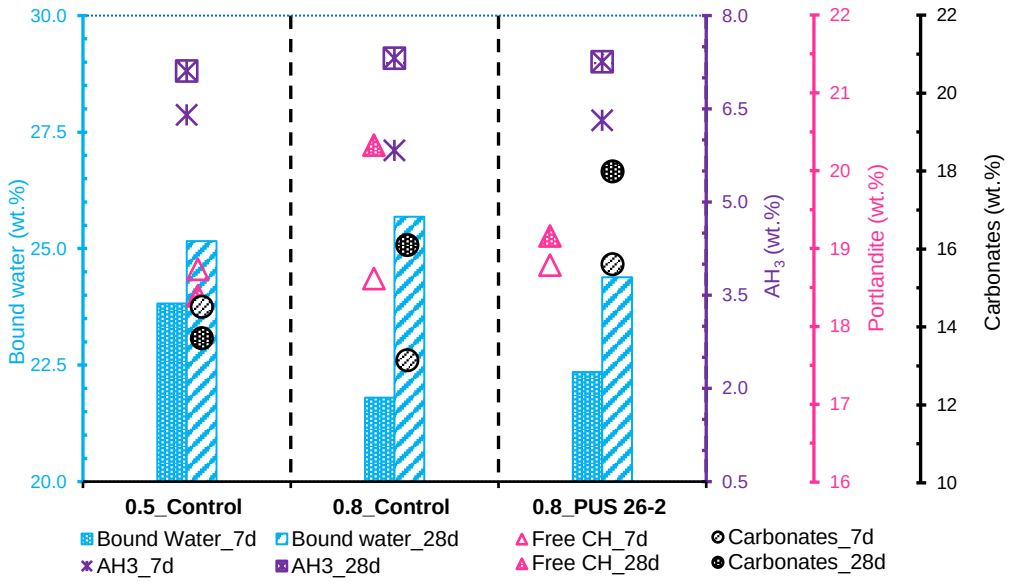

Fig. 4.12. Semi-quantification of bound water, aluminium hydroxide (AH_3), portlandite and carbonates obtained from TGA/DTG data for hardened PC pastes, mixes treated by PUS at 26 kHz for 2 min compared to untreated mixes (Control) at w/c = 0.50 and 0.80; after 7 and 28 days of sealed hydration.

It has been widely investigated that the formation of portlandite in a PC system continues after 7 days, but at a slow rate, due to the oversaturation of the pore solution with respect to calcium hydroxide from early hydration onwards (Taylor, 1997). Quantification of portlandite in pastes at w/c = 0.5 in this study, however, shows a negligible decrease in the PC sample at 28 days compared to 7 days. This could be due to the formation of hydration products which consume Ca sources e.g. carboaluminates. Additionally, the relative error of quantification based on TGA due to the sample preparation and measurement was reported to be between ±5% and 10%. Thus, the observed disagreement with the expected trend could be due to measurement error. In the sonicated sample, the portlandite was a little higher in quantity than the control pastes at 7 days which is in agreement to the comment made on the influence of PUS to induce the precipitation of calcium hydroxide. In the later stage of hydration (28 days), however, the portlandite in the control sample was rather higher than that in the sonicated paste.

As seen in the pastes at w/c = 0.5 and assuming that the curing conditions did not permit carbonation, PUS at 26 kHz markedly increased the carbonate content (see circles in Fig. 4.12) both at 7 days and 28 days of hydration. In comparison with the control sample, ultrasound intensified carbonation at 7 and 28 days by 19% and 12%, respectively. This effect might be in connection with the reduction in particle size, pitting and enhanced mass transfer due to the cavitation that can lead to ultrasound assisted carbonation. This will be discussed in section 6.2. The degree of ultrasound impact on the formation of carbonates in a higher w/c seems to be significantly higher than the ultrasound-assisted carbonation that occurred in w/c = 0.50.

6. Further discussion

6.1. *Impact on ettringite formation*

To achieve a better understanding of the overall impact of PUS on the pore solutions of PC systems, focusing on an early period of hydration is imperative, because the ultrasound irradiation in this work was applied at 15 min after mixing. This stage at which ultrasound cavitation can potentially affect the system corresponds to the period of lower hydration activity known as a dormant period (Beaudoin and Odler, 2019). The induction stage (within the first few hours) follows the initial reactions which last only a few minutes mainly due to the hydration of the aluminate and alite phases as well as the hydration of calcium sulphate hemihydrate. There is an agreement amongst the literature that the initial hydration reactions lead to the formation of an amorphous colloidal gel layer (Bullard et al., 2011; Locher, 2006; Taylor, 1997) over the surface of (typically polymineralic) cement grains. The protective gel membrane is known to be rich in Al, Si as well as Ca and S which favours the nucleation of stubby rods of ettringite at the edge of the gel within a few minutes (Taylor, 1997). This is about the time that the ultrasound was introduced to the system in this study. The results obtained from the characterisation of the pore solution and the thermal analyses as well as the particle size distribution, provide enough evidence that the primary mode of action for PUS at this stage could be the exfoliation of the surface and partial disaggregation of the already formed amorphous aluminate-rich gel layer on coarse size fractions of cement grains. Consequently, these effects increase the extent of the solid-aqueous interface, hence raising the dissolution rate of the phases and the availability of ionic species to participate in the precipitation reactions of hydration (Davies et al., 2015; Luque de Castro and Priego-Capote, 2007). The significant increase in Ca and Al concentrations as well as the limited rise in Fe, Mg and Si concentrations (in a normal w/c ratio) strengthen the position that ultrasound seems to be able to increase the availability of species to take part in hydration reactions, thus promoting the formation of corresponding phases. The relative increase in amorphous aluminium hydroxide in the system was directly confirmed by the TG/DTG analysis. Concurrently, the mode of action for surface erosion and disaggregation, however, can adversely yield a disruptive effect at the time the gel layer has formed around the grains. During ultrasound exposure, the asymmetric collapse of cavitation bubbles produces shock waves and microstreaming which induce microjets

and shear forces (Luque de Castro and Priego-Capote, 2007; Mason and Lorimer, 2002). The occurrence of these effects in the vicinity of coarser cement grains (through the large capillary water-filled space) can effectively distress the short ettringite rods already nucleated in this region. Consequently, the formation of outer product C-S-H in the initially water-filled space that normally engulfs or nucleates on ettringite rod network (Locher, 2006; Taylor, 1997) will be disturbed or delayed. In normal conditions, the C-S-H precipitation follows the extensive hydration of alite (Richardson, 2000) during the middle stage of hydration (beginning at about 3 hours). In the aftermath of ultrasonic agitation in the system, hydration normally proceeds but it may take more time for the outer product C-S-H to re-produce on the newly formed ettringite network than in the non-sonicated system. As confirmed by a comparison of the deconvolutions identified in the DTG plots that correspond to ettringite, slightly less ettringite forms when ultrasound is applied whilst the upper areas corresponding to C-S-H phases appear not to be notably changed (see Fig. 4.6 for w/c =0.50 and Fig. 4.10 and Fig. 4.11 for w/c = 0.80).

6.2. *Ultrasound-assisted precipitation and carbonation*

An additional explanation can be proposed for the impact of ultrasound on ettringite formation during initial hydration (during the pre-induction and induction periods) in relation to the initial concentrations of Ca and hydroxide in the pore solutions. The results show there are initially lower concentrations of Ca and hydroxide in all the ultrasound treated samples accounting for lower pH compared to the non-sonicated samples, in which the hydroxide continues until 28 days. This is abnormal, as we would normally expect the pore solution in PC to be supersaturated at early hydration with respect to portlandite and for ettringite to be produced as long as calcium hydroxide and gypsum are present, respectively (Rothstein et al., 2002). This is mainly because of the continuous release of Ca and Al from the dissolution of the clinker phases (mainly aluminate) and gypsum, with S from both the clinker alkali sulphate, and gypsum and hydroxide mainly from the reversible reaction of calcium hydroxide with alkali sulphates that form gypsum (Beaudoin and Odler, 2019; Taylor, 1997). However, it appears that a small amount of Ca is depleted from the system immediately upon ultrasonication that coincides with the measured decline in hydroxide ions (associated with a decrease in pH) against the non-sonicated paste. This is regardless of the free water content as can be observed in both w/c ratios studied in this work. To find an explanation for this observation, we need to focus on the effect of sonocrystallisation (Luque de Castro and Priego-Capote, 2007).This has been widely investigated in the case of ultrasound assisted crystallisation of inorganic materials (Askari et al., 2013; Mason et al., 1989) and particularly precipitation of calcium carbonate from the supersaturated solution. A number of studies (Boels et al., 2010; Nishida, 2004; Wagterveld et al., 2012) have reported that ultrasound irradiation can cause suspended crystals to mechanically break down into small fragments thereby providing many seed crystals and a larger specific surface area available for nucleation. The precipitation of calcium carbonate from concentrated calcium hydroxide slurry has also been examined (Lopez-Periago et al., 2010) where the ultrasound (in combination of supercritical CO_2) proved to significantly enhance the conversion rate of $Ca(OH)_2$ to the stable polymorph of calcium carbonate. Ultrasound was found to promote the removal of the covering $CaCO_3$ layer around the starting nucleates leading to further dissolution of $Ca(OH)_2$. Similarly, ultrasound has been proven (Santos and Van Gerven, 2011) to stimulate the breakage of the carbonate

passivating layer and enhance reaction kinetics which has enabled the intensification of mineral carbonation processes. Although the atmospheric carbonation of calcium hydroxide or calcium bearing minerals occur at a slow rate, we may observe a very low but still detectable intensification of carbonation upon ultrasonication in the systems studied in this work. The evidence from the pore solution composition where small decreases in Ca and hydroxide concentrations have occurred, may reveal the limited carbonation of supersaturated calcium hydroxide immediately after ultrasound exposure at early hydration. The consistent increases in carbonates detected by TGA in the sonicated samples in comparison with the untreated pastes (either with w/c = 0.50 by up to 10% in sonication at 26 kHz for a duration of 10 min or w/c = 0.80 by 19% at 26 kHz for only 2 min), are in agreement with the hypothesis brought forward about the ultrasound-intensified carbonation of cement paste as discussed above and highlighted in the results (sections 4.2.2 and 5.2). As discussed in section 4.2.2, both the power and duration of ultrasound exposure appeared to be influential on the extent of carbonation.

Making adjustment is difficult for the slightly lower S at the beginning of hydration due to some characteristic ultrasound irradiation. However, one conceivable explanation could be in connection with the considerable increment in the rate of sulphate precipitation from acidic sulphate-containing wastewater which was documented by Davies et al. (2015). Although being a different system, PUS at high acoustic energy (26 kHz) for durations of both 2 and 10 min in the present work could be similarly responsible for the limited precipitation of a small proportion of sulphate ions in the oversaturated pore solution with respect to gypsum, leading to a decline in the S concentration at 15 min (see Fig. 4.3 (d)).

Upon progress in hydration, ultrasound-induced cavitation during a longer irradiation (10 min was used in this study) could have led to a more effective erosion of C_3A and/or C_3S phases in the clinker, releasing more Ca, Al and Si into the pore solution as the evidence from the pore solution data demonstrated at the age of 6 hours. Based on the mechanism discussed, a pore solution with a slightly less supersaturating degree can still accommodate more dissolved Ca ions due to its relatively high saturation factor of 2-3 (compared to the gypsum saturation in which the factor never exceeds 1.3) as reported by Gartner et al. (1985). Therefore, Ca concentration in

samples under longer exposure of ultrasound increases considerably higher than the shorter treated samples whilst their pH is slightly higher.

Based on a different perspective, the postulation about the limited precipitation of calcium hydroxide due to the ultrasound-induced sonocrystallisation could also explain the marginal decrease in ettringite formation in sonicated samples during the early period of hydration, as discussed in section 6.1. At early hydration, ettringite formation is consistent with the following reactions (as per Eq. (1) and Eq. (2)) (Berry et al., 1989), which are based on two sources of sulphates available in the pore solution: gypsum and clinker alkali sulphates. Precipitation of ettringite from the latter (Eq. (2)) supplies hydroxide ions and sustains a high pH of pore solution.

$$3CaSO_4 + 3CH + 2AH_3 \rightarrow C_3A.3CS.32H_2O \qquad \text{Eq. (1)}$$

$$3M_2SO_4 + 6CH + 2AH_3 \rightarrow C_3A.3CS.32H_2O + 6M^+ + 6OH^- \qquad \text{Eq. (2)}$$

where M could be either Na or K (or both). Although ultrasound was confirmed to enable the release of more Al into the pore solution, slightly lower amounts of calcium hydroxide may affect the formation of ettringite along with the production of alkalis and hydroxide (as can be deduced from Eq. (2)). The lower amount of hydroxide (Fig. 4.4) as well as a lower concentration of K in all the sonicated samples at 6 hours (see Fig. 4.3(b)) and that of Na in samples treated by some PUS conditions (Fig. 4.3(c)) in pastes with w/c = 0.50, can altogether be evidence to support the proposed mechanism.

As discussed in section 6.1, early hydration of C_3A and C_3S are known to cause the rapid formation of crystalline products and the development of a gel layer around the cement grains, which is effective in the coagulation of components of paste during the early stages of hydration. These effects are collectively proposed to be responsible for setting in PC systems, (Neville, 2011) which transits the fluid form to a rigid state. Thus, to examine the hypothesis on possible impacts of ultrasound on the formation of ettringite (and/or C-S-H) during early hydration, the setting characteristics of cement pastes upon ultrasonication were tested. As shown in Fig. 4.13, the initial and final setting times were measured in PC pastes with w/c = 0.30 treated by ultrasound at 26, 67 and 132 kHz for duration of 2 min and compared to the untreated paste and the mix with normal consistency (w/c = 0.24). The results indicate that ultrasound slightly extends both the initial and final setting times of PC pastes that can be related to the disturbed hydration of

aluminate and alite upon ultrasound irradiation. The level of impact seems to be inversely proportional to the order of PUS power densities used in this study.

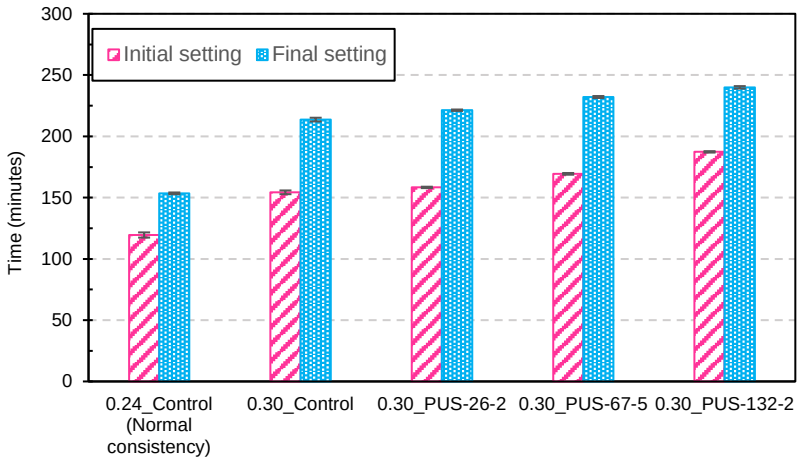

Fig. 4.13. Setting times for pastes treated by PUS at 26, 67 and 132kHz for 2 min compared to the non-sonicated (Control) paste all mixed at w/c = 0.30 and the paste at normal consistency (w/c = 0.24)

Concerning the results of the pore solution analysis that show changes in the concentration of Ca, Al, Fe and Si caused by ultrasound over the course of hydration, it appears highly probable that characteristic C-S-H with different Ca/Si and Al/Ca ratios and various concentration of foreign ions uptaken by C-S-H will be formed under the sonication treatment. For instance, the higher availability of Al during hydration may lead to the formation of C-S-H with higher Al. More investigations like X-ray microanalysis need to be carried out to characterise the C-S-H formed in the samples subjected to PUS.

6.3. *Proposing a promising application for ultrasound-enhanced formation of AH_3*

The key findings of this study are the increased supply of Al to the pore solution and the enhancement in dissolved amorphous aluminium hydroxide hydrate in PC pastes with various w/c ratios after ultrasound irradiation. This effect appears to have a promising application in the development of novel low-carbon binders based on calcium sulfoaluminate (CSA) cements (Gartner, 2004) as an alternative to PC. Ternesite has been studied by Australia's Commonwealth Scientific and Industrial Research Organisation (CSIRO) as a cementitious component of CSA clinker since the early 1990s (Sherman et al., 1995), but did not gain popularity due to its low hydration rate. However, its hydration has recently been found to be promoted by dissolved AH_3 (Ben Haha et al., 2015). More studies show that undersaturation and the availability of AH_3 enhance the dissolution of ternesite in sulphobelitic systems. In the clinker diluted with calcium sulphate, ternesite hydration appears to initiate once the sulphates are depleted from the pore solution and sufficient reactive aluminium sources are present (Bullerjahn et al., 2014; Montes et al., 2018). Accordingly, the observation made for the first time in the present research work strengthens the position that ultrasound processing has the potential to activate ternesite hydration in promising ternesite based cements by supplying more Al sources in the pore solution. Hence the author believes that this topic highly deserves further investigation.

7. Conclusions and outlook

In this research, the pore solution composition of PC pastes with two w/c ratios (0.50 and 0.80) were examined, combined with following their hydrates with XRD and TGA/DTG techniques. The following concluding remarks can be drawn from this investigation:

1) Applying PUS for up to 5 min marginally deagglomerates the coarse size fraction of PC particles in aqueous dispersion. Yet, ultrasound even at a longer exposure, may not be able to effectively disaggregate PC particles in normal pastes particularly the finer size fraction (< 10 μm).

2) Direct application of PUS to a PC paste does not alter the main types of PC hydration products but appreciably changes the pore solution composition, slightly affects the main hydrates quantity and potentially induces modifications in the composition of C-S-H hydrates e.g. the Ca/Si ratio or the levels of foreign ions uptake.

3) PC pastes at both w/c ratios of 0.50 and 0.80 upon ultrasonic processing contain substantially higher concentrations of Al in their pore solutions and accordingly higher contents of amorphous AH_3 among their hydration products. The greater the ultrasound power that is dissipated into a PC system, the more AH_3 hydrate is formed. The findings strengthen the position that ultrasound irradiation can enhance the dissolution rate of the aluminate phase in the PC clinker.

4) Sizable changes in Ca and Si concentrations upon ultrasound (particularly at a longer exposure) denote the influence of PUS on the dissolution of alite and/or aluminate phases due to the cavitation. The effect is more likely to be dominant on the coarse size fraction of the PC clinker grains.

5) The saturation of a pore solution with respect to Ca and S can be affected by ultrasound immediately after mixing and ultrasonication. The effect is more pronounced in pastes with higher w/c ratios.

6) Upon ultrasonication, the chemically bound water in normal PC pastes at 7 days reduces slightly. The theory suggested for the corresponding mechanism is that cavitation induced by PUS can temporarily disturb the formation of ettringite during a few minutes of hydration by disrupting the network of nucleates for the further formation of ettringite and the following outer product C-S-H during the initial stages of hydration. Afterwards, the system seems to recover, but it leads to a slightly reduced degree of hydration overall.

7) The results of the thermal analyses mirror the ultrasound-assisted carbonation in PC pastes which appear to be even more enhanced when PUS is applied to a PC system where higher free water is present in the PC system.

8. References

Askari, S., Alipour, S. M., Halladj, R., and Davood, A. F. (2013). Effects of ultrasound on the synthesis of zeolites: a review. *Journal of Porous Materials*, 20(1):285–302.

Beaudoin, J. and Odler, I. (2019). 5 - hydration, setting and hardening of Portland cement. In Hewlett, P. C. and Liska, M., editors, *Lea's Chemistry of Cement and Concrete (Fifth Edition)*, pages 157 – 250. Butterworth-Heinemann, fifth edition edition.

Ben Haha, M., Bullerjahn, F., and Maciej, Z. (2015). On the reactivity of ternesite. In *14th International Congress on the Chemistry of Cement, China*.

Bentz, D. P. (2006). Influence of water-to-cement ratio on hydration kinetics: Simple models based on spatial considerations. *Cement and Concrete Research*, 36(2):238–244.

Berry, E., Hemmings, R., Langley, W., and Carette, G. (1989). Beneficiated fly ash: Hydration, microstructure, and strength development in Portland cement systems. In *3rd International Conference on the Use of Fly Ash, Silica Fume, Slag, and Natural Pozzolans in Concrete, ACI SP-114, Trondheim*.

Boels, L., Wagterveld, R., Mayer, M., and Witkamp, G. (2010). Seeded calcite sonocrystallization. *Journal of Crystal Growth*, 312(7):961 – 966.

Bullard, J. W., Jennings, H. M., Livingston, R. A., Nonat, A., Scherer, G. W., Schweitzer, J. S., Scrivener, K. L., and Thomas, J. J. (2011). Mechanisms of cement hydration. *Cement and Concrete Research*, 41(12):1208–1223.

Bullerjahn, F., Schmitt, D., and Haha, M. B. (2014). Effect of raw mix design and of clinkering process on the formation and mineralogical composition of (ternesite) belite calcium sulphoaluminate ferrite clinker. *Cement and Concrete Research*, 59:87–95.

Bye, G., Livesey, P., and Struble, L. (2011). *Portland Cement*. ICE Publishing.

Davies, L. A., Dargue, A., Dean, J. R., and Deary, M. E. (2015). Use of 24khz ultrasound to improve sulfate precipitation from wastewater. *Ultrasonics Sonochemistry*, 23:424 – 431.

Fernandez, A., Garcia Calvo, J., and Alonso, M. (2018). Ordinary Portland cement composition for the optimization of the synergies of supplementary cementitious materials of ternary binders in hydration processes. *Cement and Concrete Composites*, 89:238 – 250.

Gartner, E. (2004). Industrially interesting approaches to "low-CO2" cements. *Cement and Concrete Research*, 34(9):1489–1498.

Gartner, E. M., Tang, F. J., and Weiss, S. J. (1985). Saturation factors for calcium hydroxide and calcium sulfates in fresh Portland cement pastes. *Journal of the American Ceramic Society*, 68(12):667–673.

Hackley, V., Lum, L.-S., Gintautas, V., and Ferraris, C. (2004). Particle size analysis by laser diffraction spectrometry: Application to cementitious powders. Technical report, NIST Interagency/Internal Report (NISTIR).

Ipavec, A., Gabrovsek, R., Vuk, T., Kaucic, V., Macek, J., and Meden, A. (2011). Carboaluminate phases formation during the hydration of calcite-containing Portland cement. *Journal of the American Ceramic Society*, 94(4):1238–1242.

Locher, F. W. (2006). *Cement: principles of production and use*. Verlag Bau+Technik GmbH.

Lopez-Periago, A. M., Pacciani, R., Garcia-Gonzalez, C., Vega, L. F., and Domingo, C. (2010). A breakthrough technique for the preparation of high-yield precipitated calcium carbonate. *The Journal of Supercritical Fluids*, 52(3):298 – 305.

Lothenbach, B., Saout], G. L., Gallucci, E., and Scrivener, K. (2008). Influence of limestone on the hydration of Portland cements. *Cement and Concrete Research*, 38(6):848 – 860.

Lothenbach, B. and Winnefeld, F. (2006). Thermodynamic modelling of the hydration of Portland cement. *Cement and Concrete Research*, 36(2):209 – 226.

Lothenbach, B., Winnefeld, F., Alder, C., Wieland, E., and Lunk, P. (2007). Effect of temperature on the pore solution, microstructure and hydration products of Portland cement pastes. *Cement and Concrete Research*, 37(4):483 – 491.

Luque de Castro, M. D. and Priego-Capote, F. (2007). Ultrasound-assisted crystallization (Sonocrystallization). *Ultrasonics sonochemistry*, 14(6):717–724.

Malvern Ltd (2015). Whitepaper, A basic guide to particle characterization. Technical report, Malvern Instruments Limited. Available from: https://www.cif.iastate.edu/sites/default/files/uploads/Other_Inst/Particle%20Size/Particle%20Characterization%20Guide.pdf.

Mason, T. J., Lindley, J., Lorimer, J. P., Maan, R., and Roberts, C. W. (1989). The effects of ultrasound on the synthesis of zeolite naa.

Mason, T. J. and Lorimer, J. P. (2002). *Applied Sonochemistry: Uses of Power Ultrasound in Chemistry and Processing*. Wiley-VCH.

Matschei, T., Lothenbach, B., and Glasser, F. (2007). The AFm phase in Portland cement. *Cement and Concrete Research*, 37(2):118 – 130.

Montes, M., Pato, E., Carmona-Quiroga, P., and Blanco-Varela, M. (2018). Can calcium aluminates activate ternesite hydration? *Cement and Concrete Research*, 103:204 – 215.

Neville, A. M. (2011). *Properties of Concrete, 5th edition*. Prentice Hall.

Nishida, I. (2004). Precipitation of calcium carbonate by ultrasonic irradiation. *Ultrasonics Sonochemistry*, 11(6):423–428.

Peters, S. (2017). *The Influence of Power Ultrasound on Setting and Strength Development of Cement Suspensions*. PhD thesis, Bauhaus-University Weimar.

Richardson, I. (2000). The nature of the hydration products in hardened cement pastes. *Cement and Concrete Composites*, 22(2):97 – 113.

Rothstein, D., Thomas, J. J., Christensen, B. J., and Jennings, H. M. (2002). Solubility behavior of Ca-, S-, Al-, and Si-bearing solid phases in Portland cement pore solutions as a function of hydration time. *Cement and Concrete Research*, 32(10):1663 – 1671.

Santos, R. M. and Van Gerven, T. (2011). Process intensification routes for mineral carbonation. *Greenhouse Gases: Science and Technology*, 1(4):287–293.

Scrivener, K., Snellings, R., and Lothenbach, B. (2016). *A Practical Guide to Microstructural Analysis of Cementitious Materials*. CRC Press US. Taylor & Francis Group.

Sherman, N., Beretka, J., Santoro, L., and Valenti, G. (1995). Long-term behaviour of hydraulic binders based on calcium sulfoaluminate and calcium sulfosilicate. *Cement and Concrete Research*, 25(1):113 – 126.

Taylor, H. (1997). *Cement chemistry, 2nd edition*. Thomas Telford Publishing, 2nd edition.

Vollpracht, A., Lothenbach, B., Snellings, R., and Haufe, J. (2016). The pore solution of blended cements: a review. *Materials and Structures*, 49(8):3341–3367.

Wagterveld, R. M., Miedema, H., and Witkamp, G.-J. (2012). Effect of ultrasonic treatment on early growth during CaCO3 precipitation. *Crystal Growth & Design*, 12(9):4403–4410.

Zajac, M., Rossberg, A., Le Saout, G., and Lothenbach, B. (2014). Influence of limestone and anhydrite on the hydration of Portland cements. *Cement and Concrete Composites*, 46:99 – 108.

5

Chapter 5: Effect of ultrasound on the extent of PC hydration and mechanical performance of PC mortars

1. Introduction [1]

In the previous chapter, the effects of ultrasound on the pore solution compositions of Portland cement (PC) paste with both water-to-cement ratios (w/c) of 0.50 and 0.80 plus the particle size distribution of PC particles were discussed. Although the main hydration products were not changed when ultrasound was applied at various frequencies and irradiation times, appreciable changes in the pore solution compositions were observed. Amongst various ion species in the pore fluid, aluminium concentrations were substantially increased upon the ultrasonication of PC pastes at both w/c ratios, denoting an enhanced dissolution of the aluminate phases of the PC clinker. Additionally, small changes in the calcium and silicon concentrations were detected. The evidence of increasing the carbonates in the pore solution was observed whilst a temporarily limited disruption to the formation of ettringite in early age upon ultrasonication was postulated. Negligible disaggregation of PC particles in aqueous dispersion were measured using a particle size analyser, thereby changes in the dissolution rate of the phases were connected to the enhanced mass transfer, erosion and exfoliation of the anhydrous grains. These could be subsequent effects of acoustic cavitation which leads to shock waves and jet streams. Moreover cavitation, particularly at a longer exposure, can lead to degassing or deaeration, removing the air entrapped and influencing the mechanical properties of cement-based composites.

[1] A paper with title of "*Insights into the positive effects of the direct application of power ultrasound to Portland cement pastes and mortars, study of chemical shrinkage and mechanical performance*", based on the results discussed in this chapter, has been submitted to the "Construction and Building Materials" journal.

In this chapter, the effect of PUS on the extent of PC hydration is investigated by precisely measuring the chemical shrinkage, using a self-developed automated dilatometry method to 14 days of hydration. Additionally, the mechanical performances of the PC mortars up to 91 days of age are evaluated. In this regard, ultrasound was directly applied at two different stages of mortar mixes preparation. First, the whole fresh mortar mix was treated whilst in the second scenario, the aggregates were added to the sonicated PC paste to cast the mortar mixes. 26 kHz and 132 kHz ultrasound were used as the respective high and low power densities available in this study. Durations of ultrasound treatment for 2 and 10 minutes were selected for all the experiments and all the PC pastes and mortar mixes were prepared with w/c ratios of 0.50. Finally, a microstructural analysis was undertaken on the fracture surfaces of both the hardened PC pastes and the mortars, to shed light on the effects of PUS on the microstructure of bulk cement paste together with the interface between the aggregates and the cement paste.

2. Chemical shrinkage of PC paste

To evaluate the repeatability of the automatic measurement method developed in this study, Table 5.1 shows the mean values of chemical shrinkages at specific hydration ages with the corresponding standard deviation of three independent samples. The accepted repeatability value specified in ASTM C1608-17 (2017) for measurements made at 24 hours after mixing is 0.00193 mL/g. As shown in Table 5.1, all the standard deviations obtained by the automated set-up developed in this work were far better than those specified in the ASTM precision requirements, denoting the excellent repeatability of the method used in this study. Deploying a high precision setup and image processing software for dilatometry was very important in this work, because the differences between the results generated by various ultrasonication conditions used in this study were found to be small (the absolute values were close to each other during initial trials). The results of the chemical shrinkage for the non-sonicated paste determined in this investigation were consistent with the data measured by Zhang et al. (2013) at the same w/c.

Table 5.1. The mean values of the measured chemical shrinkages (mL/g) of PC pastes at specific hydration times, reported with the values of standard deviation of three replicates

Paste mixes	Specific hydration ages					
	12h	24h	48h	72h	168h	336h
Control*	0.0174 ±0.0003	0.0250 ±0.0004	0.0353 ±0.0007	0.0390 ±0.0006	0.0473 ±0.0014	0.0534 ±0.0014
PUS26kHz-2min	0.0184 ±0.0004	0.0279 ±0.0006	0.0366 ±0.0006	0.0415 ±0.0005	0.0498 ±0.0010	0.0554 ±0.0016
PUS26kHz-10min	0.0183 ±0.0001	0.0269 ±0.0001	0.0351 ±0.0002	0.0391 ±0.0004	0.0472 ±0.0010	0.0526 ±0.0017
PUS132kHz-2min	0.0188 ±0.0004	0.0275 ±0.0006	0.0359 ±0.0004	0.0407 ±0.0005	0.0499 ±0.0004	0.0551 ±0.0011
PUS132kHz-10min	0.0182 ±0.0004	0.0270 ±0.0005	0.0355 ±0.0006	0.0397 ±0.0007	0.0478 ±0.0007	0.0527 ±0.0015

*Nine replicates were measured for the non-sonicated sample (Control) and three replicates for the other mixes.

Fig. 5.1 represents the evolution of the chemical shrinkage as a function of the PC pastes aged up to 336 hours (14 days) of hydration. The curves show the measured mean values for pastes mixed at w/c = 0.50 and immediately treated by ultrasound at 26 and 132 kHz for both 2 and 10 minutes after mixing. The level of water in the capillary tubes at 1 hour after the first contact of the cement was set as the initial value in calculating the chemical shrinkage. The automatic measurement was performed at intervals of 5 minutes, leading to obtaining the curves that consisted of more than 4000 data points (Fig. 5.1). To obtain a clear image of very early hydration, the initial data acquired during the first 4 and 24 hours have been enlarged and depicted in the plots. Also, for better comparison, Fig. 5.2 illustrates the amplitude of the PC pastes' chemical shrinkage at specific ages.

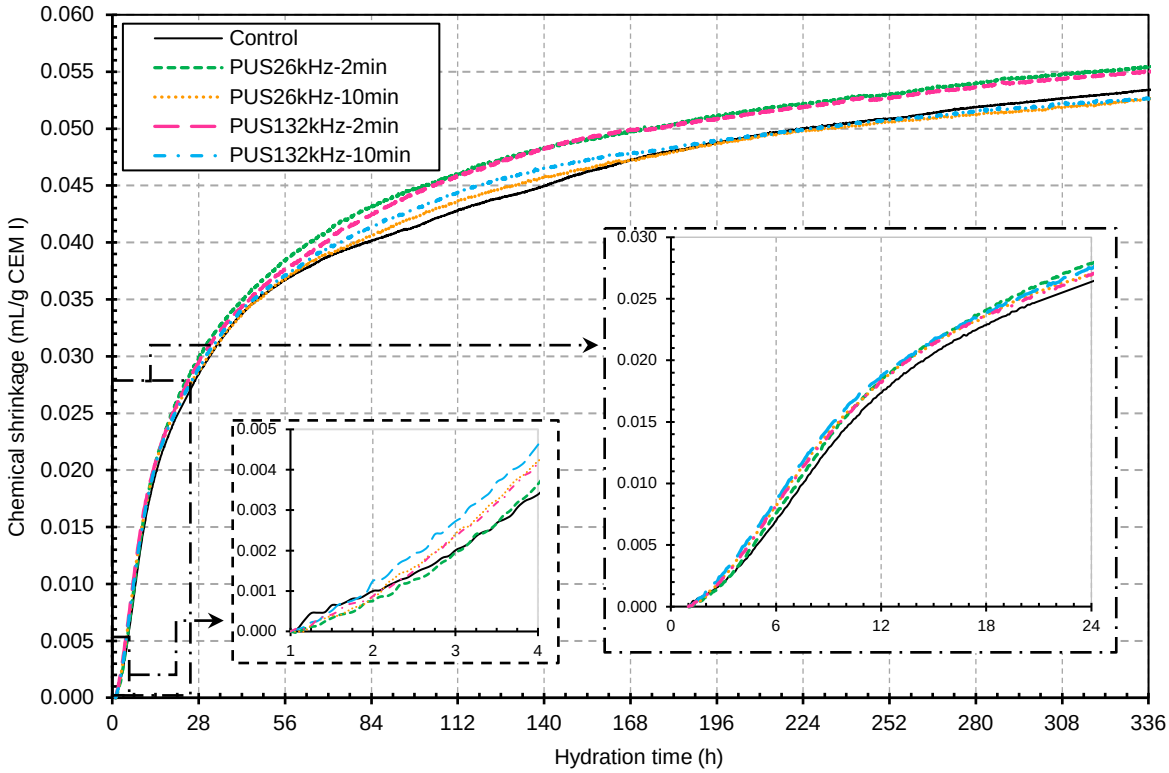

Fig. 5.1. Comparison of the measured chemical shrinkages of PC pastes treated by ultrasound at 26 and 132 kHz for 2 and 10 minutes to the non-sonicated sample (Control). All pastes were mixed at w/c = 0.50

Overall, for a given age, the measured chemical shrinkage was higher for the cement pastes treated by ultrasound for only 2 minutes. As shown in Figs. 5.1 and 5.2, sonication at 26 kHz for 2 minutes leads to a slightly higher rate of chemical shrinkage in the PC pastes than the same irradiation time of PUS but at 132 kHz. These results indicate the potentially positive effect of ultrasound at a relatively shorter time on the acceleration of the cement hydration reactions. This could be related to the disaggregation and dispersion of cement particle clusters, as seen in the results of the particle size analysis (chapter 4, section 2). In addition, the analysis of the pore solution compositions discussed in the previous chapter showed a significant increase in concentrations of Ca and especially Al, together with a limited rise in that of Fe, Mg and Si in the pore fluids of PC pastes treated by the same ultrasonication parameters. As discussed, the observations can be linked to the enhancement in the dissolution rate of the cement phases due to the ultrasound-induced cavitation, leading to the acceleration of hydration and consequently, inducing an increase in the chemical shrinkage rate compared with the non-sonicated paste. The results are also in agreement with the data on the heat of hydration obtained by Peters (2017),

which confirmed the acceleration of cement paste hydration (at w/c = 0.37 with superplasticiser) due to the application of PUS. Nevertheless, the comparison could be difficult as an ultrasonic horn system was used in that study and the actual sonication energy dissipated in the system has not been reported.

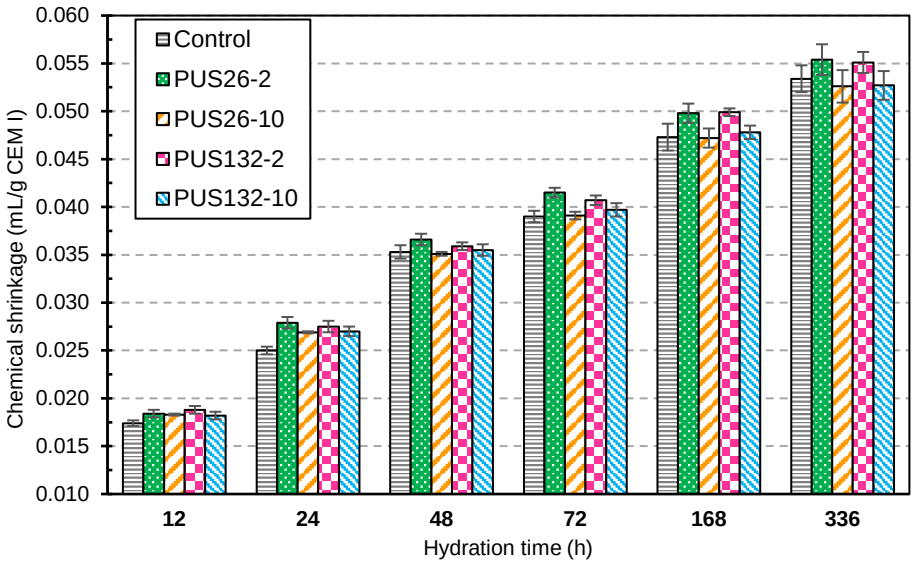

Fig. 5.2. Evolution of chemical shrinkages for the non-sonicated paste and pastes treated by ultrasound at 26 and 132 kHz for 2 and 10 minutes, the standard deviation bars are shown for all measurements.

The longer exposures of ultrasonication - up to 10 minutes - generated no sign of improvement in the rate of cement hydration development, however. Both PUS frequencies of 26 and 132 kHz for 10 minutes yielded lower values of ultimate chemical shrinkage than the non-sonicated sample, starting from 7 days to 14 days of hydration. This could be attributed to the particle re-agglomeration after being de-agglomerated at a longer sonication specially at PUS with a higher power density, leading to partially fusing the cement particles together due to the extensive shockwaves and shear forces induced by the ultrasonic cavitation. The evidence for the negative effect of long-time sonication on the aggregation of PC particles in an aqueous medium was observed in the results of particle size distribution in chapter 4 (section 2).

As can be seen in the enlarged area of initial-stage hydration (1 to 4 hours) displayed in Fig. 5.1, the control sample started hydration with a relatively higher value of chemical shrinkage than all the sonicated pastes. The rate of change in shrinkage for the non-sonicated paste then

gradually became slower, until its value was observed as lower than the other pastes at 4 hours onwards. This could be related to the slight disrupting effect of ultrasound postulated in chapter 4, but it needs more evidence to be confirmed.

3. Compressive and flexural strength development

The relative compressive and flexural strength indices of sonicated PC mortars at each curing age (up to 91 days) in percentages were calculated compared to the non-sonicated sample and are shown in Fig. 5.3. The sonication at 26 and 132 kHz was applied to the fresh state mortars for durations of 2 and 10 minutes immediately after finishing the mixing procedures. The relative strength indices of 100% correspond to the non-sonicated (Control) mortars.

3.1. *Effects of ultrasonic power*

Sonication at all frequencies and duration decreases both the compressive and flexural strengths of mortars at 1 day (as can be seen in Fig. 5.3(a) and (b)), reducing the relative strength indices compared with the non-sonicated sample. Ultrasound at 26 kHz for 2 minutes, which delivers a higher level of acoustic power than PUS at 132 kHz, reduced the relative compressive and flexural strength values for samples aged 1 day to 81% and 84%, respectively, which are the lowest values amongst all the mixes and ages. However, PUS at 132 kHz which dissipates gentler ultrasound led to a lower adverse effect on strength values at 1 day, having approximately the same mechanical performance as the control mortar at this age. Hence, when less insonation power density was applied to the mortars, a lower degree of interruption was observed in the compressive and flexural strengths of the mortars when demoulded, compared to the control mortar. These results support the potential disturbing effect of ultrasound on the very early formation of ettringite in PC pastes that was observed in the previous chapter. As postulated, the cavitation induced by more intense sonication (here, at 26 kHz) could temporarily distress the primarily formed network of nucleates for the further formation of ettringite and subsequent outer product C-S-H during the initial stages of hydration. This can result in a lower strength gain for the bulk cement paste surrounding the aggregates in mortars at very early ages and reduced strengths. Nevertheless, following the ultrasound agitation, the network of ettringite and C-S-H can be recovered and will continue to form, contributing to space filling and strength development (as discussed in chapter 4). This can be confirmed by the results shown in Fig. 5.3 where the relative compressive and flexural strength indices of the sonicated mortars surpass or become close to the reference samples from 3 and 7 days onwards, respectively.

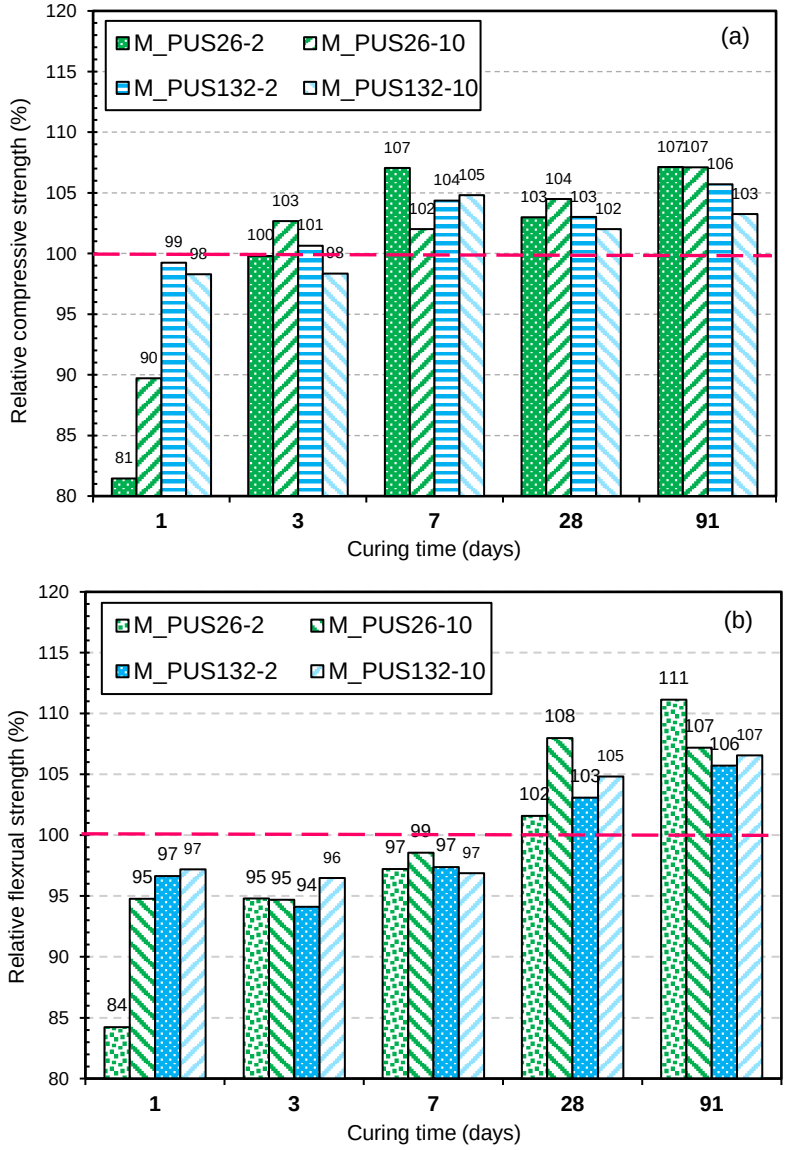

Fig. 5.3. Effect of ultrasound frequency and time of irradiation on (a) compressive strength and (b) flexural strength development of PC mortars, PUS applied to fresh mortar at w/c = 0.50

As shown in Fig. 5.3(a), ultrasound at 26 kHz for 2 minutes increased the relative compressive strength of the mortar to 107% at 7 and 91 days, when the samples were cured in water. The same sonication condition enhanced the flexural strength index up to 111% at 91 days (Fig. 5.3(b)). However, changes in the strength development of the mortars sonicated at a lower acoustic intensity (132 kHz) were not as considerable as those of treated at a higher intensity. These results agree with the data obtained for the evolution of the chemical shrinkages, where cement pastes sonicated at 26 kHz showed a slightly higher amplitude of chemical shrinkage than those treated at 132 kHz, over 14 days hydration.

3.2. *Effect of ultrasound exposure time*

At 1 day, a longer exposure of ultrasonication at the frequency associated with a higher power density (26 kHz) for up to 10 minutes markedly increased both the compressive and flexural strengths (Fig. 5.3), partially counteracting the negative effect of insonation and improving the relative strength indices to become closer to the control mortar at this age. This behaviour can be due to the degassing/deaeration effect of ultrasound cavitation (Lorimer and Mason, 1987; Mason, 1999) (particularly at a higher intensity), in which the total volume of entrapped air in fresh paste or mortar is reduced as reviewed in chapter 2 and experimentally confirmed by Peters (2017). Even the partial removal of entrapped air is particularly critical to enhance the mechanical properties of cement-based composites at a very early age when the porosity of the hardened cement paste surrounding the aggregates (especially pores larger than 20 nm) is still high because its hydration is not yet well advanced (Neville, 2011; Taylor, H.F.W., 1997). Fig. 5.3 shows that, in contrast with 26 kHz, the performance of a longer ultrasound duration at a lower power/intensity (132 kHz) is apparently not strong in deaeration and in improving the mechanical properties of mortars.

Nevertheless, the effect of longer ultrasound duration on compressive strength becomes less profound by progress of hydration at 3 days curing onward. From 7 to 91 days, 10 minutes ultrasound duration (both at 26 and 132 kHz) generally do not help (and has a negative effect to some extent) to enhance the compressive strength development compared to the shorter exposure duration.

3.3. *Effect of sonicated component*

Figs. 5.4 and 5.5 show the results of the compressive and flexural strengths development together with the relative strength indices for both “sonicated mortars” (labelled as M_PUS) and mortars obtained from sonicated paste, is called “paste-sonicated mortars” (labelled as P_PUS) at 26 and 132 kHz respectively, both for a duration of 2 and 10 minutes. It is of note that in this investigation an equivalent volume of materials was sonicated for the two different mixing procedures and to the study of various components sonication. Similar to the previous sections, the relative strength indices in percentages were calculated by normalising the strength values

based on the non-sonicated mortar (indicating the value of 100%). The results are illustrated for each curing age.

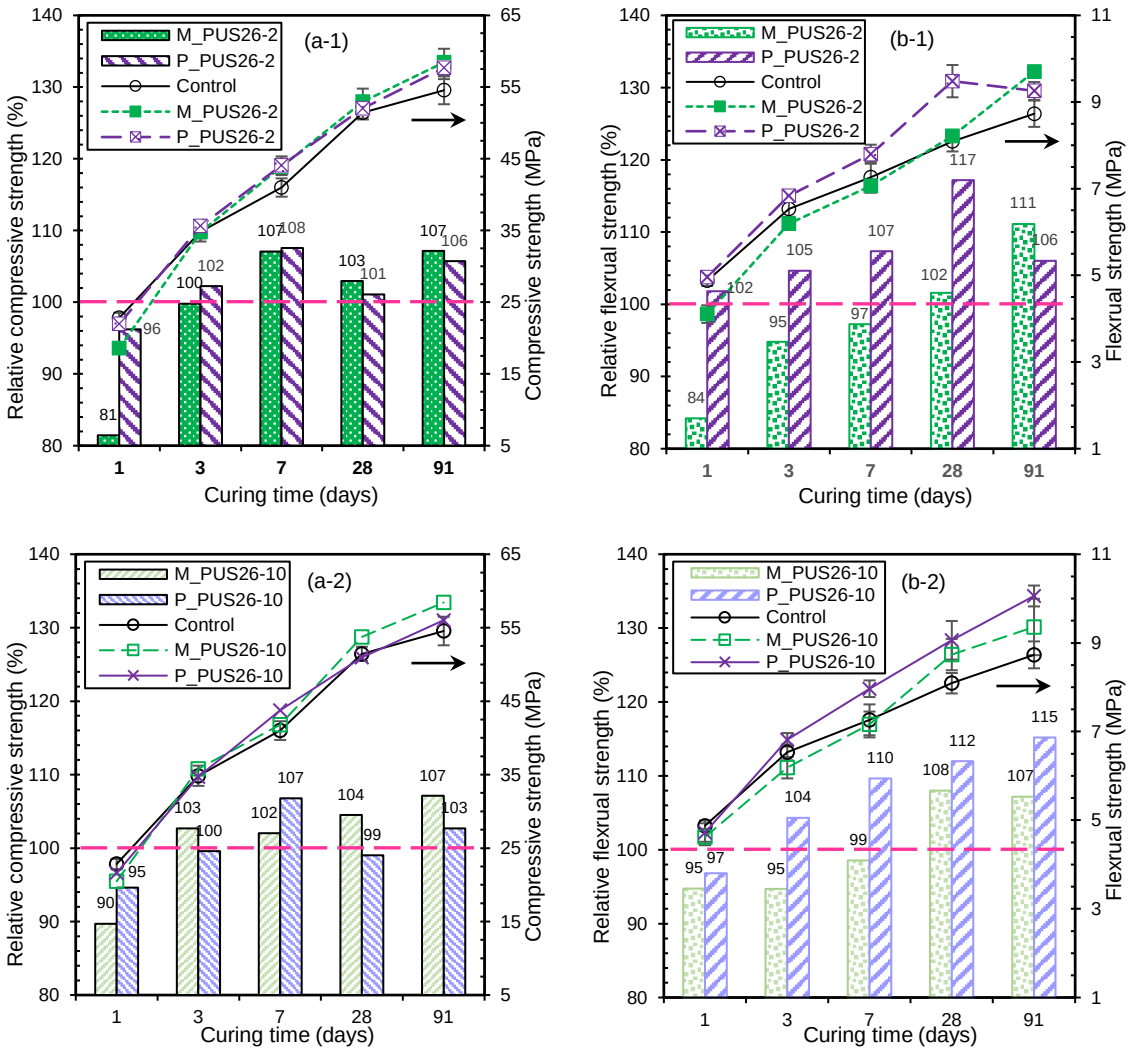

Fig. 5.4. Variation of relative compressive strength and relative flexural strength indices plus the measured values of compressive and flexural strengths for mortar specimens after applying ultrasound at 26 kHz to "sonicated mortars" (M_PUS26) and "paste-sonicated mortars" (P_PUS26) for irradiation times of 2 minutes ((a-1) and (b-1)) and 10 minutes ((a-2) and (b-2)), versus curing ages

At 1 day, the results highlight a significant enhancement in both the compressive and flexural strengths of mortar mixes, in which the PC paste was sonicated at 26 kHz before the addition of aggregates compared with the "sonicated mortars" samples (Fig. 5.4). However, an entirely opposite trend was observed for the samples treated at a lower sonication power of 132 kHz (see Fig. 5.5). The results are in contrast with Peters' (2017) report of only 24 hours compressive

strength. This could be related to the significant differences between these two studies including the mortar mixtures (w/c and the aggregate/cement ratio which was 1:1), the ultrasonic set-up (horn) and other testing conditions.

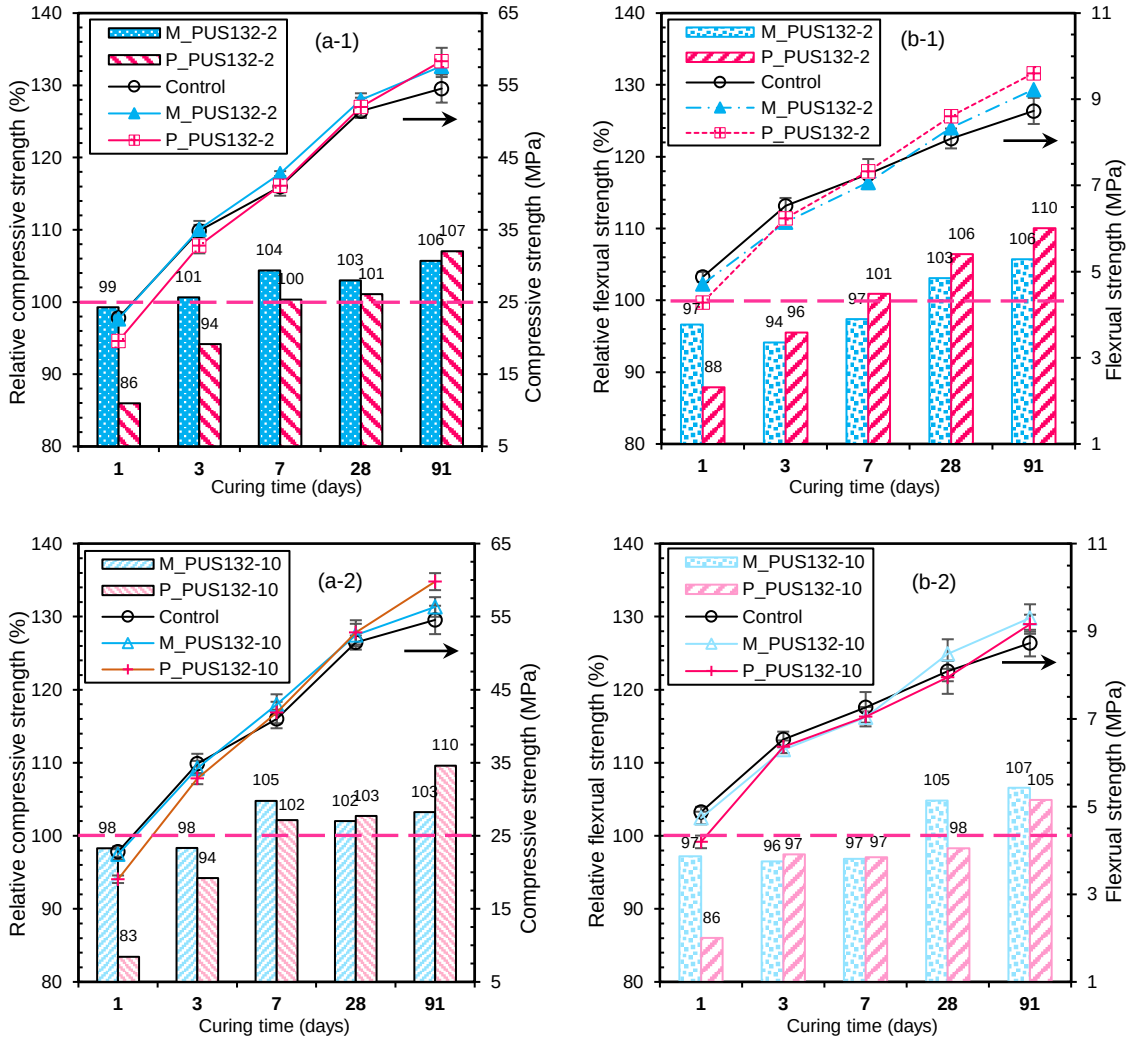

Fig. 5.5. Variation of relative compressive strength and relative flexural strength indices plus the measured values of compressive and flexural strengths for mortar specimens after applying ultrasound at 132 kHz to "sonicated mortars" (M_PUS132) and "paste-sonicated mortars" (P_PUS132)) for irradiation times of 2 minutes ((a-1) and (b-1)) and 10 minutes ((a-2) and (b-2)), versus curing age

There are two explanations for this effect. First, due to using equivalent volumes of materials, the presence of aggregates in mortar may affect the propagation of ultrasound waves by the attenuation of amplitude and intensity in the case of "sonicated mortar". This can reduce the possibility of effective ultrasound cavitation occurring in the fresh mortar in comparison with the

case of applying ultrasound solely to the paste. Therefore, together with the positive effect of PUS on accelerating the rate of hydration at an early age and the deaeration of cement paste discussed in section 3.2, the higher strength indices of “paste-sonicated mortars” treated by PUS at 26 kHz for 2 and 10 minutes can be attributed to the more effective improvement in the properties of the bulk cement paste. Also, despite the fact that addition of aggregates to the sonicated paste may entrapped unexpected air voids (which has not been measured here), it is yet observed higher strength indices in “paste-sonicated mortars” compared to “sonicated mortar” samples. It should be noted that a direct comparison of cement paste properties in the mortar matrix to that discussed in the chemical shrinkage may not be appropriate as the PUS energy per volume of these were not the same. This means that the relatively smaller quantity of paste studied in the chemical shrinkage may experience higher degree of particle re-agglomeration than the paste treated to make the “paste-sonicated mortar” mix. Thus, the comparison was carried out amongst samples treated by the corresponding PUS condition in each experiment.

Secondly, the changes observed in the strength values due to the different mixing procedures could be attributed to changes in the properties of the so-called interfacial transition zone (ITZ) between the aggregates and the surrounding bulk cement paste in the mortar matrix. This region in mortar or concrete microstructure is characterised by the presence of a relatively higher porosity than the bulk cement paste and a zone of stress concentrations arising from the difference in the modulus of the elasticity of the paste and the aggregates (Scrivener et al., 2004; Wong et al., 2009). Also, Darwin (1994) pointed out that the structure of bulk cement paste is different from cement paste within the ITZ. In this regard, it is proposed that the water/cement ratio of the cement paste within the ITZ may be slightly higher in the microstructure of “sonicated mortars” than “pastes-sonicated mortars”. Initial trials with various ultrasonic systems confirmed that the application of high-power ultrasound increases the possibility of bleeding occurring in fresh cement paste. During this phenomenon, the sedimentation/settlement of solid cement particles in the cement suspension under the shockwaves and shear forces induced by the ultrasound cavitation can cause the contraction of the paste and the ascent of free mixing water. This finally can increase the possibility of the partial precipitation of cement particles from the freshly made cement paste upon the application of high-intensity PUS. The effects and the

mechanisms in which ultrasound facilitates the production of some inorganic compounds (barium sulphate, potassium sulphate etc.) by precipitation and crystallisation have been reported by Dodds et al. (2007). Generally, bleeding in cement paste is caused by the inability of the cement particles to hold the mixing water when they tend to settle downwards under gravity. However, in the case of high intensity ultrasonication, the mechanical effect of intense cavitation can quickly lead to the local sedimentation of cement particles and the partial stiffening of cement paste in the high energy cavitation zone or on the surface of vessel's wall. An example of this can occur at the area close to the tip of a probe in an ultrasonic horn system. Although a high-power ultrasound system was never used in this study and no signs of bleeding were observed from the visual inspections, it is still possible to have some limited degree of separation of water from the cement particles on the microstructural scale of the mortar matrix due to the cavitation disruption. In this regard, the solid surface of aggregates within the ITZ that is widespread throughout the mortar matrix could be the area in which the water to cement ratio is likely to be increased and hence negatively affect the strength development of the mortar. At a very early age when the degree of hydration of the bulk cement paste is still relatively low and the porosity is yet high, the effect of a weak ITZ on strength gain becomes paramount. Accordingly, this could be an explanation for obtaining much lower values for 1-day strength in "sonicated mortars" than "paste-sonicated mortars" at 26 kHz compared to the gentler insonation at 132 kHz. As shown in Figs. 5.4(a-2) and (b-2), this effect is seen to have subsided in the samples treated by a longer exposure of PUS of up to 10 minutes, perhaps because of the effective deaeration performance of longer sonication.

At later ages, a difference can be observed between the behaviour of compressive and flexural strengths with the progress of hydration. As can be seen in Figs. 5.4 and 5.5, the differences between the application of 26 kHz PUS at two different stages appear to be less profound for the results of compressive strengths. However, a still considerable enhancement can be seen in the rate of the flexural strength gain for the "paste-sonicated mortars" compared with both the sonicated mortar and the control sample. As can be expected, this improvement is lower in the case of less intense ultrasound at 132 kHz (Fig. 5.5), most likely due to the positive deaeration effect of 26 kHz ultrasound on the mortars' strength as discussed in section (3.2). As Figs. 5.4(b-

1) and (b-2) present, the relative flexural strength indices of “paste-sonicated mortar” treated by PUS at 26 kHz for 2 and 10 minutes increased by up to 17% and 12% respectively, compared with the “sonicated mortar” at 28 days. This highlights the fact that the choice of ultrasonication of mortar constituents (either the whole mixes or only the paste) does not affect the load-bearing capacity of mortars in compression and tension modes in the same manner. In other words, the tensile strength of mortars (which has been measured by the flexure test in this study) is more sensitive to the ultrasound intensity and treatment approach than the compressive strength. This is possibly because of the differences induced in the bound within the hydrated bulk cement paste and/or between the paste and the aggregates (i.e. the ITZ) upon ultrasonication. The relatively improved rates of hydration were supported by the evidence obtained from the chemical shrinkage (section 2) for the cement pastes treated by ultrasonication at 26 and 132 kHz for 2 minutes. Even for pastes sonicated for up to 10 minutes, a slight acceleration in the rate of hydration was seen for up to 7 days. Thus, the enhanced hydration of the bulk cement paste in the “paste-sonicated mortars” can be inferred from the results of the chemical shrinkage. However, the role of the ITZ should also be considered in interpreting the observed improvement in flexural strength in “paste-sonicated mortars” compared to “sonicated mortars”.

This could be linked to the differences in compression and the flexure failure mechanism of mortar or concrete. Under the compression mode, the crack propagation initiates from the interface between the cement paste and the aggregates (in which microcracks exist, even prior to loading (Neville, 2011)) due to the tensile strain. Then, extensive cracking develops in the mortar matrix leading to failure. Thus, the aggregate interlock would be influential in distributing the stresses and should counteract the microstructure failure after the failure of the bulk cement paste (Chhorn et al., 2018). However, flexural loadings create both the tension and compression forces (Mehta and Monteiro, 2006). Hence, in the flexure tensile mode, both the compressive and tensile zones stresses occur at the failure section. In this regard, the cracks are initiated in the ITZ at low stresses and develop into the mortar matrix at high stresses while the cement paste resists the crack propagation (Ahmed et al., 2016). This indicates the critical role of the bulk cement paste and the ITZ in flexural tensile mode of rupture in mortars and concrete. Therefore, in an equivalent condition, the enhancement in the flexural strength in PC mortar for a given

compressive strength can be attributed to an improvement in the properties of the bulk paste matrix and modification of the ITZ.

To obtain a better image of the changes in strength development, the relationship between the compressive and flexural strength is analysed in the next section for the whole of the mortar mixes made by various mixing approaches and sonication conditions.

3.4. *Relationship between compressive and flexural strength*

Fig. 5.6 shows the correlation between the compressive and flexural strength test results for the entire population of mortar specimens treated at different ultrasonic frequencies and durations tested at various curing ages plus the control samples. A power regression analysis was conducted to determine the best-fit relationship between all the measured strength mean values for all the curing times. The proposed equations and the derived regression coefficients (R^2) based on the analysis are given in Fig. 5.6 and are presented with the corresponding trend lines. Generally, the relations are similar to those reported in the literature for cement mortars and concrete (Al-Swaidani et al., 2017; Huang et al., 2013; Neville, 2011).

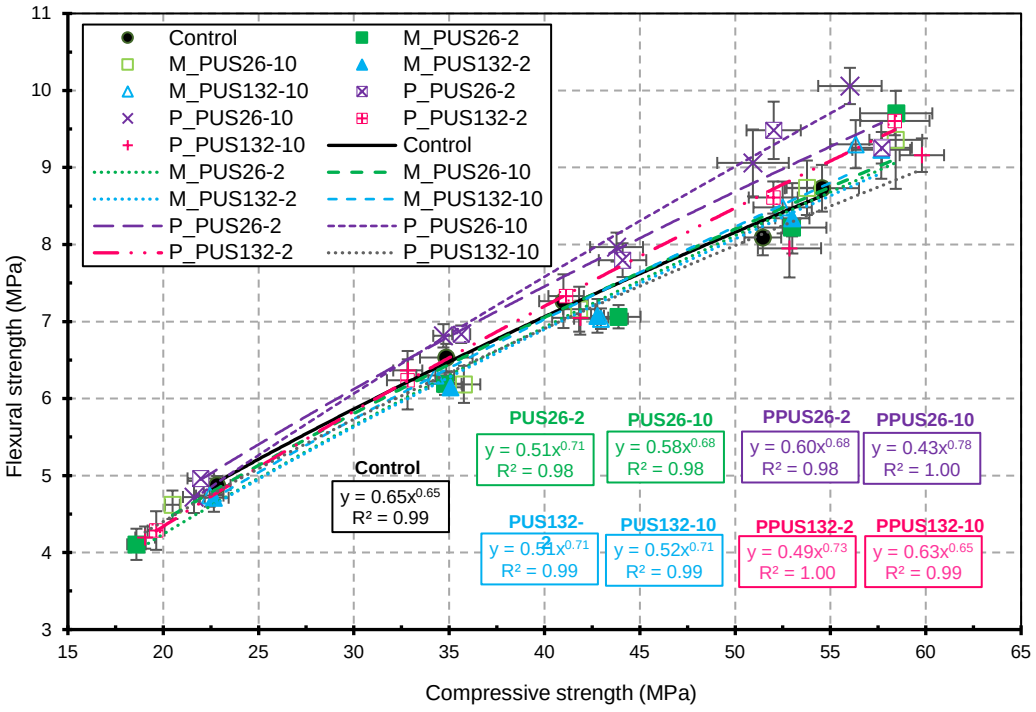

Fig. 5.6. Correlation between the compressive and flexural strengths of the whole population of mortar specimens

The results indicate that for a given compressive strength at later ages (3 days onwards), the flexural strengths of mortars obtained from “paste-sonicated mortars” treated at 26 kHz for 2 and 10 minutes and 132 kHz for 2 minutes are higher than the non-sonicated mortar and the other mixes. The order of the degree of enhancement is as follows: PUS 26 kHz for 10 minutes > 26 kHz for 2 minutes > 132 kHz for 2 minutes. It is concluded that the addition of aggregates to the sonicated paste enhances the mechanical properties of the mortars in comparison to the sonicated fresh mortar or the non-sonicated mortar. As discussed in section 3.3.3, this could be the result of improving the bulk paste matrix and/or the bound between the paste and the aggregates (i.e. ITZ). The relatively higher improvement observed for the ultrasound at 26 kHz over 132 kHz is consistent with the results of the chemical shrinkage. The case of a longer sonication at 26 kHz for 10 minutes over 2 minutes could be due to the deaeration effect of PUS discussed in section 3.2, which plays a significant role in the strength of mortar.

4. Microstructural Studies

4.1. *Cement paste*

Figs 5.7 and 5.8 show the microstructure of hardened cement pastes hydrated under saturated and sealed curing conditions at 23 °C. Fig 5.7 shows SEM micrographs with both 5 KX and 10 KX magnifications and Fig 5.8 provides more images at 10 KX. From these, the fracture surface microstructure of the control cement paste can be compared to that of paste sonicated at 26 kHz for 2 minutes as well as 132 kHz for 2 and 10 minutes.

The SEM micrographs at various magnifications and points reveal that significantly larger pores are observed in the microstructure of the non-sonicated paste (Control_7d) compared with all the sonicated pastes. Sonication at 26 kHz leads to a relatively denser microstructure than 132 kHz when applied for 2 minutes. These qualitative results are in agreement with the deaeration/degassing effects of ultrasound discussed in previous sections. In this regard, the effect of a higher intensity of ultrasound (26 kHz compared with 132 kHz) is also highlighted. Denser microstructure is also seen in the case of a longer exposure of ultrasound (PUS132-10_7d images in both Fig. 5.7 and Fig. 5.8).

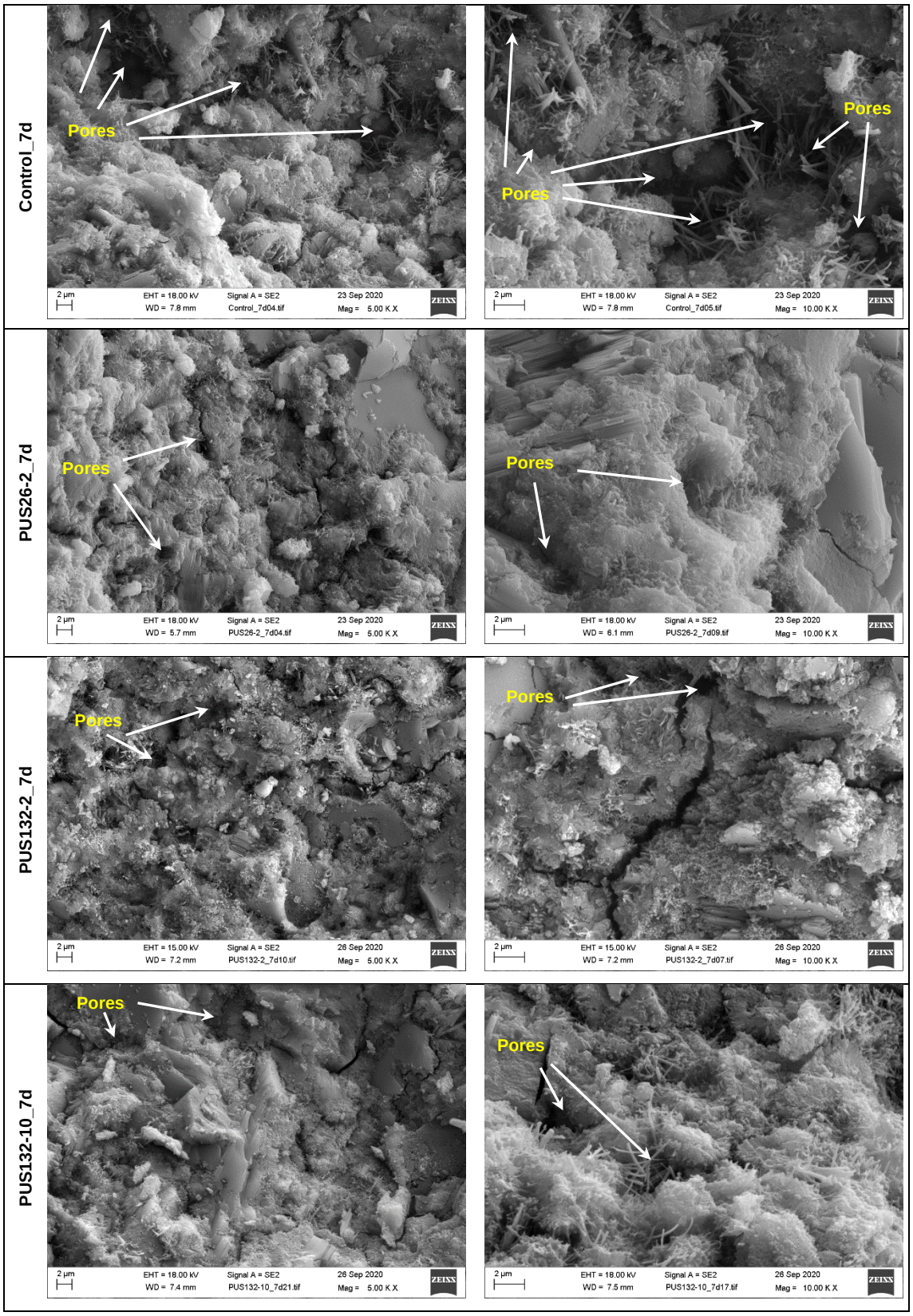

Fig. 5.7. Microstructure of the hardened cement paste at 7 days sealed hydration and 5 KX and 10 KX magnifications; non-sonicated paste (Control) versus sonicated pastes at 26 kHz for 2 minutes (PUS26-2) and 132 kHz for 2 and 10 minutes (PUS132-2 and PUS132-10).

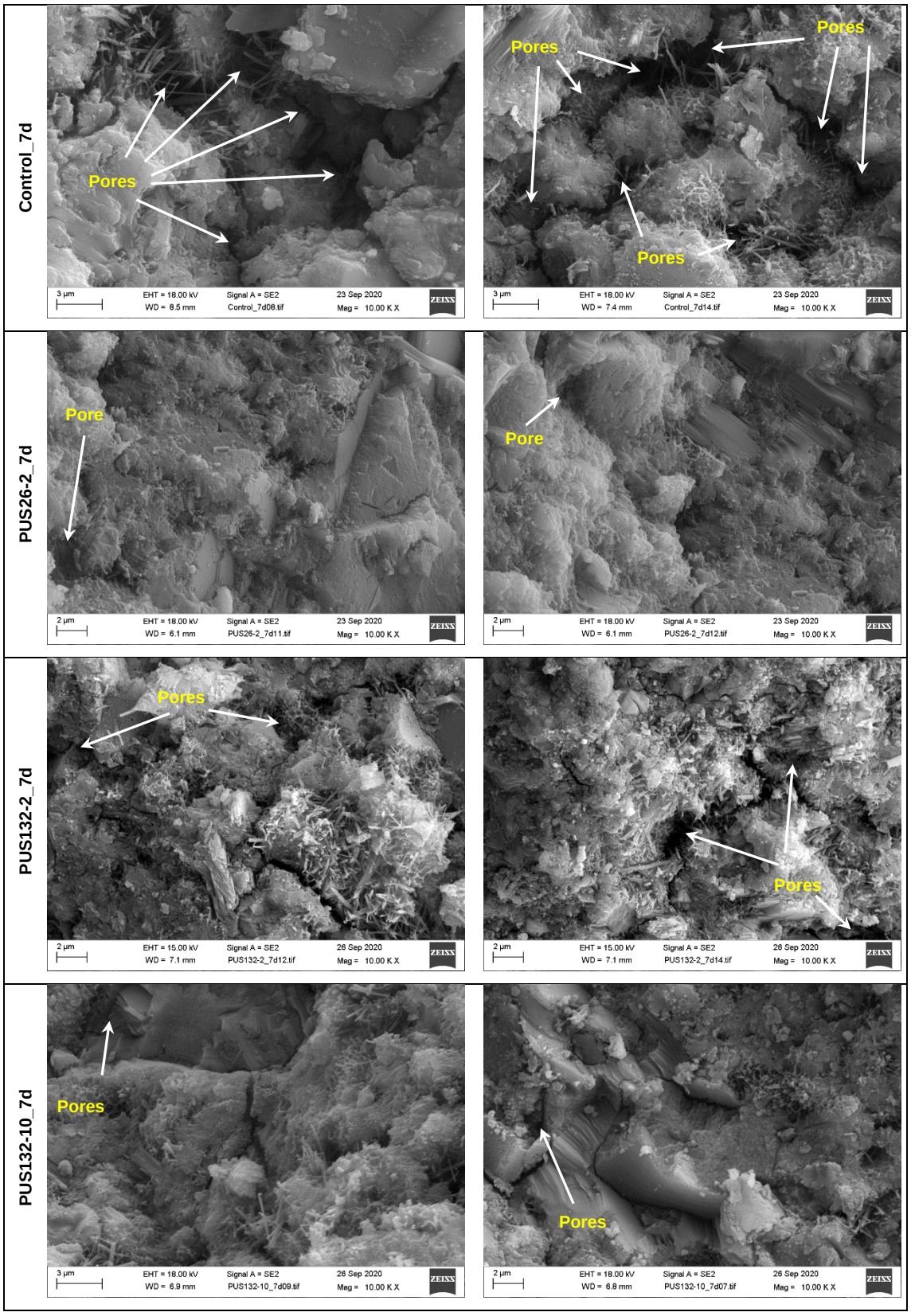

Fig. 5.8. Microstructure of the hardened cement paste at 7 days sealed hydration and 10 KX magnification; non-sonicated paste (Control) versus sonicated pastes at 26 kHz for 2 minutes (PUS26-2) and 132 kHz for 2 and 10 minutes (PUS132-2 and PUS132-10).

4.2. *Microstructure of the ITZ in PC mortars*

Figs. 5.9 to 5.12 show the microstructural study of the ITZ between the aggregate and the bulk paste in respect of the control sample, the 26kHz ultrasound treated "sonicated mortars" for a duration of 2 and 10 minutes and the “paste-sonicated mortar” for 2 minutes, all aged at 28 days. In addition to the SEM micrographs of the interface regions, qualitative EDS line scan elemental analysis (for Ca, Si, O, Al, S, Na, K, Fe and Mg) were performed corresponding to the same SEM images and shown below each micrograph.

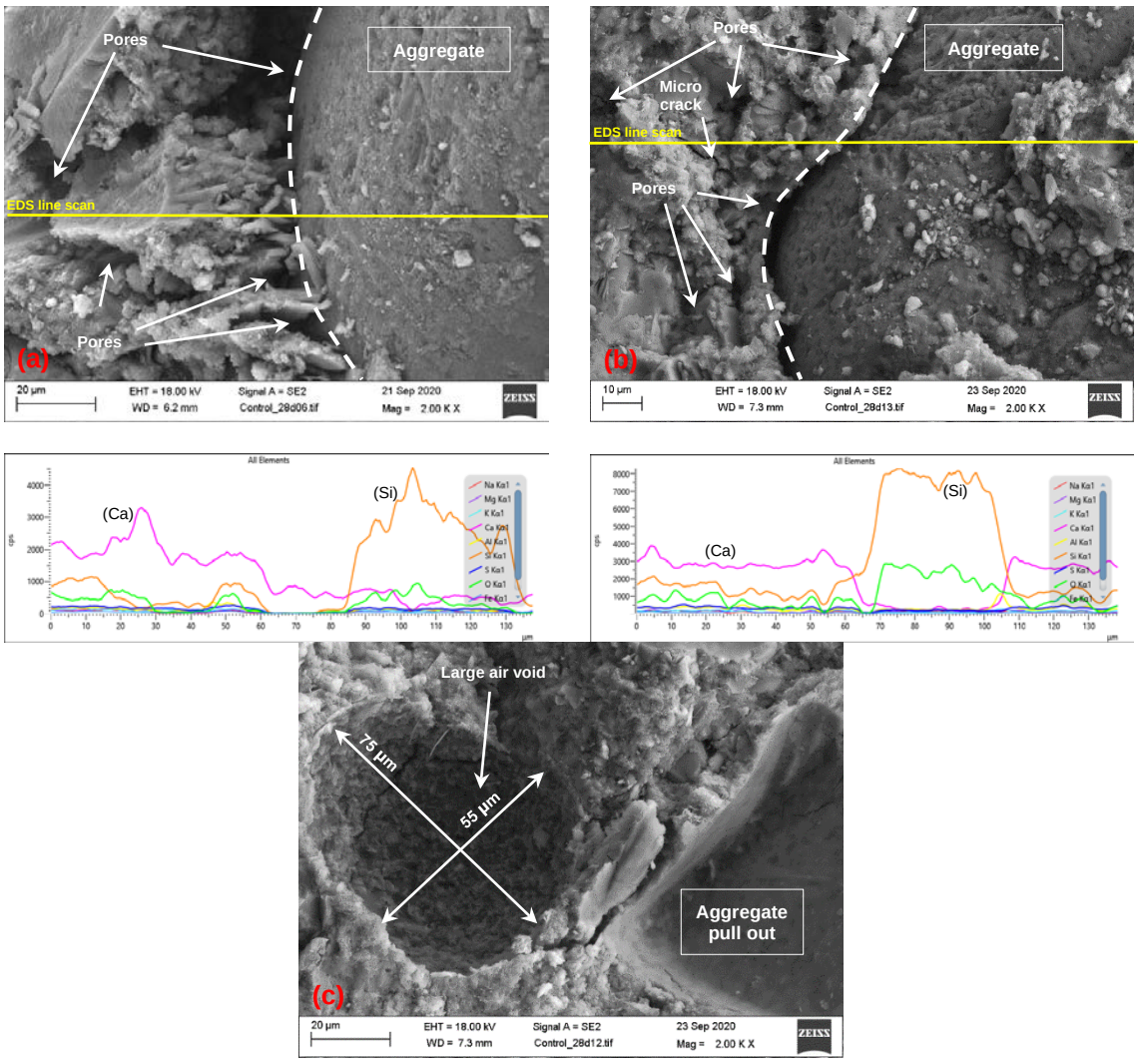

Fig. 5.9. The SEM micrographs and the EDS line scan profiles of the ITZ for the 28-days cured control mortar specimens.

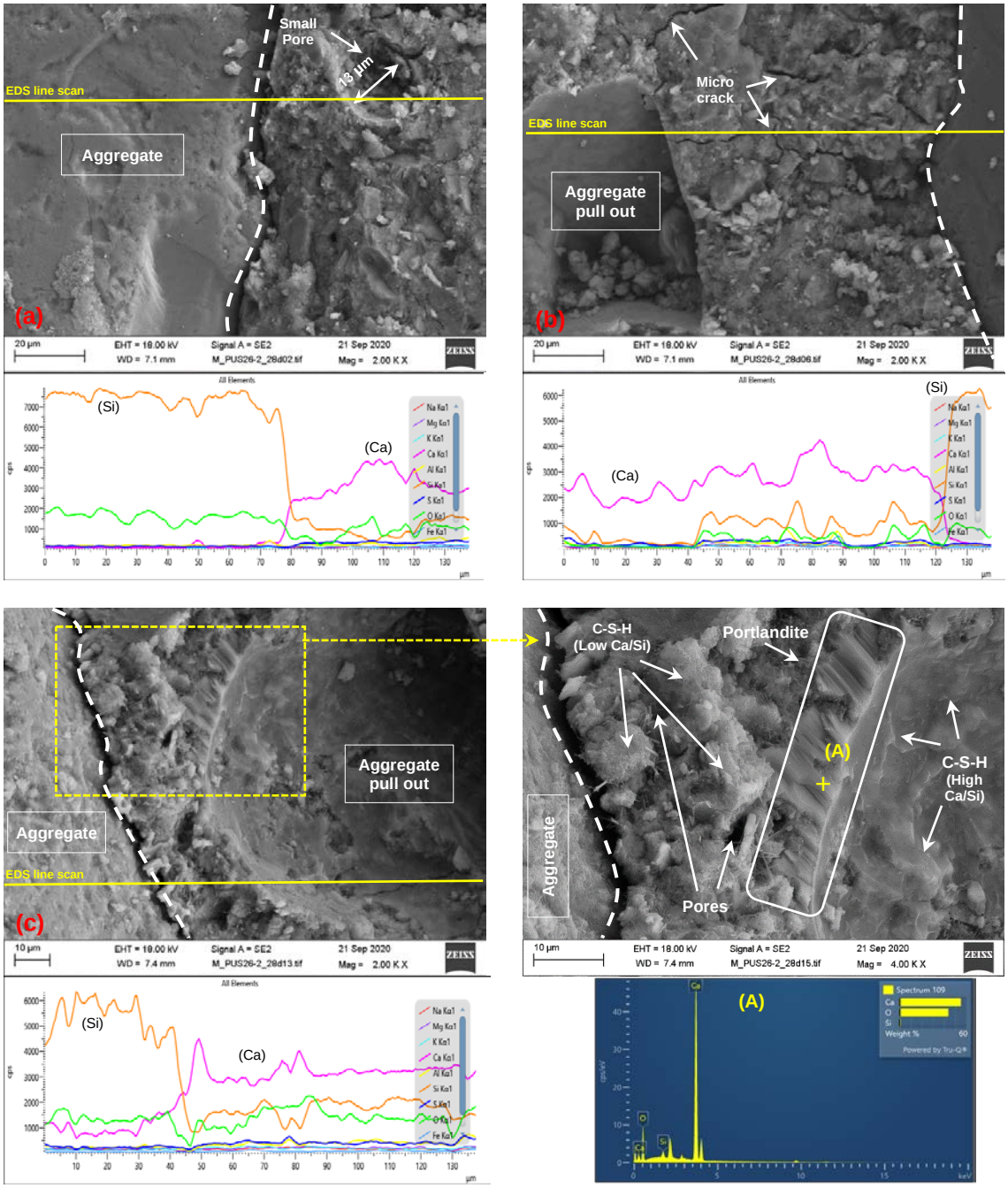

Fig. 5.10. The SEM micrographs, the EDS line scan profiles and a microanalysis of the ITZ for the 28-days cured mortar specimens treated by applying ultrasound at 26 kHz to the “sonicated mortar” (M_PUS26) for 2 minutes.

As can be seen in Fig. 5.9((a) and (b)), a highly non-uniform area of porous matrix and irregularly structured hydration products with large pores in between has been formed in the ITZ of the control mortar specimens. The microstructures of the specimens contain different sizes of

air voids, one of which is shown in Fig. 5.9(c), indicating a very large air void directly next to an aggregate pull out region.

In contrast to the control mortar, the microstructure of the ITZ regions observed in the mortars treated by ultrasound are relatively denser and more uniform (Figs. 5.10 to 5.12). Additionally, the ITZ structures in the sonicated specimens are not very different from those of the bulk cement paste matrix. However, there are some subtle differences between the microstructure of "sonicated mortar" and "paste-sonicated mortar" treated at 26 kHz for 2 minutes. As shown in Fig. 5.10(a), small air voids are observed in the ITZ of the "sonicated mortars" whilst the ITZ and the cement paste farther away in the interface of the "paste-sonicated mortar" are relatively air-void free and denser (Fig. 5.11(a) and (b)). Moreover, many regions of aggregate pull-out with various sizes of aggregates are observed in the microstructure of the "sonicated mortars".

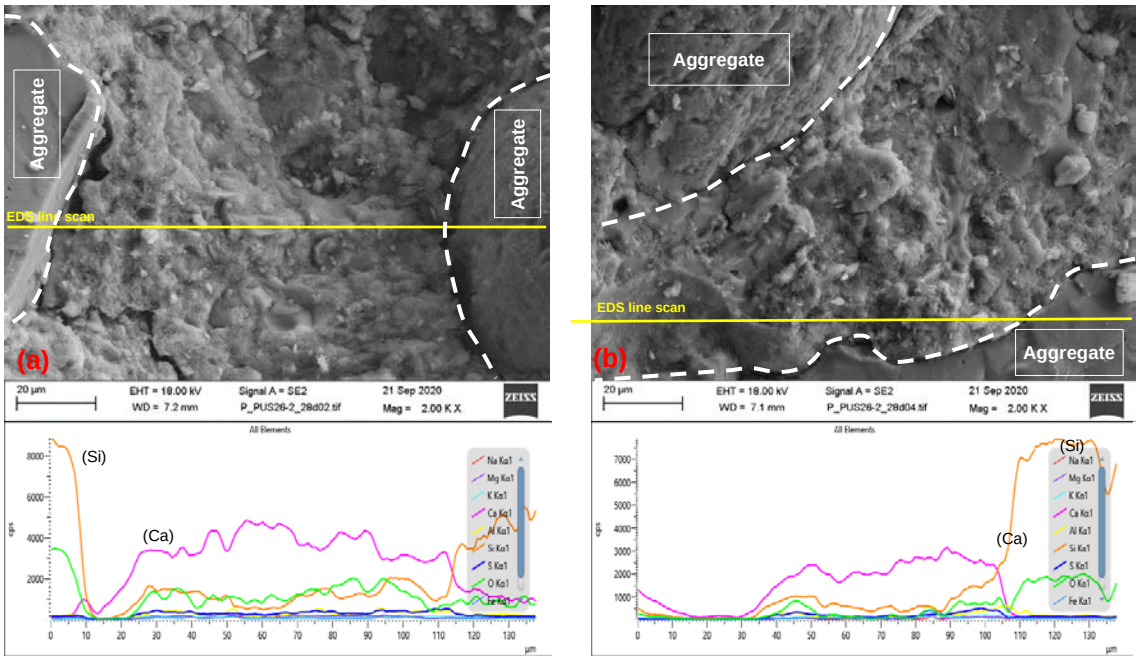

Fig. 5.11. The SEM micrographs and the EDS line scan profiles of the ITZ for the 28-days cured mortars specimens treated by applying ultrasound at 26 kHz "paste-sonicated mortar" (P_PUS26) for 2 minutes.

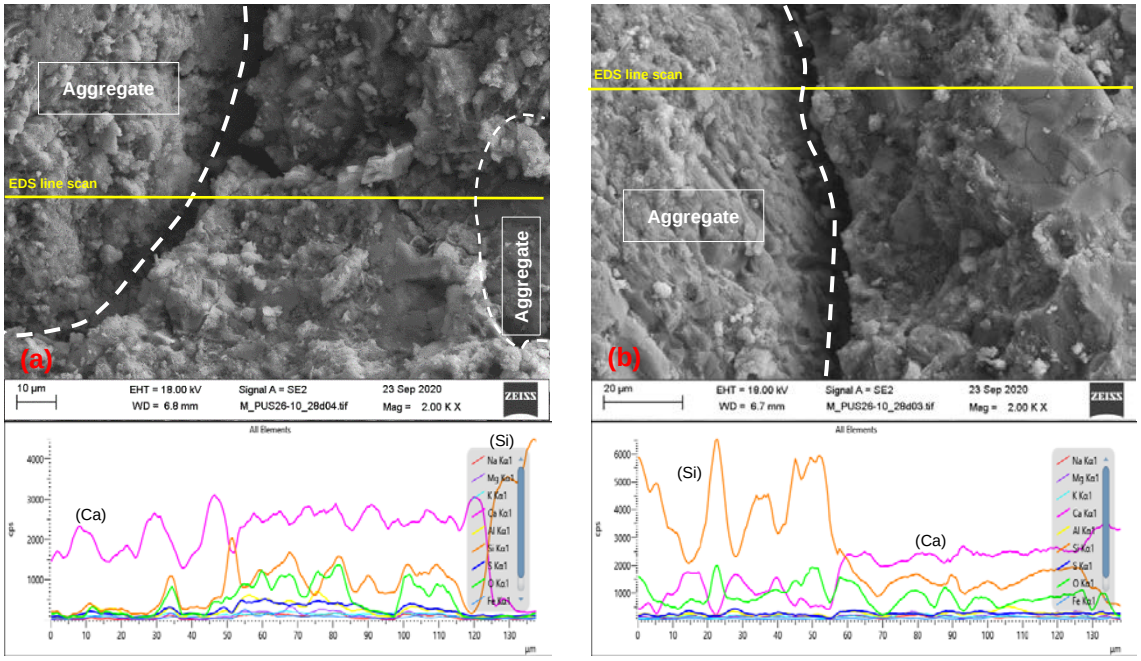

Fig. 5.12. The SEM micrographs and the EDS line scan profiles of the ITZ for the 28-days cured mortar specimens treated by applying ultrasound at 26 kHz to “sonicated mortar” (M_PUS26) for 10 minutes.

An enlarged area of one of these cases is shown in Fig. 5.10(c). Its corresponding microanalysis presents a relatively large portlandite crystal rim observed in the interface of the aggregate pull out region and the surrounding paste. The paste located between the two aggregates is also porous and contains non-uniform C-S-H products. However, the space around the aggregates in the “paste-sonicated mortar” (Fig. 5.11) is surrounded by a denser and more uniform solid matrix without a borderline between the paste matrix and the ITZ. These observations can support the improvement in the ITZ when mortars are cast with the addition of aggregates to the sonicated paste (“paste-sonicated mortars”) as discussed in section 3.3. Also, this is in agreement with the compressive/flexural strengths relationship indicated in Fig. 5.6 (section 3.4), which showed a higher flexural strength of samples obtained from “paste-sonicated mortars” treated at 26 kHz for 2 and 10 minutes and 132 kHz for 2 minutes.

5. Conclusions

In this part of study, the chemical shrinkage of the cement pastes was studied, together with the mechanical performance of the corresponding cement mortars made by two different mixing approaches (ultrasonicated at 26 and 132 kHz for durations of 2 and 10 minutes). Qualitative analyses of the hardened pastes and mortars were also undertaken using the SEM technique. The following conclusions can be drawn from this investigation:

1) A short ultrasonication at both the higher and lower intensities used in this study leads to enhancing the rate of chemical shrinkage in the PC paste by up to 5.5% and 4% at 7 and 14 days hydration, respectively.
2) PC pastes sonicated at 26 kHz for 2 minutes show a slightly higher rate of chemical shrinkage (up to about 2% at 3 days) than those treated at 132 kHz for the same irradiation time. Similarly, the corresponding mortars yield a higher rate of the evolution of compressive and flexural strengths over 91 days curing in water, when subjected to a higher acoustic intensity at 26 kHz than when treated by a gentler insonation at 132 kHz. The maximum improvement is about 5% for the flexural strength at 91 days.
3) The application of PUS to fresh mortar mixes reduces the compressive and flexural strengths of hardened cement mortars at 1 day compared to the non-sonicated mortar up to 19% and 16%, respectively, for 2 minutes ultrasound at 26 kHz. In this regard, the effect of ultrasound at a higher intensity of 26 kHz is more profound than PUS at 132 kHz. However, at later ages, ultrasonication leads to significant increases in both the compressive and flexural strengths: up to 7% and 11%, respectively at 91 days curing. Mortars treated at 26 kHz acquire higher compressive and flexural strength than those treated at 132 kHz as well as the control samples.
4) Longer exposure of PUS at 26 kHz considerably enhances 1-day strength that could be related to the deaeration effect of ultrasound on the partial removal of entrapped air in fresh mortar.
5) Ultrasonication of paste before the addition of aggregates leads to a considerably better mechanical performance in mortars. With respect to this enhancement, the effect of PUS at 26 kHz is more profound where it results in up to 17% improvement in the flexural

strength of mortars at 28 days. Results of the SEM analysis shows that this could be due to the improvement in the bulk cement paste and/or modification of the interface between the aggregates and the cement paste (ITZ).

6. References

Ahmed, M., Mallick, J., and Abul Hasan, M. (2016). A study of factors affecting the flexural tensile strength of concrete. *Journal of King Saud University - Engineering Sciences*, 28(2):147 – 156.

Al-Swaidani, A., Soud, A., and Hammami, A. (2017). Improvement of the early-age compressive strength, water permeability, and sulfuric acid resistance of scoria-based mortars/concrete using limestone filler. *Advances in Materials Science and Engineering*, 2017:1–17.

ASTM C1608-17 (2017). *Standard Test Method for Chemical Shrinkage of Hydraulic Cement Paste*. ASTM International, West Conshohocken, PA.

Chhorn, C., Hong, S. J., and Lee, S. W. (2018). Relationship between compressive and tensile strengths of roller-compacted concrete. *Journal of Traffic and Transportation Engineering (English Edition)*, 5(3):215 – 223.

Darwin, D. (1994). The interfacial transition zone: Direct evidence on compressive response. *MRS Proceedings*, 370:419.

Dodds, J., Espitalier, F., Louisnard, O., Grossier, R., David, R., Hassoun, M., Baillon, F., Gatumel, C., and Lyczko, N. (2007). The effect of ultrasound on crystallisation-precipitation processes: Some examples and a new segregation model. *Particle & Particle Systems Characterization*, 24(1):18–28.

Huang, C.-H., Lin, S.-K., Chang, C.-S., and Chen, H.-J. (2013). Mix proportions and mechanical properties of concrete containing very high-volume of class f fly ash. *Construction and Building Materials*, 46:71 – 78.

Lorimer, J. P. and Mason, T. J. (1987). Sonochemistry. Part 1-The physical aspects. *Chemical Society Reviews*, 16:239–274.

Mason, T. J. (1999). *Sonochemistry*. Oxford University Press.

Mehta, P. and Monteiro, P. (2006). *Concrete: Microstructure, Properties, and Materials*. McGraw-Hill.

Neville, A. M. (2011). *Properties of Concrete, 5th edition*. Prentice Hall.

Peters, S. (2017). *The Influence of Power Ultrasound on Setting and Strength Development of Cement Suspensions*. PhD thesis, Bauhaus-University Weimar.

Scrivener, K., Crumbie, A., and Laugesen, P. (2004). The interfacial transition zone (ITZ) between cement paste and aggregate in concrete. *Interface Science*, 12(4):411–421.

Taylor, H.F.W. (1997). *Cement chemistry, 2nd edition*. Thomas Telford Publishing, 2nd edition.

Wong, H., Zobel, M., Buenfeld, N., and Zimmerman, R. (2009). Influence of the interfacial transition zone and microcracking on the diffusivity, permeability and sorptivity of cement-based materials after drying. *Magazine of Concrete Research*, 61(8):571–589.

Zhang, T., Gao, P., Luo, R., Guo, Y., Wei, J., and Yu, Q. (2013). Measurement of chemical shrinkage of cement paste: Comparison study of ASTM C 1608 and an improved method. *Construction and Building Materials*, 48:662 – 669.

6

Chapter 6: Conclusions and Perspectives

1. An overview

The present work first identified the gap in the knowledge about the effect of power ultrasound in the field of cement-based systems. Previous works in this field had been limited to the characterisation of ultrasonic dispersion of pozzolanic materials when used as a partial replacement of cement in cementitious systems. The predominant mode of action for PUS in such studies was identified mainly as the enhancement of the dispersion of agglomerates. Despite providing some important evidence for the acceleration of alite hydration due to ultrasound, the only substantial previous study of the direct application of PUS to cement-based systems also failed to shed light on fundamental changes that ultrasound can bring to the conventional Portland cement system with a normal water-to-cement ratio (w/c). In this current study, the underlying mechanisms through which power ultrasound can affect the hydration and properties of cementitious systems have been reviewed, together with the disaggregation and dispersion of cement particles. It is also suggested that ultrasound can potentially influence the hydration of cement and have some positive effects on the performance of cementitious materials.

An ultrasound delivery system operating at several power densities suitable for the treatment of cementitious systems, was set up and used in this investigation. The effect of ultrasound on the pore solution compositions of PC pastes with two water-to-cement ratios (w/c) of 0.50 and 0.80 were investigated together with the size distribution of PC particles. Any changes in the main hydrates brought about by PUS were also studied. The progress of hydration under ultrasonication was explored by developing a precise method for measuring the chemical

shrinkage. In addition, the effect of ultrasound on the interface between the aggregates and cement paste in PC mortars was explored by measuring early age and long-term compressive and flexural strength development, together with SEM microstructural analysis.

2. Conclusions

2.1. *Effect of ultrasound on PC particle distribution*

Ultrasound slightly disaggregates the coarse size fraction of PC dispersed in an aqueous medium, but it has little effect on changing the particle size distribution of the finer size fraction (less than 10 μm). Also, a small re-agglomeration was observed after a longer exposure to ultrasound (10 minutes). Taking into consideration that there is a significantly lower ratio of water to solids in a cement paste with a normal w/c ratio of 0.50 compared with the diluted suspension used for PSD studies, PUS would be unlikely to deagglomerate PC particles to any great extent in normal pastes. This observation suggests that any changes induced by the application of ultrasound to either the pore solution and/or the hydrates cannot be primarily attributed to the deagglomeration of particles.

2.2. *Effect of ultrasound on the pore solution and hydration products*

The main hydration products in the PC pastes were not noticeably changed when ultrasound was applied at various frequencies and irradiation times. However, appreciable changes in the pore solution compositions were observed. Amongst various ion species in the pore fluid, aluminium concentrations were substantially increased upon the ultrasonication of PC pastes at both w/c ratios of 0.50 and 0,80, denoting enhanced dissolution of the aluminate phases of the PC clinker. Subsequently, the TG analysis showed a slight increase of amorphous AH_3 hydrate due to sonication. Small changes in calcium and silicon concentrations were also detected, especially after longer exposure to ultrasound. In addition, evidence for an increase in the carbonates was observed whilst a temporary limiting of disruption to the formation of ettringite in an early age of ultrasonication was postulated. Since there was almost negligible disaggregation of PC particles during PUS, it was concluded that the observed changes in the dissolution rates of the phases must be connected to enhanced mass transfer, erosion and the exfoliation of

anhydrous grains. These could be due to the effects of acoustic cavitation bubble collapse, which produces shock waves and jet streams.

2.3. *Effect of ultrasound on the progress of PC hydration*

An enhanced extent of hydration was indicated by meaningful increases in the rate of chemical shrinkage in the PC pastes subjected to short periods of ultrasound (2 minutes). The effect of PUS at the lower frequency of 26 kHz was more pronounced than at 132 kHz. Longer exposure of PUS of up to 10 minutes adversely affected the chemical shrinkage development of the PC pastes.

2.4. *Effect of ultrasound on the mechanical performance of PC mortars*

In Chapter 2, it was hypothesised that cavitation can lead to degassing/deaeration and that the removal of the entrapped air could influence the mechanical properties of cement-based composites. A study of the compressive and flexural strength development of PC mortars revealed that very early age mechanical properties of mortars treated by ultrasound was reduced compared to non-sonicated mortars. However, ultrasonication generally enhanced the mechanical performance of mortars over long-term hydration. At higher acoustic energies ultrasound was found to have a significant influence on both the lowering of the 1-day strengths and an increase in long-term compressive and flexural strengths (91 days curing). Longer exposure (10 minutes) at a higher intensity of ultrasound (26 kHz) was found to reverse and recover the adverse effects of a shorter treatment (2 minutes) on the 1-day strength. This can be related to the deaeration effect of ultrasound on the removal of entrapped air from fresh mortar. Deaeration was confirmed by SEM studies of cement paste microstructure, which showed a denser microstructure of sonicated samples at all frequencies and durations.

Application of ultrasound at two different stages in the casting of mortars highlighted the importance of the timing of aggregate addition. If the aggregates were added to the pre-sonicated cement paste, a significantly enhanced compressive and flexural strength was obtained in comparison to the mortar mixes sonicated after the addition of aggregates. This was supported by SEM microstructural studies of the interface between the aggregates and the bulk cement

paste, which revealed a more compact and uniform matrix for the sonicated samples. Additionally, the correlation made between the compressive and flexural strength test values of the entire mortar specimens indicated an improvement in flexural strength and accordingly the bound between the cement paste and the aggregates (the ITZ) when aggregates were added to the treated paste. Again, the higher intensity ultrasound at 26 kHz was shown to have a more positive effect in the enhancement of the mechanical properties than 132 kHz.

Many regions of aggregate pull-out with various size of aggregates were observed in the microstructure of the mortars sonicated with aggregates. These are in agreement with the hypothesis that directly applying ultrasound to mortars when aggregates are present in fresh mixes could lead to a decrease in the quality of the ITZ. In contrast, the ITZ showed an improved microstructure when the cement paste was treated before the addition of aggregates. These findings could well be important if ultrasound was to be used in ready mixed mortars and concrete applications.

3. Recommendations for future work

Further investigations are needed to understand the underlying effects of ultrasound on PC hydration kinetics. Specifically, this would be the study of ultrasound interaction during the onset and continuation of various phases of heat evolution during hydration. This could be measured using isothermal calorimetry which was a methodology not available to the present study.

Chapter 4 (Section 6.3) discussed the theory for deploying ultrasound to promote the hydration of ternesite cements. This is important for the development of novel low carbon binders. Also in the same chapter evidence for ultrasound-intensified carbonation in cement-based systems was observed. This will be hugely important and also practical for the conversion of waste recycled cementitious materials fines to pozzolanic materials.

Further investigations are also needed to understand the underlying effects of ultrasound on PC composites. More evidence is required to understand the deaeration effect of ultrasound and its performance in cement mortars and concrete by quantifying the entrapped air in each of them.

Changes in entrapped air can be measured using an air meter for mortar/concrete in the ultrasonication of fresh mixes.

It would also be useful to develop bespoke ultrasonic equipment suitable for the treatment of cementitious systems at various intensities.

The following are also important to more fully understand the potential applications of PUS for cement-based materials:

- To conduct more in-depth studies of the effects of acoustic cavitation on cementitious materials.
- To investigate the hydration kinetics of binary and ternary blended cementitious systems (i.e. calcined clay, slags, PFA, silica fume) subjected to the direct application of PUS.
- To undertake low temperature thermodynamic modelling of cementitious systems, comparing sonicated to conventional cement pastes. Specifically, this could examine the solid and pore solution chemistry to determine how far from thermodynamic equilibrium the system becomes during ultrasonic treatment.
- To explore the effects of various ultrasonic frequencies and intensities on the sonocrystallisation of cementitious materials, hydration kinetics and hydrate assemblages.
- To perform microstructural studies to identify changes in the early hydration of Portland cement phases immediately upon ultrasonication, using advanced imaging techniques.
- Electron density, as shown by secondary electron (SE) imaging, will show average solid/porosity maps to use to examine the densification effects due to ultrasonic processing. It may be interesting to use neutron imaging to map water-filled porosity as a comparison to SE (or backscattered electron) imaging in such studies.

List of publications

Ganjian, E., Ehsani, A., Mason, T. J., Tyrer, M. (2018) Application of power ultrasound to cementitious materials: Advances, issues and perspectives. *Materials & Design*, 160:503-513

Manuscript Submitted:

"Insights into the positive effects of power ultrasound on the pore solution of Portland cement pastes", based on the results discussed in this chapter, submitted to the "*Cement and Concrete Composite*" journal.

"Insights into the positive effects of the direct application of power ultrasound to Portland cement pastes and mortars, study of chemical shrinkage and mechanical performance", submitted to the "*Construction and Building Materials*" journal.

Conferences presentations:

Presentation at *"39th Cement and Concrete Science Conference*, Sep 2019"

Title: Influence of power ultrasound on the Portland cement pore solution compositions at early ages.

Presentation at *"40th Cement and Concrete Science Conference*, Sep 2020"

Title: Effect of Power Ultrasound on the Portland cement paste and mortar: study of chemical shrinkage and compressive and flexural strength development